UNIVERSIDADE FEDERAL DE SANTA CATARINA
CENTRO TECNOLÓGICO
GRADUATE PROGRAM IN ELECTRICAL ENGINEERING

Guilherme Corrêa Danielski

Identification of the Feasible Region for Convexified Nonlinear Security-Constrained Optimal Power Flow Problem

Forianopolis
2022

Guilherme Corrêa Danielski

IDENTIFICATION OF THE FEASIBLE REGION FOR CONVEXIFIED NONLINEAR SECURITY-CONSTRAINED OPTIMAL POWER FLOW PROBLEM

Thesis submitted to the Graduate Program in Electrical Engineering in partial fulfillment of the requirements for the degree of Master of Science in Electrical Engineering.

Supervisor: Prof. Katia Campos de Almeida, PhD

Florianópolis

2021

Ficha de identificação da obra elaborada pelo autor,
através do Programa de Geração Automática da Biblioteca Universitária da UFSC.

Danielski, Guilherme Corrêa
Identification of the Feasible Region for Convexified Nonlinear Security-Constrained Optimal Power Flow Problem / Guilherme Corrêa Danielski ; orientadora, Katia Campos de Almeida, 2022.
116 p.

Dissertação (mestrado) - Universidade Federal de Santa Catarina, Centro Tecnológico, Programa de Pós-Graduação em Engenharia Elétrica, Florianópolis, 2022.

Inclui referências.

1. Engenharia Elétrica. 2. umbrella constraints. 3. fluxo de potência ótimo com restrição de segurança. 4. restrições guarda-chuva. 5. programação semidefinida. I. de Almeida, Katia Campos. II. Universidade Federal de Santa Catarina. Programa de Pós-Graduação em Engenharia Elétrica. III. Título.

Guilherme Corrêa Danielski

IDENTIFICATION OF THE FEASIBLE REGION FOR CONVEXIFIED NONLINEAR SECURITY-CONSTRAINED OPTIMAL POWER FLOW PROBLEM

The present Master's thesis was evaluated and approved by the following examiners:

Prof. Roberto de Souza Salgado, PhD
Universidade Federal de Santa Catarina

Prof. Marcos Julio Rider Flores, Dr.
Unicamp

Eng. Miguel Paredes Quiñones, Dr.
IBM Research

We certify that this is the original and final version of the conclusion work that has been judged suitable for obtaining the title of Master of Science in Electrical Engineering.

Documento assinado digitalmente
Telles Brunelli Lazzarin
Data: 26/02/2022 19:09:14-0300
CPF: 023.400.719-25
Verifique as assinaturas em https://v.ufsc.br

Prof. Telles Brunelli Lazzarin, Dr.
Graduate Program Coordinator
Universidade Federal de Santa Catarina

Documento assinado digitalmente
Katia Campos de Almeida
Data: 14/02/2022 06:59:50-0300
CPF: 503.911.516-49
Verifique as assinaturas em https://v.ufsc.br

Prof. Katia Campos de Almeida, PhD
Supervisor
Universidade Federal de Santa Catarina

Florianópolis, 2022.

To my forever loved grandmother, Isa.

ACKNOWLEDGEMENTS

First and foremost, I am grateful to my supervisor Prof. Katia Campos de Almeida. Thanks to her, I was able to develop as a researcher. She was my first supervisor in 2012, and since then, she has helped me in many ways.

I am in debt to my supportive husband Renan, who always helped me and for his feedback. He is always by my side during trying times. Thank you.

I am also grateful for the committee's insightful observations and knowledge. Moreover, for the opportunity they gave me to showcase my work to them.

To my supportive family, especially my mother Silvani, father Jefferson, and brother Gabriel. Thanks for the emotional support and incentive to always give my best. To my beloved grandmother, Isa, who always loved me and never let me feel alone. May she rest in peace. You will always be remembered and loved.

I am thankful for the scholarship from CAPES; without the financial support, I wouldn't be able to pursue my Masters.

ABSTRACT

Security-constrained optimal power flow (SCOPF) is a powerful tool for power system planning and operation. However, due to the problem non-convexivity and number of variables and constraints, this optimization problem is computationally demanding. This work proposes a new methodology to identify the constraints that bound the feasible set of the nonlinear SCOPF problem, thus considerably reducing the processing time for its solution. The methodology convexify the nonlinear problem using semidefinite programming (SDP) and employs a recovery method to reveal the required and sufficient constraints to solve the SCOPF problem. An illustrative example details the approximations resulting from SDP relaxation, and the New England test system and a 34-bus equivalent of the Hydro-Québec system are used to verify the performance of the proposed approach.

Keywords: security constrained optimal power flow; umbrella constraints; semidefinite programming.

RESUMO

O fluxo de potência ótimo com restrições de segurança (FPORS) é uma poderosa ferramenta para o planejamento e operação de sistemas de potência. Porém, devido ao grande número de variáveis e restrições, além de sua não-convexidade, esse problema de otimização apresenta alto custo computacional. O presente trabalho propõe uma nova metodologia para a identificação de restrições que limitem o conjunto viável do problema FPORS não-linear, reduzindo consideravelmente o tempo de processamento para a sua solução. A metodologia transforma o problema não-convexo em convexo usando programação semidefinida (PSD) e emprega um método de recuperação para revelar as restrições requeridas e suficientes para resolver o problema FPORS. Um exemplo ilustrativo detalha as aproximações resultantes da relaxação PSD. Além disso, o sistema New England de 39 barras e um equivalente de 34 barras do sistema Hidro-Québec são usados para verificar a performance da estratégia proposta.

Palavras-chave: fluxo de potência ótimo com restrição de segurança; restrições guarda-chuva; programação semidefinida.

RESUMO EXPANDIDO

A habilidade de um sistema de energia elétrica de operar respeitando limites pré-especificados, tanto em regime permanente e após um distúrbio (por exemplo, curto-circuito ou falha de equipamento), é chamada de segurança operacional. O objetivo do operador do sistema é garantir que o sistema esteja no estado seguro. De forma a poder analisar a segurança do sistema elétrico, foram classificadas cinco condições de operação do sistema: estado normal de operação, estado de alerta, estado de emergência corretivo, estado de emergência não-corretivo, e estado restaurativo de operação [1].

A operação segura do sistema de potência exige uma margem de segurança para poder permanencer em estado normal de operação mesmo após um distúrbio. Há diversos critérios de segurança que podem ser adotados. Um deles é o critério $N-1$, introduzido após o apagão de 1961 nos EUA. O critério de segurança $N-1$ impõe que a operação do sistema elétrico não seja comprometida após um distúrbio que causa a perda de um de seus componentes. Os limites que devem ser respeitados podem ser classificados genericamente como físicos e operacionais. Os primeiros são limites construtivos dos componentes do sistema. Os limites operacionais são obtidos através de simulações e dependem das condições operativas (carregamento, despacho de geração, topologia da rede, etc.). Entre os limites operacionais podem ser citados: limites nas magnitudes das tensões, limites de carregamento de linhas e transformadores e limites de geração impostos para garantir reserva girante no sistema. O carregamento de linhas pode ser restringido tanto pela queda de tensão ao longo das mesmas, pelo limite térmico ou de estabilidade dinâmica. Neste trabalho, um distúrbio é uma pertubação no sistema de potência que ocasiona a queda de uma linha de transmissão.

O fluxo de potência ótimo com restrições de segurança (FPORS) é uma poderosa ferramenta para o planejamento e operação de sistemas de potência. O objetivo do FPORS é obter uma condição operacional do sistema que respeita a condição $N-1$, enquanto ao mesmo tempo otimiza um critério de desempenho. Entretanto, resulta num problema de otimização não linear, não convexo e com número considerável de variáveis e restrições, pois é necessário considerar no problema todas as restrições de operação do sistema intacto e após cada contingência. Desta forma, a resolução do problema FPORS apresenta um custo computacional elevado.

Entretanto, muitas das restrições do problema FPORS são redundantes, ou seja, não necessárias para formar o conjunto viável do problema de otimização. Desta forma, as restrições que formam a fronteira do conjunto viável são denominadas restrições *umbrella*. Em outras palavras,o problema FPORS pode ser reduzido quando consideradas somente suas restrições *umbrella*, uma vez que não há modificação no conjunto viável. Vale salientar que essas restrições são independentes da função objetivo. Como consequência, restrições *umbrella* não são necessariamente restrições ativas numa dada solução, mas todas as restrições ativas são *umbrella*. Portanto, pode-se afirmar que há somente um único conjunto de restrições *umbrella* para cada problema.

No últimos anos foram publicados diferentes estratégias para se obter as restrições *umbrella* de um sistema [2–6], porém, encontram-se métodos de determinação de restrições *umbrella* válidos somente para problemas convexos. Consequentemente, são válidos apenas quando se adota o modelo linearizado para as equações da rede elétrica. O presente trabalho propõe uma nova metodologia para a identificação de restrições *umbrella*, ou seja, que limitam o conjunto viável do problema FPORS não-convexo. Desta forma, reduz-se consideravelmente o tempo de processamento do problema FPORS.

Para se identificar as restrições *umbrella* de um problema de otimização não-

convexo, o mesmo relaxado por um problema convexo usando programação semidefinida (PSD) [7]. A PSD permite elevar o problema a um espaço convexo de maior dimensão, permitindo assim obter sua solução ótima global. Este trabalho usa uma relaxação de segunda ordem para montar o problema PSD. No problema PSD as restrições do problema não convexo são linearizadas e insere-se uma restrição matricial que impõe que a matriz formada pelos monômios presentes nas restrições originais, denominada matriz de momentos, seja semidefinida positiva. Todavia, tal metodologia aumenta consideravelmente a dimensão do problema original ao aumentar, em especial, o número de variáveis. Além disso, dependendo do tipo de problema, a PSD somente consegue obter apenas uma solução aproximada. Em outras palavras, o conjunto viável da PSD engloba o do problema não-convexo. Como consequência, obtêm-se uma solução conservadora para a função objetivo (um valor menor que o global), além da solução não necessariamente respeitar todas as restrições do problema.

Devido a essa aproximação, é necessário recuperar uma solução factível a partir daquela obtida via PSD, de forma que todas as restrições do problema não convexo original sejam respeitadas. A recuperação proposta minimiza o desvio padrão entre o ponto ótimo PSD e o do problema não-linear, enquanto resolve o problema não-convexo de identificação de restrições *umbrella*. Como o ponto inicial do problema é a solução da PSD, tal ponto está próximo da solução global do problema não-convexo.

Como mencionado anteriormente, a relaxação via PSD aumenta consideravelmente o problema a ser resolvido. Por outro lado, o problema de identificação de restrições *umbrella* é muito custoso computacionalmente, pois seu tamanho aumenta quadraticamente em relação ao número de restrições a serem verificadas. Isto torna a identificação de restrições *umbrella* não-convexas usando PSD uma tarefa árdua, do ponto de vista computacional. Como um exemplo, para identificar todas as restrições *umbrella* do equivalente de 34 barras do sistema Hydro-Québec, é necessário resolver um problema com mais de 1 bilhão de restrições e 8 milhões de variáveis. Ao aumentar o número de barras do sistema teste, o número de restrições e variáveis cresce significamente.

A fim de diminuir o custo computacional, o presente trabalho propõe as seguintes técnicas de partição do problema de identificação das restrições *umbrella*: partição por contingência, partição por segurança e partição por linha. A partição por contingência separa o problema por contigência, ou seja, supondo que o problema FPORS considera n_c contigências, então divide-se o problema FPORS em $n_c + 1$ subproblemas, cada um formulado, ou ainda com variáveis e restrições, associadas a uma das contingências. A partição por segurança divide o problema FPORS em n_c subproblemas com as restrições associadas ao sistema intacto e a cada uma contigência. A separação é feita da seguinte maneira: todas as contigências têm como referência o sistema intacto (sem distúrbio), desta forma, ao resolver cada subproblema, identificam-se as restrições *umbrella* para um FPORS que considera somente o sistema intacto e uma dada contigência. A última partição separa o problema FPORS em dois subproblemas, sendo o primeiro subproblema formulado apenas considerando as restrições de fluxo de linha. Isto é feito devido à expectativa que a maioria das restrições não *umbrella* são restrições de fluxo de linha. Portanto, remove-se o maior número de restrições primeiramente, para então resolver o segundo subproblema considerando somente as restrições de fluxo de linha que foram consideradas *umbrella*.

A estratégia proposta anteriormente fornece um conjunto *umbrella* aproximado, isto é, que contém restrições que não são *umbrella*. Para obter o conjunto final de restrições *umbrella*, é necessário resolver o problema de identificação das restrições *umbrella* considerando somente o conjunto de restrições obtidos pelas partições. Se preciso,

é recomendada a combinação de partições para minimizar o número de restrições em cada problema de identificação de restrições *umbrella*.

A estratégia de partição reduz somente o número de restrições a serem testadas, mas não necessariamente o número de variáveis do problema PSD. Para tal, é empregado uma problema PSD obtido pela análise da estrutura esparsa do problema não convexo original. A metodologia transforma a matriz de momentos numa matriz bloco diagonal, diminuindo assim o número de variáveis a serem consideradas.

A metodologia proposta é constituída, portanto, de duas etapas: na primeira obtêm-se uma solução relaxada para o problema de identificação das restrições *umbrella* e, na segunda etapa, recupera-se a solução e as restrições *umbrella* do problema FPORS original. Um exemplo ilustrativo detalha como obtêm-se as restrições *umbrella* e as aproximações resultantes da relaxação PSD. Além disso, o sistema New England de 39 barras e um equivalente do sistema Hidro Quebec de 34 barras foram usados para verificar a performance da estratégia proposta.

LIST OF FIGURES

LIST OF TABLES

LIST OF ABBREVIATIONS AND ACRONYMS

SCOPF	Security-Constraint Optimal Power Flow.
SC-LOPF	Security-Constrained Linear Optimal Power Flow.
OPF	Optimal Power Flow.
AC	Alternate current.
SDP	Semidefinite Programming.
FACTS	Flexible AC Transmission System.
SC	Synchronous Condenser.
LP	Linear Programming.
SOS	Sum od Squares.
LOPF	Linear Optimal Power Flow.
UCOPF	Umbrella Constraint Optimal Power Flow.
UCD	Umbrella Constraint Discovery.

LIST OF SYMBOLS

Indices

i, l, m	Bus index.
j	Constraint index.
k	Contingency index.

Functions

f_c, F_c, F	Cost function.
$p(x)$	$2d$-degree Real-valued polynomial.
$L_y\{\cdot\}$	Linear functional.
$h_j(\mathbf{x})$	Inequality constraint j.
dev	Deviation objetive function.

Constants

n_b	Number of buses.
n_l	Number of lines.
n_g	Number of generators.
n_c	Number of contingencies.
J_{AC}	Number of constraints for the SCOPF problem.
J_{DC}	Number of constraints for the SC-LOPF problem.
P_{D_i}	Active power load at bus i.
Q_{D_i}	Reactive power load at bus i.
$P_{G_{\min}}$	Active power generation lower limit.
$Q_{G_{\min}}$	Reactive power generation lower limit.
$P_{G_{\max}}$	Active power generation upper limit.
$Q_{G_{\max}}$	Reactive power generation upper limit.
$V_{\min}$	Voltage magnitude lower limit.
$V_{\max}$	Voltage magnitude upper limit.
$F_{\max}$	Active power flow upper limit.
$\Delta P_{\max}^{(k)}$	Maximal variation in active power generation at state k.
$\Delta Q_{\max}^{(k)}$	Maximal variation in reactive power generation at state k.
r_{ik}	Resistance of the line connecting bus i to k.
x_{ik}	Reactance of the line connecting bus i to k.
$b_{sh_{ik}}$	Shunt susceptance of the line connecting bus i to k.
$\bar{z}_{ik}$	Series impedance of the line connecting bus i to k.
$\bar{y}_{ik}$	Series admittance of the line connecting bus i to k.
g_{ik}	Series conductance of the line connecting bus i to k.
b_{ik}	Series susceptance of the line connecting bus i to k.
J	Number of constraints.

Variables

e_i	Real voltage at bus i.
f_i	Imaginary voltage at bus i.
$\bar{V}_i$	Complex voltage at bus i.
F_{lm}	Active power flow from bus l to m.
S_{lm}	Apparent power flow from bus l to m.

I_i	Current injection at bus i.
$\bar{S}$	Apparent power.
P_i	Active injected power at bus i.
S_P	Security constraint for the SC-LOPF problem.
P_{G_i}	Active power generated at bus i.
Q_{G_i}	Reactive power generated at bus i.
δ_i	Bus i voltage angle in radians.
s	Slack variable.

Vectors and variable matrices

$\mathbf{x}$	Variable vector.
$\mathbf{f}_P$	Active power injection vector.
$\mathbf{f}_Q$	Reactive power injection vector.
$\mathbf{f}_F$	Active power flow vector.
$\mathbf{f}_T$	Reverse active power flow vector.
$\mathbf{f}_V$	Voltage magnitude vector.
$\mathbf{f}_{S_P}$	Variation in active power generation between two states.
$\mathbf{f}_{S_Q}$	Variation in reactive power generation between two states.
$\mathbf{I}$	Identity matrix.
$\mathbf{u}$	Unity vector.
$\bar{\mathbf{Y}}$	Bus admittance matrix.
$\mathbf{B}_\delta$	DC load flow admittance matrix.
A_{inc}	Bus-line incidence matrix.
$\boldsymbol{\lambda}$	Lagragian multiplier vector.
$\mathbf{y}$	Vector of lifting variables.
$\mathbf{C}$	Constant symmetric matrix.
$\mathbf{X}$	Symmetric monomial matrix.
$\mathbf{M}(\mathbf{y})$	Moment matrix.
$\hat{\mathbf{M}}(\mathbf{y})$	Block diagonal moment matrix.
$\mathbf{Z}$	Order-1 moment matrix.
$\mathbf{b}$	Constant column vector.
$\mathbf{A}_j$	Constant sparse matrix associated with constraint j.
$\mathbf{w}_j$	Variable vector associated with constraint j.
$\mathbf{R}$	Adjacency matrix.
$\mathbf{x}_{rec}$	Recovered variable matrix.
$\mathbf{e}_{rec}$	Recovered real valued voltage vector.
$\mathbf{f}_{rec}$	Recovered imaginary valued voltage vector.

Sets

$\mathcal{N}$	Set of the system buses.
$\mathcal{G}$	Set of the system generators.
$\mathcal{S}$	Set of the system generators considered for the security constraint.
$\mathcal{K}$	Set of contingency states.
$\mathcal{J}$	Set of constraints.
$\mathcal{J}(k)$	Set of constraints associated with state k.
$\mathcal{J}_1, \mathcal{J}_2, \mathcal{J}_3$	Subset of $\mathcal{J}$.
$\mathcal{J}_\pi$	Power balance, generation, and line constraint set.
$\mathcal{J}_\pi^b$	Power balance constraint set.

$\mathcal{J}_\pi^g$	Power generation constraint set.
$\mathcal{J}_\pi^l$	Line limit constraint set.
$\mathcal{J}_\pi^v$	Voltage magnitude constraint set.
$\mathcal{J}_\pi^{g,v}$	Power generation and voltage constraints set.
$\mathcal{J}_\pi(k)$	$\mathcal{J}_\pi$ constraints associated with state k.
$\mathcal{J}_\pi^U$	Union of the umbrella sets associated with each $\mathcal{J}_\pi(k)$.
$\tilde{\mathcal{J}}_\pi$	Constraint subset of $\mathcal{J}_\pi$.
$\mathcal{J}_\lambda$	Set of security constraints.
$\mathcal{J}_\lambda(k)$	Set of security constraints associated with state k.
$\mathcal{U}$	Set of umbrella constraints.
$\mathcal{U}_1$	Umbrella constraint set of $\mathcal{J}_1$.
$\mathcal{U}_2$	Umbrella constraint set of $\mathcal{J}_2$.
$\mathcal{U}_3$	Umbrella constraint set of $\mathcal{J}_3$.
$\mathcal{U}^l$	Set of umbrella constraints associated with line constraints.
$\mathcal{U}_k$	Set of umbrella constraints of $\mathcal{J}_\pi(k)$.
$\mathcal{U}(k)$	Set of umbrella constraints associated with state 0 and k.
$\tilde{\mathcal{U}}$	Approximate umbrella constraint set.
$\tilde{\mathcal{U}}_k$	Set of umbrella constraints of $\tilde{\mathcal{J}}_\pi(k)$.
$\tilde{\mathcal{U}}^\alpha$	Union of all $\tilde{\mathcal{U}}_k$.
$\tilde{\mathcal{J}}_\alpha$	Union of $\tilde{\mathcal{U}}^\alpha$ and $\mathcal{J}_\lambda$.
$\tilde{\mathcal{J}}_\alpha(k)$	$\tilde{\mathcal{J}}_\alpha$ constraints associated with state k.
$\tilde{\mathcal{U}}^\beta(k)$	Set of umbrella constraints of $\tilde{\mathcal{J}}_\alpha(k)$.
$\mathcal{B}$	Bag set.

Other symbols

$2d$	Polynomial degree.
x^α	α degree monomial.
p_α	Polynomial coefficient associated with x^α.
$\min$	Subscript indicating lower limit.
$\max$	Subscript indicating upper limit.
(k)	Superscript indicating the contingency state.
$\top$	Superscript indicating transpose.
$\bullet$	Inner product operation.
$*$	Superscript indicating optimal solution.
$sign(\cdot)$	Sign of the variable.
$\subseteq_U$	Umbrella constraints subset in the constraint set.
G	Undirected graph.
V	Graph G node set.
E	Graph G edge set.

CONTENTS

1 INTRODUCTION

Electric power transmission has gone through considerable development since its first conception. In the first systems, power was supplied via direct currents. For this reason, transmission losses were so high that the extension of the lines could not exceed 2 km. It was not until the development of the alternate current that the power grid would start assuming its current shape. The power plants began to expand in order to accommodate the ever-increasing demand [8].

As a result of a continuously increasing demand, modern societies have become even more energy-dependent. For instance, the blackout of 2003 in North America caused an economic cost in the range of $7 and $10 billion for the national economy and estimation of further lost earnings for U.S. workers, consumers, and taxpayers around $6.4 billion [9]. Another example took place in Amapá, Brazil at the end of 2020. This blackout lasted 22 days, during the height of the COVID-19 pandemic, affecting almost 800 thousand residents. Hospitals, businesses, government bodies, traffic and utilities were impaired by it. Consequently, COVID-19 numbers ceased to be reported due to this event [10, 11]. In other words, a secure and reliable power grid is of utmost importance for the country's economy.

1.1 POWER SYSTEM SECURITY

Considering the power system steady-state operation, its ability to operate within the specified limits of safety and supply quality after a disturbance is called system security. That is, if the grid is operating in a safe state (i.e. within its operational limits and load requirements), in case of a disturbance (e.g. short-circuits, equipment failure, etc.), it should not go to an unsafe state [12].

With the improvement of computers and the implementation of new algorithms to help the system operators in control centers analyze and operate the system network, security functions were introduced to help keeping the power system in a "normal" state. In addition, in 1978 Dy Liacco proposed the classification of power system operating conditions into states [13].

For the purpose of analysis of the power system security, the system operating conditions are classified into five states: *normal*, *alert*, *correctable emergency*, *noncorrectable emergency* and *restorative* [1]. The objective of this classification is to show how the power system is satisfying its load and operational constraints. The operating condition of each state is as follows:

- Normal state: All the system variables are within normal range. There is no equipment overload. This also represents a secure state, as in the case of a disturbances, there will be no violations;

- Alert state: This is an insecure state. All variables are within the normal range, however a disturbances can cause equipment overload. This state can become active if a disturbance happened while on normal operation state, or there is a considerable increase in the system load. Therefore, system operators should take action to revert the system to a normal state;

- Correctable Emergency state: This state may be active when a severe disturbance occurs or the preventive controls fail. In this state, the power balance constraints are still satisfied, but some inequality constraints are being violated (i.e. equipment are overloaded). Emergency control actions must be taken to bring back to an alert or normal state. This can be done without load loss;
- Noncorrectable Emergency state: Similar to the Correctable Emergency state, but the emergency control action will cause load loss;
- Restorative state: No operating limits violated, but loss of load has occurred. If the control actions to restore the load is successful, the system transitions to normal or alert states.

The secure operation of power systems demands appropriate security margins so it can remain secure after different disturbances. There are many security criteria to determine a sufficient security margins. One such criterion is the $N-1$ criterion, introduced after the 1965 Northeast USA blackout. The criterion dictate that the system should withstand a loss of any component without compromising the system operation [14]. For a system to operate in $N-1$ condition, the power system operators have to take into consideration many different types of system limitations, such as: physical limits, sag limits, safety limits, disturbances, and operational limits. Furthermore, power flows can be restricted, especially over long distances, by voltage limits, voltage collapse, thermal limit or transient instability (e.g. electromechanical) [15].

Finally, the complexity of modern power systems causes their operation and expansion planning to be more difficult, especially when we consider that these tasks should reduce costs without affecting quality, security, and reliability [16].

Therefore, system operators usually do not consider all the possible disturbances, as it might prove computationally prohibitive for time-sensitive operations. Thus, an approach to identify and rank the severity of each disturbances is required. First, by performing a series of simulations, all disturbances are screened, and the system performance indices under every disturbances are obtained. Afterwards, disturbances are ranked according to the performance indices obtained in the simulations. This mainly helps classify the disturbances by severity and identify which one does not change the system's state to insecure [17].

In this study, a contingency is a disturbance in the power system that leads to the outage of a transmission line. In order to decrease the changes in operating states, security constraints are introduced. One method to achieve the $N-1$ operational condition is by using the Security-Constraint Optimal Power Flow algorithm (SCOPF) [18].

1.2 SECURITY-CONSTRAINED OPTIMAL POWER FLOW

The Optimal Power Flow (OPF) is a planning problem that, given a static loading condition, considers the system network (mathematical models for buses, transmission lines, transformers, etc.) to obtain an optimal active and reactive power dispatch. The

power dispatch is just a part of the power system operational and planning process, but essential [12].

The OPF was initially formulated by Carpentier in 1962 [19] and originally intended to discover the operational conditions in which the power system would respect all its limits and have the lowest operational cost associated with it. A great advantage of the OPF problem is its flexibility to represent a wide range of equipment that may be of interest to system operators. Usually the OPF problem has the following form:

$$\begin{aligned} \min_{\mathbf{x}} \quad & f_c(\mathbf{x}) \\ \text{subject to} \quad & \mathbf{g}(\mathbf{x}) \leq \mathbf{c}, \end{aligned}$$

where f_c is the objective function of the problem (e.g. economic dispatch), $\mathbf{g}$ is a set of constraints of interest, and $\mathbf{x}$ is a vector of control variables.

However, it has been observed that operating conditions obtained by solving the OPF problem may not be secure. This has led to the development of the security-constrained dispatch, which may be considered when solving an OPF problem. By doing so, preventive actions may be taken so the system can operate in a secure manner. However, such dispatch is seen as conservative, as it does not account for the system corrective capabilities (e.g. generation rescheduling, switching, overload rotation, etc.) [20].

The OPF problem with secured-constrained dispatch is called Security-Constrained Optimal Power Flow (SCOPF). The SCOPF's objective is to obtain an operational condition for the system so it may operate in a $N-1$ state, while minimizing the objective function [12].

Nevertheless, taking system security into consideration brings many challenges, especially regarding its significant increase in the number of constraints of the optimization problem. This is due to the need of adding all operation constraints pre-contingency and for each contingency to the problem [16].

One solution to overcome the hurdles associated with system expansion is to use the SC-LOPF model. This model was first proposed by Stott in 1978 [21, 22], and is based on the DC linearized load flow equations. After linearization, there are many linear programming algorithms readily available that are very efficient in solving large-scale problems. Moreover, the number of constraints decreases significantly, as the reactive power balance constraints are not taken into consideration and the bus voltage magnitudes are supposed to be equal to the nominal values [23]. However, this approach neither takes into account any reactive and apparent power control variables, thus there is a considerable reduction in the system complexity [18].

1.3 THESIS RATIONALE

Computational programs that solve the OPF and SCOPF problems are among the tools used to reliably operate the grid [18]. Nonetheless, these optimization problems may become difficult to solve due to their complexity, non-linearity and size. Usually, power system constraints for SCOPF are in the million [12, 24].

However, some studies observed that just a fraction of those constraints is not redundant [2, 3]. For this reason, [2] introduced the concepts of umbrella constraints

and umbrella set. Umbrella constraints are the ones that set the border of the feasible set of the problem. In other words, they are the constraints necessary and sufficient to solve the original problem without affecting the original solution. Another essential characteristic of the umbrella constraints is that they are independent of the objective function of the problem. That means that a set of umbrella constraints is unique and does not change when the objective function does. Therefore, the umbrella constraints are not necessarily binding constraints but a set of potentially binding ones, where the cost function will determine the ones to be active. In other words, there is just one possible set of umbrella constraints for each power system operation point. Nevertheless, the linear OPF model has some limitations. These include no guarantee in feasibility for the nonlinear problem, only local optima, and no reactive power representation, which are not necessarily relevant for some applications [25].

[2] also uses the fact that the feasible set of the linear SCOPF problem, also known as Security-Constrained Linear Optimal Power Flow (SC-LOPF) is a convex polytope to derive a methodology to identify the umbrella constraints of the problem. As will be discussed in this thesis, the extension of such methodology to the nonlinear OPF or SCOPF is not trivial.

Considering the research developed so far, we may say that the problem of reducing the set of constraints of the SC-LOPF is fairly solved. Nevertheless, the SC-LOPF model has some limitations: it does not take into consideration the reactive power requirements of the system and reactive power controls, which, in spite of not being relevant for some applications, may result in unfeasible steady-state operating points [25]. Moreover, this linear model may affect the system operator´s decisions and corrective actions, specially regarding system stability and reactive power control. Due to these limitations, in many situations it is advantageous to represent steady state operation through the active and reactive power balance equations, which raises the questions: how to identify the umbrella constrains of the nonlinear SCOPF?

One way to extend the umbrella identification method described in [2] is via convex relaxation of the SCOPF. One such relaxation would be the semidefinite programming (SDP) [25].

1.4 THESIS GOALS

The present study describes an algorithm to identify the umbrella set of the nonlinear SCOPF problem. The SCOPF is represented in rectangular coordinates and semidefinite programming relaxation and is used to describe the feasible set of the problem, in the lifted space, by a set of linear constraints. The algorithm described in [2] is then extended to obtain the umbrella set of the relaxed SCOPF.

1.5 THESIS CONTRIBUTION

This thesis addressed the proposed large-scale non-convex umbrella identification problem. To tackle it, three partitioning methods were developed. Furthermore, the sparsity exploitation method introduced by [45] was extended for the proposed problem.

Finally, as the SDP relax the original problem to convexify it, a new recovery method was proposed to identify the umbrella constraints of the non-convex SCOPF problem.

1.6 THESIS OUTLINE

This thesis is divided in 7 chapters, as follows:

Chapter 2 introduces the SCOPF problem, its uses and formulation. It also shows the approximations used in the SC-LOPF.

Chapter 3 briefly demonstrates the concept of the semidefinite programming and how the convexification of a set of equations may affect the original nonlinear solution.

Chapter 4 introduces the umbrella identification problem and analyzes the challenges imposed by such problem. Three umbrella detection examples applied to SC-LOPF are also presented.

Chapter 5 proposes and formulates a new method for identifying the umbrella constraints of the SCOPF problem. An illustrative example is used to show how it works and its limitations.

Chapter 6 analyzes the results of simulations with the following test systems: 2-bus network, 34-bus Hydro-Québec equivalent and the IEEE 39-bus network.

Chapter 7 draws some conclusions about the study and proposes future work.

2 SECURITY-CONSTRAINED OPTIMAL POWER FLOW

2.1 INTRODUCTION

The power system is usually represented by its single line diagram. Each branch can represent a wide array of equipment, such as transmission lines, transformers, Flexible Transmission System (FACTS) devices, among others. Each node (or bus) is a substation that can be connected to power generators, FACTS devices, synchronous condensers or loads. The power balance equations are essentially a mathematical representation of the conservation of energy in every node of the system. In other words, the sum of all the power coming in is equal to the one coming out of every node [26].

Load flow and optimal power flow (OPF) programs can be used to calculate the voltage magnitudes and angles that satisfy the energy balance in the system. The main difference between these tools is that OPF programs determine the voltage magnitudes and angles that optimize a performance criterion. This chapter introduces the nonlinear Optimal Power Flow and the Security Constrained Optimal Power Flow problems, and their respective linearized mathematical modelling.

2.2 THE POWER SYSTEM

There are mainly two ways to calculate the bus voltage magnitudes and angles that satisfy the energy balance in the system. One of them is a direct approach, in which the active and reactive power balance equations are solved. The other one is by calculating the network's current flows. No matter the approach adopted, the set of equations being solved can be expressed in polar or rectangular coordinates. Each formulation has its particularities, which need to be taken into consideration when using computational solvers [26].

As previously stated, power flow equations can have different representations. However, the set of equations are nonlinear. In order to reduce computational costs, a linearized load flow model was derived based on properties of high voltage power networks [27]. Although the linearized model is very useful to provide information regarding the active power balance in the system and line loading, it disregards the reactive power balance in the system. Therefore, the linearized model is useful in some particular operational studies only, such as time-sensitive operations or long-term planning simmulations. This section, first of all, presents the nonlinear load flow model represented in rectangular coordinates and, subsequently the linearized load flow [26].

2.2.1 Nonlinear Load Flow Model

This model is also known as alternate current (AC) model. In this case, the active and reactive power balance in every bus must be respected. In addition, a set of physical and operational constraints must be satisfied, among them: minimum and maximum limits on voltage magnitudes, active and reactive power generation and variable transformer taps; maximum line loading limits.

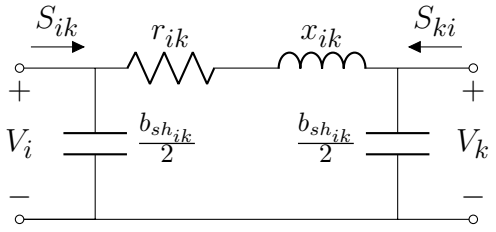

Figure 2.1: Nominal π model of Transmission Line.

2.2.1.1 Power Balance Constraints

Consider that the grid consists of a set of $\mathcal{N} = 1, 2, \ldots, n_b$ buses, the set of n_g generator buses $\mathcal{G} \subseteq \mathcal{N}$, and the set of lines $\mathcal{L} = 1, 2, \ldots, n_l$.

The complex bus voltages are expressed in rectangular coordinates as $\bar{V}_1 = e_1 + \mathrm{j}f_1, \ldots, \bar{V}_{n_b} = e_{n_b} + \mathrm{j}f_{n_b}$, where $\mathrm{j} = \sqrt{-1}$. These can be stored in vector $\bar{\mathbf{V}} = \mathbf{e} + \mathrm{j}\mathbf{f}$, where

$$\mathbf{e} = \begin{bmatrix} e_1 \\ e_2 \\ \vdots \\ e_{nb} \end{bmatrix}, \quad \mathbf{f} = \begin{bmatrix} f_1 \\ f_2 \\ \vdots \\ f_{nb} \end{bmatrix} \tag{2.1}$$

In this study, the π model is used to represent the transmission line, as shown in Fig. 2.1. The model is composed of the series resistance r_{ik} and reactance x_{ik}, and the shunt susceptance $b_{sh_{ik}}$ for the line that connects bus i to k. Therefore, the series impedance is $\bar{z}_{ik} = r_{ik} + \mathrm{j}x_{ik}$, and the series admittance is $\bar{y}_{ik} = \bar{z}_{ik}^{-1} = g_{ik} + \mathrm{j}b_{ik}$. The series conductance g_{ik} and the series susceptance b_{ik} are calculated by equations (2.2) and (2.3), respectively.

$$g_{ik} = \frac{r_{ik}}{r_{ik}^2 + x_{ik}^2} \tag{2.2}$$

$$b_{ik} = \frac{-x_{ik}}{r_{ik}^2 + x_{ik}^2} \tag{2.3}$$

The power balance equation can be deduced by the use of Kirchhoff's current law, as shown by Fig. 2.2 [27]. Thus, we have:

$$\bar{I}_i = \sum_{k \in \Omega_i} \bar{I}_{ik} \tag{2.4}$$

where $i = 1, \ldots, n_b$, Ω_i is the set of buses connected to bus i. The line currents from bus i to bus k and from bus k to bus i are expressed as:

$$\bar{I}_{ik} = [\bar{y}_{ik} + \mathrm{j}b_{sh_{ik}}]\bar{V}_i - [\bar{y}_{ik}]\bar{V}_k \tag{2.5}$$

$$\bar{I}_{ki} = [-\bar{y}_{ik} + b_{sh_{ik}}]\bar{V}_i - [\bar{y}_{ik} + \mathrm{j}b_{sh_{ik}}]\bar{V}_k \tag{2.6}$$

Substituting (2.5) in (2.4) yields:

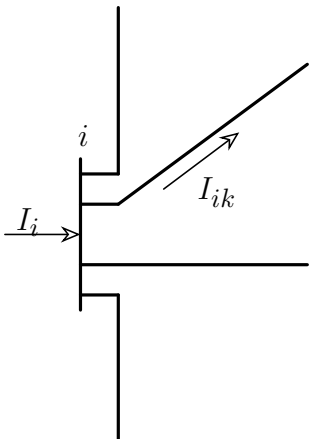

Figure 2.2: Current injection at bus i.

$$\bar{I}_i = [\sum_{k\in\Omega_i} (\bar{y}_{ik} + \mathrm{j}b_{sh_{ik}})]\bar{V}_i + \sum_{k\in\Omega_i} \bar{y}_{ik}\bar{V}_k \tag{2.7}$$

Thus, the current injection at each bus for the whole network can be expressed in the matrix form:

$$\bar{\mathbf{I}} = \bar{\mathbf{Y}}\bar{\mathbf{V}} \tag{2.8}$$

where $\bar{\mathbf{Y}}$ is the bus admittance matrix of size $n_b \times n_b$ expressed by equations (2.9) and (2.10):

$$\bar{Y}_{ii} = \bar{y}_i + \sum_{k\in\Omega_i} \bar{y}_{ik}, \tag{2.9}$$

$$\bar{Y}_{ij} = \bar{Y}_{ji} = -\bar{y}_{ij} \tag{2.10}$$

Thus, the matrix can be represented as:

$$\bar{\mathbf{Y}} = \mathbf{G} + \mathrm{j}\mathbf{B} \tag{2.11}$$

where $\mathbf{G}$ and $\mathbf{B}$ are the bus conductance and susceptance matrices, respectively.

Let $diag$ be an operator that translates a vector into a diagonal matrix or the diagonal elements of a matrix into a vector, and * an operator that indicates the complex conjugate. The vector of complex power injections at the system buses is defined as

$$\bar{\mathbf{S}} = diag(\bar{\mathbf{V}}).(\bar{\mathbf{Y}}\bar{\mathbf{V}})^* \tag{2.12}$$

By combining (2.11) and (2.12), we obtain the vector of apparent bus power:

$$\bar{\mathbf{S}} = \mathbf{f}_P(\mathbf{e},\mathbf{f}) + \mathrm{j}\mathbf{f}_Q(\mathbf{e},\mathbf{f}) \tag{2.13}$$

where f_P and f_Q are the vectors of active and reactive power injections, which are expressed as:

$$\mathbf{f}_P(\mathbf{e},\mathbf{f}) = diag(\mathbf{e})\left[\mathbf{G}\,\mathbf{e} - \mathbf{B}\,\mathbf{f}\right] + diag(\mathbf{f})\left[\mathbf{B}\,\mathbf{e} + \mathbf{G}\,\mathbf{f}\right] \tag{2.14}$$

$$\mathbf{f}_Q(\mathbf{e},\mathbf{f}) = -diag(\mathbf{e})\left[\mathbf{B}\,\mathbf{e} + \mathbf{G}\,\mathbf{f}\right] + diag(\mathbf{f})\left[\mathbf{G}\,\mathbf{e} - \mathbf{B}\,\mathbf{f}\right] \tag{2.15}$$

Therefore, the active and reactive power balance at bus i are expressed by equations (2.16) and (2.17), respectively.

$$P_{G_i} - P_{D_i} - f_{P_i}(\mathbf{e},\mathbf{f}) = 0 \tag{2.16}$$

$$Q_{G_i} - Q_{D_i} - f_{Q_i}(\mathbf{e},\mathbf{f}) = 0 \tag{2.17}$$

where P_{G_i} and Q_{G_i} are the active power and reactive power generation, and P_{D_i} and Q_{D_i} are the active and reactive load at bus i, respectively.

Load flow computational programs use numerical methods to calculate the solutions to (2.16) and (2.17). As the number of variables is larger than the number of equations, some of the variables are specified: voltage magnitudes at generation buses, active power generation at all but one generation bus and the angle of the reference bus, which is set to zero [26]. In rectangular coordinates, the angle at the reference bus (ref) is fixed by imposing $f_{ref} = 0$

2.2.1.2 Active Power Flows over the Lines

The active power flow over line l that connects bus i to bus k is given by:

$$f_{F_l} = \Re\{\bar{V}_i \bar{y}_l^* (\bar{V}_i - \bar{V}_k)^*\} \tag{2.18}$$

The vector containing all the n_l active power flows over the lines can be represented by a matrix expression as follows:

$$\mathbf{f}_F = \Re\{diag(\mathbf{A}_f\mathbf{V})\mathbf{Y}_f^*\mathbf{V}^*\}, \tag{2.19}$$

where the $n_l \times n_b$ bus incident matrix $\mathbf{A}_f$ elements are defined in (2.20), and the $n_l \times n_b$ line admittance matrix $\mathbf{Y}_f$ elements are obtained as shown in (2.21).

$$a_{f_{lj}} = \begin{cases} 1, & \text{if the } l\text{th line starts at bus } j \\ 0, & \text{otherwise} \end{cases}, \tag{2.20}$$

$$\bar{y}_{f_{lj}} = \begin{cases} y_l, & \text{if the } l\text{th line starts at bus } j \\ -y_l, & \text{if the } l\text{th line ends at bus } j \\ 0, & \text{otherwise} \end{cases}, \tag{2.21}$$

By expressing $\bar{V}_i$ and $\bar{V}_k$ in rectangular coordinates the active power flow over line is written:

$$\mathbf{f}_F = diag([\Re\{\mathbf{Y}_f\}(\mathbf{e}\mathbf{e}^\top + \mathbf{f}\mathbf{f}^\top) + \Im\{\mathbf{Y}_f\}(\mathbf{e}\mathbf{f}^\top - \mathbf{e}^\top\mathbf{f})]\mathbf{A}_f^\top) \tag{2.22}$$

For the active power flow in the inverse direction (from bus k to i):

$$\mathbf{f}_T = diag([\Re\{\mathbf{Y}_t\}(\mathbf{e}\mathbf{e}^\top + \mathbf{f}\mathbf{f}^\top) + \Im\{\mathbf{Y}_t\}(\mathbf{e}\mathbf{f}^\top - \mathbf{e}^\top\mathbf{f})]\mathbf{A}_t^\top) \tag{2.23}$$

where $\mathbf{A}_t$ and line admittance matrix $\mathbf{Y}_t$ are analogous to $\mathbf{A}_f$ and $\mathbf{Y}_f$ and are given by (2.24) and (2.25), respectively.

$$a_{t_{lj}} = \begin{cases} 1, & \text{if the } l\text{th line ends at bus } j \\ 0, & \text{otherwise} \end{cases}, \tag{2.24}$$

$$\bar{y}_{t_{lj}} = \begin{cases} -y_l, & \text{if the } l\text{th line starts at bus } j \\ y_l, & \text{if the } l\text{th line ends at bus } j \\ 0, & \text{otherwise} \end{cases} \tag{2.25}$$

2.2.1.3 System Constraints

System constraints either represent physical limits of the components of the system or be defined by operational performance indices, which require, for example, that voltages do not fall above or below given values. Operational constraint can be imposed, in steady state operation, when the system is intact, or if one or more of its components are out of service; taking into consideration the behavior of the system under small or large disturbances.

The optimal secure power dispatch must respect the physical and operational limits of the system. Consider that the subscripts $\min$ and $\max$ indicate the lower and upper limits, respectively. The main constraints imposed in the dispatch are:

- Active and reactive power balance equations for every bus;
- Active and reactive power generation limits, which can be expressed in vector form as
$$\mathbf{P}_{G_{\min}} \leq \mathbf{P}_G \leq \mathbf{P}_{G_{\max}}$$
$$\mathbf{Q}_{G_{\min}} \leq \mathbf{Q}_G \leq \mathbf{Q}_{G_{\max}}$$
where $\mathbf{P}_G$ and $\mathbf{Q}_G$ are $(n_b \times 1)$ vectors of active and reactive generation;
- Upper and lower limits on the voltage magnitude of all buses. For rectangular coordinates, these limits can be expressed by the square of the voltage magnitudes:
$$diag(\mathbf{V}_{\min})\mathbf{V}_{\min} \leq diag(\mathbf{e})\mathbf{e} + diag(\mathbf{f})\mathbf{f} \leq diag(\mathbf{V}_{\max})\mathbf{V}_{\max}$$
- Maximum loading limit of every line, which can be expressed in terms of the current, complex or active power flow over the line. If we limit the active power

flow for all the lines, we have:

$$-\mathbf{F}_{\max} \leq \mathbf{f}_F(\mathbf{e}, \mathbf{f}) \leq \mathbf{F}_{\max}$$
$$-\mathbf{F}_{\max} \leq \mathbf{f}_T(\mathbf{e}, \mathbf{f}) \leq \mathbf{F}_{\max}$$

where $\mathbf{f}_F$ is given by (2.19) and $\mathbf{f}_T$ is given by (2.23).

Other constraints may also be imposed, depending on the characteristics of the system.

Using (2.16) and (2.17), we can express the active and reactive power balance of the system in vector form:

$$\mathbf{P}_G = \mathbf{P}_D + \mathbf{f}_P(\mathbf{e}, \mathbf{f}) \tag{2.26}$$
$$\mathbf{Q}_G = \mathbf{Q}_D + \mathbf{f}_Q(\mathbf{e}, \mathbf{f}) \tag{2.27}$$

Thus, it is possible to rewrite the active and reactive power generation limits as:

$$\mathbf{P}_{G_{\min}} \leq \mathbf{P}_D + \mathbf{f}_P(\mathbf{e}, \mathbf{f}) \leq \mathbf{P}_{G_{\max}} \tag{2.28}$$
$$\mathbf{Q}_{G_{\min}} \leq \mathbf{Q}_D + \mathbf{f}_Q(\mathbf{e}, \mathbf{f}) \leq \mathbf{Q}_{G_{\max}} \tag{2.29}$$

It should be noticed that, for every load bus i, inequalities (2.28) and (2.29) become equalities since, in this case, the active and reactive power generation upper and lower limits are all set to zero. A similar situation occurs when a synchronous condenser (SC) is connected to a bus, as the upper and lower limit of its active power generation are zero.

2.3 OPTIMAL POWER FLOW

The power flow equations are nonlinear, as shown by equations (2.16) and (2.17). Therefore, there are many possibles solutions in a computationally demanding problem. Furthermore, there are also many constraints to take into account, as stated before. One possible way to solve this problem is through the Optimal Power Flow (OPF) algorithms. The algorithms find a solution (i.e. if one exists) that optimizes a given performance criterion and does not violate any constraint. The criterion to be optimized can be chosen according to operational requirements, such as generation cost, active power loss, voltage profile, among others [26]. There are many methods to solve the OPF problem, however traditional methods usually only solve for local solutions [28].

Considering the set of constraints that must be respected in steady state operation, in rectangular coordinates, the OPF problem can be expressed as:

$$\begin{aligned}
\min_{\mathbf{e},\mathbf{f}} \quad & f_c(\mathbf{e},\mathbf{f}) \\
\text{subject to} \quad & P_{G_{i\min}} \leq f_{P_i}(\mathbf{e},\mathbf{f}) \leq P_{G_{i\max}},\ \forall i \in \mathcal{N} \\
& Q_{G_{i\min}} \leq f_{Q_i}(\mathbf{e},\mathbf{f}) \leq Q_{G_{i\max}}, \forall i \in \mathcal{N} \\
& V_{i_{\min}}^2 \leq f_{V_i}(e_i,f_i) \leq V_{i_{\max}}^2,\ \ \forall i \in \mathcal{N} \\
& |f_{F_l}(\mathbf{e},\mathbf{f})| \leq F_{l_{\max}}, \qquad \forall l \in \mathcal{L} \\
& |f_{T_l}(\mathbf{e},\mathbf{f})| \leq F_{l_{\max}}, \qquad \forall l \in \mathcal{L} \\
& f_{ref} = 0
\end{aligned} \tag{2.30}$$

where $f_c(\mathbf{e},\mathbf{f})$ is the objective function, and

$$f_{V_i}(e_i,f_i) = e_i^2 + f_i^2 \tag{2.31}$$

For $\mathbf{x} = [\mathbf{e}^\top, \mathbf{f}^\top]^\top$, the OPF problem can be expressed, in compact form, as:

$$\begin{aligned}
\min_{\mathbf{x}} \quad & f_c(\mathbf{x}) \\
\text{subject to} \quad & \mathbf{g}(\mathbf{x}) \leq \mathbf{c}
\end{aligned} \tag{2.32}$$

where,

$$\begin{aligned}
\mathbf{g} = [\mathbf{f}_P^\top, -\mathbf{f}_P^\top, \mathbf{f}_Q^\top, -\mathbf{f}_Q^\top, \mathbf{f}_V^\top, -\mathbf{f}_V^\top, \mathbf{f}_F^\top, -\mathbf{f}_F^\top, \mathbf{f}_T^\top, -\mathbf{f}_T^\top, \mathbf{f}_{ref}^\top, \\
-\mathbf{f}_{ref}^\top]^\top,
\end{aligned} \tag{2.33}$$

$$\begin{aligned}
\mathbf{c} = [\mathbf{P}_{G_{\max}}^\top, -\mathbf{P}_{G_{\min}}^\top, \mathbf{Q}_{G_{\max}}^\top, -\mathbf{Q}_{G_{\min}}^\top, \mathbf{V}_{\max}^{2^\top}, -\mathbf{V}_{\min}^{2^\top}, \mathbf{F}_{\max}^\top, \\
-\mathbf{F}_{\max}^\top, \mathbf{F}_{\max}^\top, -\mathbf{F}_{\max}^\top, \mathbf{0}, \mathbf{0}]^\top.
\end{aligned} \tag{2.34}$$

2.3.1 Linearized Load Flow Equations

A linear expression can be derived for the active power flow f_{F_l} by making the following suppositions [26]:

- the angular difference between bus i and k is small, thus $sin(\delta_i - \delta_k) \approx \delta_i - \delta_k$ in radians;
- reactive power balance equations are satisfied in all the buses;
- bus voltage magnitudes are equal to the nominal values;
- the series resistances of the lines are considerably smaller than the series reactance. Thus, they can be neglected.

Using the previous simplifications the active power flow over line $l = (i,k)$ is expressed as:

$$f_{F_l} = \frac{1}{x_{ik}}(\delta_i - \delta_k) \tag{2.35}$$

where δ_i and δ_k are the voltage angles at bus i and k, respectively.

The active power injected at bus i is, therefore:

$$P_i = \sum_{k=1}^{n_b} \frac{1}{x_{ik}}(\delta_i - \delta_k) \tag{2.36}$$

Using (2.36), we can express the active power injections in all the buses in vector form as:

$$\mathbf{P} = \mathbf{B}_\delta \boldsymbol{\delta} \tag{2.37}$$

where $\boldsymbol{\delta}$ is the vector of voltage angle, and the components of the DC load flow admittance matrix, $\mathbf{B}_\delta$, are defined as

$$\begin{array}{l} B_{\delta_{ik}} = -\frac{1}{x_{ik}}, \\ B_{\delta_{ii}} = \sum_{k=1}^{n_b} \frac{1}{x_{ik}} \end{array} \tag{2.38}$$

Using (2.37), the active power balance in the system can be expressed, in vector form, as:

$$\mathbf{P}_G - \mathbf{P}_D = \mathbf{B}_\delta \boldsymbol{\delta} \tag{2.39}$$

In vector form, the active power flows over all the lines in the system can be expressed as:

$$\mathbf{f}_F = \boldsymbol{\Gamma} \mathbf{A}_{inc}^\top \boldsymbol{\delta} \tag{2.40}$$

where $\mathbf{A}_{inc}$ is the $n_b \times n_l$ bus-line incidence matrix and $\boldsymbol{\Gamma}$ is a $n_l \times n_l$ diagonal matrix whose elements are the series susceptances of the lines.

Choose a reference bus in the system and set $\delta_{ref} = 0$. As, in the DC model, transmission losses are not taken into consideration, the power provided by $P_{G_{ref}}$ can be written in terms of the P_{G_i}, for $i \neq ref$. Thus, we can eliminate one equation in (2.37). As one component of δ is fixed, the resulting linear system has $n_b - 1$ equations and unknowns. Let $\hat{\mathbf{P}}_G$ and $\hat{\mathbf{P}}_D$ be the vectors of power generation load, $\hat{\mathbf{B}}_\delta$ the DC load flow admittance matrix after eliminating the row and column of the reference bus and, $\hat{\mathbf{A}}_{inc}$ be the $n_b - 1 \times n_l$ matrix obtained by eliminating the row in $\mathbf{A}_{inc}$ associated with the reference bus. $\hat{\mathbf{B}}_\delta$ is invertible. Therefore, we can rewrite equation (2.40) as:

$$\mathbf{f}_F = \boldsymbol{\Gamma} \hat{\mathbf{A}}_{inc}^\top \hat{\mathbf{B}_\delta}^{-1} (\hat{\mathbf{P}}_G - \hat{\mathbf{P}}_D) \tag{2.41}$$

As the generation units have upper and lower output limits and transmission lines have maximum loading limits, power dispatch in the system should respect the following inequalities:

$$\hat{\mathbf{P}}_{G_{\min}} \leq \hat{\mathbf{P}}_G \leq \hat{\mathbf{P}}_{G_{\max}} \tag{2.42}$$

$$|\mathbf{f}_F| \leq \mathbf{f}_{\max} \tag{2.43}$$

Combining equations (2.41) and (2.43), we obtain the following inequalities:

$$-\mathbf{f}^{\max} \leq \mathbf{\Gamma}\hat{\mathbf{A}}_{inc}^{\top}\hat{\mathbf{B}_{\delta}}^{-1}(\hat{\mathbf{P}}_G - \hat{\mathbf{P}}_D) \leq \mathbf{f}^{\max} \tag{2.44}$$

As all the limits that must be respected in the power dispatch are expressed in terms of the vector of active power generation, P_G, the DC optimal power flow can be written, in compact form, as:

$$\begin{aligned} \min_{\mathbf{P}_G} \quad & f_c \\ \text{subject to} \quad & \mathbf{A}_{\delta}\hat{\mathbf{P}}_G \leq \mathbf{c}_{\delta} \end{aligned} \tag{2.45}$$

where

$$\mathbf{A}_{\delta} = \begin{bmatrix} -\mathbf{u}^{\top} \\ \mathbf{u}^{\top} \\ \mathbf{I} \\ -\mathbf{I} \\ \mathbf{\Gamma}\hat{\mathbf{A}}_{inc}^{\top}\hat{\mathbf{B}_{\delta}}^{-1} \\ -\mathbf{\Gamma}\hat{\mathbf{A}}_{inc}^{\top}\hat{\mathbf{B}_{\delta}}^{-1} \end{bmatrix}, \tag{2.46}$$

$$\mathbf{c}_{\delta} = \begin{bmatrix} P_{G_{\max_{ref}}} - \mathbf{u}^{\top}\hat{\mathbf{P}}_D \\ -P_{G_{\min_{ref}}} + \mathbf{u}^{\top}\hat{\mathbf{P}}_D \\ \hat{\mathbf{P}}_{G_{\max}} \\ -\hat{\mathbf{P}}_{G_{\min}} \\ \mathbf{f}^{\max} + \mathbf{\Gamma}\hat{\mathbf{A}}_{inc}^{\top}\hat{\mathbf{B}_{\delta}}^{-1}\hat{\mathbf{P}}_D \\ \mathbf{f}^{\max} - \mathbf{\Gamma}\hat{\mathbf{A}}_{inc}^{\top}\hat{\mathbf{B}_{\delta}}^{-1}\hat{\mathbf{P}}_D \end{bmatrix} \tag{2.47}$$

$\mathbf{I}$ is a $(n_b - 1) \times (n_b - 1)$ identity matrix, and $\mathbf{u}$ is a $(n_b - 1) \times 1$ unit vector. The first two constraints of (2.45) are the generation limits for the slack bus.

In a secure operating strategy, the previous limits should be respected for the intact system (i.e., in the original configuration) and in a set configurations described by credible contingencies. Each contingency leads to a particular system topology, for which we have different vectors $\mathbf{P}_G$, $\mathbf{P}_D$ and $\boldsymbol{\delta}$ and a different matrix $\mathbf{B}_{\delta}$. However the previous equations remain valid.

2.4 SCOPF FORMULATION

As an extension of the OPF problem, the Security Constrained Optimal Power Flow (SCOPF) problem takes into account the pre-contingency and post-contingency constraints. It is a nonlinear, noncovex, and a large-scale optimization problem. The SCOPF main objective is to optimize a cost function (F_c) by using available control means, while respecting equality and inequality constraints [29].

In this study, the SCOPF problem takes into consideration all the limits described in the previous section for a set of contingent states, $\mathcal{K}$. Let $k = 0, 1, ...n_c$, be the states in $\mathcal{K}$, where $k = 0$ is the no-contingency state. If a state k makes the problem unfeasible, it is disregarded. To each state k is associated a set of operational constraints, that is, a

set of power balance equations and a set of limits. This is due to the fact that the vectors $\mathbf{P}_G$ and $\mathbf{Q}_G$ and, the admittance matrix $\mathbf{Y}$ change for each state k. A superscript $^{(k)}$ is used to indicates which state an optimization variable is associated to.

Two different control strategies can be adopted when formulating the SCOPF [18]:

Preventive control: the optimal dispatch should respect all the system limits in all contingent states without resorting to corrective actions.

Corrective Control: the optimal dispatch takes into consideration that corrective actions can be carried out after contingencies. The amplitude of these corrections is pre-specified.

The SCOPF formulation adopted in the present study is built using the corrective control strategy. It is supposed that active and reactive power generation may be corrected after contingencies.

Let the vectors of variables of the problem be $\mathbf{e}$ and $\mathbf{f}$ with $\mathbf{e} = [(\mathbf{e}^0)^\top, \ldots, (\mathbf{e}^{(n_c)})^\top]^\top$ and $\mathbf{f} = [(\mathbf{f}^{(0)})^\top, \ldots, (\mathbf{f}^{(n_c)})^\top]^\top$. Thus, the vector of variables is $\mathbf{x} = \left[\mathbf{e}^\top, \mathbf{f}^\top\right]^\top$. The cost function F_c is the sum of the same optimization criterion (f_c) for each state k considered. Also, consider that generation outputs at selected buses $\mathcal{S} \subseteq \mathcal{G}$ can be adjusted after each contingency in order to maintain a secure operation. The problem can be written as

$$
\begin{aligned}
\min_{e,f} \quad & F_c = \textstyle\sum_{k=0}^{n_c} f_c(\mathbf{x})^{(k)} \\
\text{subject to} \quad & P_{G_{i\min}}^{(k)} \leq f_{P_i}^{(k)} \leq P_{G_{i\max}}^{(k)}, \forall k \in \mathcal{K}, \forall i \in \mathcal{N} \\
& Q_{G_{i\min}}^{(k)} \leq f_{Q_i}^{(k)} \leq Q_{G_{i\max}}^{(k)}, \forall k \in \mathcal{K}, \forall i \in \mathcal{N} \\
& V_{i_{\min}}^{(k)^2} \leq f_{V_i}^{(k)} \leq V_{i_{\max}}^{(k)^2}, \quad \forall k \in \mathcal{K}, \forall i \in \mathcal{N} \\
& |f_{F_l}^{(k)}| \leq F_{l_{\max}}^{(k)}, \qquad \forall k \in \mathcal{K}, \forall l \in \mathcal{L} \\
& |f_{T_l}^{(k)}| \leq F_{l_{\max}}^{(k)}, \qquad \forall k \in \mathcal{K}, \forall l \in \mathcal{L} \\
& |f_{S_{P_i}}^{(k)}| \leq \Delta P_{i_{\max}}^{(k)}, \qquad \forall k \in \mathcal{K}, \forall i \in \mathcal{S} \\
& |f_{S_{Q_i}}^{(k)}| \leq \Delta Q_{i_{\max}}^{(k)}, \qquad \forall k \in \mathcal{K}, \forall i \in \mathcal{S} \\
& f_{ref}^{(k)} = 0 \qquad \forall k \in \mathcal{K} \quad \text{(reference)}
\end{aligned}
\tag{2.48}
$$

where,

$$
\begin{aligned}
f_{P_i}^{(k)} &= e_i^{(k)} \left[\sum_{j=1}^{n_b} \left(G_{ij}^{(k)} e_j^{(k)} - B_{ij}^{(k)} f_j^{(k)} \right) \right] + f_i^{(k)} \left[\sum_{j=1}^{n_b} \left(G_{ij}^{(k)} f_j^{(k)} + B_{ij}^{(k)} e_j^{(k)} \right) \right], \\
f_{Q_i}^{(k)} &= f_i^{(k)} \left[\sum_{j=1}^{n_b} \left(G_{ij}^{(k)} e_j^{(k)} - B_{ij}^{(k)} f_j^{(k)} \right) \right] + e_i^{(k)} \left[\sum_{j=1}^{n_b} \left(G_{ij}^{(k)} f_j^{(k)} + B_{ij}^{(k)} e_j^{(k)} \right) \right], \\
f_{V_i}^{(k)} &= e_i^{(k)^2} + f_i^{(k)^2}, \\
\mathbf{f}_{F_l}^{(k)} &= g_l^{(k)} \left(e_i^{(k)^2} + f_i^{(k)^2} - e_i^{(k)} e_j^{(k)} - f_i^{(k)} f_j^{(k)} \right) + b_l^{(k)} \left(e_i^{(k)} f_j^{(k)} - e_j^{(k)} f_i^{(k)} \right), \\
\mathbf{f}_{T_l}^{(k)} &= g_l^{(k)} \left(e_j^{(k)^2} + f_j^{(k)^2} - e_j^{(k)} e_i^{(k)} - f_j^{(k)} f_i^{(k)} \right) + b_l^{(k)} \left(e_j^{(k)} f_i^{(k)} - e_i^{(k)} f_j^{(k)} \right), \\
f_{ref}^{(k)} &= f_1^{(k)},
\end{aligned}
$$

the coupling constraints,

$$
\begin{aligned}
f_{S_{P_i}}^{(k)} &= f_{P_i}^{(0)} - f_{P_i}^{(k)}, \\
f_{S_{Q_i}}^{(k)} &= f_{Q_i}^{(0)} - f_{Q_i}^{(k)},
\end{aligned}
$$

$f_{P_i}^{(k)}$ and $f_{Q_i}^{(k)}$ are the active and reactive power injection at bus i and state k, respectively. These injections are expressed in terms of the components of the bus admittance matrix of the system in the contingency state k, $\mathbf{Y}^{(k)} = \mathbf{G}^{(k)} + \mathrm{j}\mathbf{B}^{(k)}$; $f_{F_l m}^{(k)}$ is the active power flow at line l and state k; $f_{V_i}^{(k)}$ is the bus i squared voltage magnitude at state k; and $f_{S_{P_i}}^{(k)}$ and $f_{S_{Q_i}}^{(k)}$ are, respectively, the variations in active and reactive power generation at the buses in $\mathcal{S}$ between the no-contingency state and state k.

The upper and lower limits imposed to $f_{P_i}^{(k)}$ and $f_{Q_i}^{(k)}$ can vary according to the system state and depend on the characteristics of the bus (i.e., whether this is a load, a SC or generation bus). The upper and lower limits for $f_{F_l}^{(k)}$ and $f_{T_l}^{(k)}$ are usually the same magnitude and varies accordingly to operational requirements. $\Delta P_{i_{\max}}^{(k)}$ and $\Delta Q_{i_{\max}}^{(k)}$ are, respectively, the maximum corrections allowed in the active and reactive power generation between the no-contingency state and state k.

Similarly to problem (2.32), the compact notation is also used. Define vectors $\mathbf{f}_P^\top = \left[f_{P_1}^{(0)}, ..., f_{P_{nb}}^{(n_c)} \right]$, $\mathbf{f}_Q^\top = \left[f_{Q_1}^{(0)}, ..., f_{Q_{nb}}^{(n_c)} \right]$, $\mathbf{f}_V^\top = \left[f_{V_1}^{(0)}, ..., f_{V_{nb}}^{(n_c)} \right]$, $\mathbf{f}_{S_{P_S}}^\top = \left[f_{S_{P_1}}^{(1)}, ..., S_{P_{nb}}^{(n_c)} \right]$ and $\mathbf{f}_{S_Q}^\top = \left[f_{S_{Q_1}}^{(1)}, ..., f_{S_{Q_{nb}}}^{(n_c)} \right]$, vectors of upper and lower generation limits, $\mathbf{P}_{G_{\max}}$, $\mathbf{P}_{G_{\min}}$, $\mathbf{Q}_{G_{\max}}$, $\mathbf{Q}_{G_{\min}}$, upper and lower voltage limits, $\mathbf{V}_{\max}$, $\mathbf{V}_{\min}$, line loading limits $\mathbf{P}_{F_{\max}}$, maximum and minimum active and reactive power adjustments $\Delta\mathbf{P}_{\max}$, $\Delta\mathbf{P}_{\min}$, $\Delta\mathbf{Q}_{\max}$, $\Delta\mathbf{Q}_{\min}$ and vector of the imaginary components of the voltage at the reference bus, $\mathbf{f}_{ref} = \left[f_{ref}^{(0)}, \ldots, f_{ref}^{(n_c)} \right]$. Thus, problem (2.48) can be rewritten as:

$$
\begin{aligned}
\min_{\mathbf{x}} \quad & f_c(\mathbf{x}) \\
\text{subject to} \quad & \mathbf{g}(\mathbf{x}) \leq \mathbf{c}
\end{aligned}
\tag{2.49}
$$

where the vectors function $\mathbf{g}$ and $\mathbf{c}$ are declared by equations (2.50) and (2.51), respectively.

$$\begin{aligned}\mathbf{g} = [&\mathbf{f}_P^\top, -\mathbf{f}_P^\top, \mathbf{f}_Q^\top, -\mathbf{f}_Q^\top, \mathbf{f}_V^\top, -\mathbf{f}_V^\top, \mathbf{f}_F^\top, -\mathbf{f}_F^\top, \mathbf{f}_T^\top, -\mathbf{f}_T^\top, \mathbf{f}_{S_P}^\top, -\mathbf{f}_{S_P}^\top, \mathbf{f}_{S_Q}^\top, \\ &- \mathbf{f}_{S_Q}^\top, \mathbf{f}_{ref}^\top, -\mathbf{f}_{ref}^\top]^\top, \end{aligned} \tag{2.50}$$

$$\begin{aligned}\mathbf{c} = [&\mathbf{P}_{G_{\max}}^\top, -\mathbf{P}_{G_{\min}}^\top, \mathbf{Q}_{G_{\max}}^\top, -\mathbf{Q}_{G_{\min}}^\top, \mathbf{V}_{\max}^{2^\top}, -\mathbf{V}_{\min}^{2^\top}, \mathbf{F}_{\max}^\top, -\mathbf{F}_{\max}^\top, \\ &\mathbf{F}_{\max}^\top, -\mathbf{F}_{\max}^\top, \Delta\mathbf{P}_{\max}^\top, -\Delta\mathbf{P}_{\max}^\top, \Delta\mathbf{Q}_{\max}^\top, -\Delta\mathbf{Q}_{\max}^\top, \mathbf{0}, \mathbf{0}]^\top \end{aligned} \tag{2.51}$$

Therefore, the number of constraints (J_{AC}) of (2.49) is:

$$J_{AC} = 2(n_c + 1)(2n_g + n_b + 2n_l) + 4n_c(n_g - 1) \tag{2.52}$$

2.4.1 SCOPF Linearization

The security constrained linear optimal power flow problem (SC-LOPF) can be expressed as

$$\begin{aligned} \min \quad & c(\hat{\mathbf{P}}_g) \\ \text{subject to} \quad & \hat{\mathbf{A}}_\delta \, \hat{\mathbf{P}}_g \leq \hat{\mathbf{c}}_\delta \end{aligned} \tag{2.53}$$

where $c(\cdot)$ is the total generation cost, $\hat{\mathbf{A}}_\delta$ is the expanded $\mathbf{A}_\delta$ to accommodate all contingency states variables and the security constraints considered, $\hat{\mathbf{c}}_\delta$ is he expanded vector of limits, and $\hat{\mathbf{P}}_g = [\hat{\mathbf{P}}_g^{(0)^\top}, \hat{\mathbf{P}}_g^{(1)^\top}, \ldots, \hat{\mathbf{P}}_g^{(n_c)^\top}]^\top$. The superscript $(\cdot)$ denotes the contingency state associated to the variable. The security constraints used in this study are:

$$S_{P_i}^{(k)} = P_{G_i}^{(0)} - P_{G_i}^{(k)} \tag{2.54}$$

Taking into consideration every constraint of (2.53) associated to a load bus reduces to an equality (as $P_{G_{i\max}}^{(k)} = P_{G_{i\min}}^{(k)}$), the number of constraints in this problem is

$$J_{DC} = 2(n_g + 1)(n_g + n_l) + 2n_c(n_g - 1) \tag{2.55}$$

2.5 CONCLUSION

This chapter introduced the SCOPF and the linearized secure optimal power flow problems used in this work. The latter has linear constraints. Thus, it is possible through the umbrella discovery algorithm proposed in [4] to identify the constraints that define its feasible set. This algorithm it will be introduced in Chapter 3.

However, as the SCOPF is a non-covex problem, it is not possible to use known algorithms to identify its umbrella constraints. Thus, the following Chapter introduces a possible approach to have a an approximate representation of the power system in steady-state operation with linear constraints by the use of semidefinite programming.

3 SEMIDEFINITE PROGRAMMING

3.1 INTRODUCTION

When solving a nonconvex optimization problem, classical algorithms may not obtain the global optimal solution since they converge to generic stationary points. Semidefinite programming (SDP) defines, in a higher dimension space, a convex problem whose optimal solution is close to the global optimum of the original problem. For this reason, SDP can be used to obtain near global optimal solutions.

Nevertheless, there are setbacks regarding this approach. Mainly the increase in the number of variables and the relaxation of the problem's feasible set. Some strategies to mitigate these problems are discussed in Chapter 4.

3.2 PRELIMINARY NOTIONS

3.2.1 Linear Programming

A linear programming optimization problem (LP) can be represented in the primal standard form [30]:

$$\begin{array}{ll} \min\limits_{\mathbf{x}} & \mathbf{c}^\top \mathbf{x} \\ \text{subject to} & \mathbf{A}\mathbf{x} = \mathbf{b}, \\ & \mathbf{x} \geq 0, \end{array} \tag{3.1}$$

where $\mathbf{x}$ and $\mathbf{c}$ are $n \times 1$ vectors, $\mathbf{A}$ is a $m \times n$ matrix, and $\mathbf{b}$ is a $m \times 1$ scalar vector.

Let $\mathbf{a}_i^\top$ be the ith line of matrix $\mathbf{A}$, and b_i the ith element of vector $\mathbf{b}$. Consider a inequality constraint $\mathbf{a}_i^\top \mathbf{x} \leq b_i$. The inequality can become an equality constraint, and thus be incorporated into the standard problem (3.1), by introducing a new variable, also know as slack variable:

$$\begin{aligned} \mathbf{a}_i^\top \mathbf{x} + s &= b_i \\ s &\geq 0 \end{aligned}$$

Thus, we can conclude that any linear problem can be manipulated to fit the standard form (3.1).

Let $\boldsymbol{\lambda}$ be the Lagrangian multiplier vector. As such, we can conclude the dual problem of (3.1) is:

$$\begin{array}{ll} \max & \boldsymbol{\lambda}^\top \mathbf{b} \\ \text{subject to} & \mathbf{A}^\top \boldsymbol{\lambda} \leq \mathbf{c}^\top. \end{array} \tag{3.2}$$

The dual problem provides a lower bound for the optimal cost. Therefore, if $\mathbf{x}^\star$ is a feasible solution to the primal problem, and $\boldsymbol{\lambda}^\star$ is a feasible solution for the dual problem, then $\boldsymbol{\lambda}^{\star\top} \mathbf{b} \leq \mathbf{c}^\top \mathbf{x}^\star$. This is also know as weak duality. As an extension of this, if $\boldsymbol{\lambda}^\top \mathbf{b} = \mathbf{c}^\top \mathbf{x}^\star$, then $\mathbf{x}^\star$ and $\boldsymbol{\lambda}^\star$ are optimal solutions to the primal and dual problems, respectively. The strong duality implies that if a linear problem has an optimal solution, its dual is also feasible. Furthermore, their respective optimal costs are equal [30].

3.2.2 Polynomial problems and SDP

Polynomial problems are present in many technical fields. As such, there are well established tools to solve them. Usually an optimization algorithm searches for a locally or globally solution; it solves for complex or real number; and it can use a numerical or symbolic method [31]. The use of semidefinite programming to obtain a relaxed solution to a nonconvex quadratic problem was firstly proposed by Shor [7]. By doing so, a convex problem is solved. Due to the relaxation, the optimal solution is equal or lower to the original's.

To better demonstrate this relaxation, consider the following $2d$-degree real-valued polynomial [32]:

$$p(\mathbf{x}) = \sum_{\alpha} p_\alpha x^\alpha \tag{3.3}$$

where $\alpha \coloneqq \{\alpha_1\alpha_2\cdots\alpha_n \,|\, \alpha \in \mathbb{N}^n\}$, $x_\alpha \coloneqq x_1^{\alpha_1}x_2^{\alpha_2}\cdots x_n^{\alpha_n}$, $\sum_i \alpha_i \leq 2d$, and p is the coefficient vector of $p(\mathbf{x})$ in the basis

$$1, x_1, x_2, \ldots, x_n, x_1^2, x_1x_2, \ldots, x_1x_n, x_2x_3, \ldots, x_n^2, \ldots, x_1^m, \ldots, x_n^m \tag{3.4}$$

Let the quadratic polynomial $p(\mathbf{x}) = (x_1 - 1)^2 + x_2^2$, or its equivalent is $p(\mathbf{x}) = 1 - 2x_1 + x_1^2 + x_2^2$. This can also be written as $p(\mathbf{x}) = 1x_1^0x_2^0 - 2x_1^1x_2^0 + x_1^2x_2^0 + x_1^0x_2^2$. The basis is $1, x_1, x_2, x_1^2, x_1x_2, x_2^2$. There are two exponents, α_1 and α_2 that can be equal to 0, 1 or 2, provided that $\alpha_1 + \alpha_2 \leq 2$. The coefficients of the polynomial are: for $\alpha_1 = \alpha_2 = 0 \implies \alpha = \{00\}, p_\alpha = p_{00}$; for $\alpha_1 = 1$ and $\alpha_2 = 0 \implies \alpha = \{10\}, p_\alpha = p_{10}$; for $\alpha_1 = 0$ and $\alpha_2 = 1 \implies \alpha = \{01\}, p_\alpha = p_{01}$; for $\alpha_1 = 2$ and $\alpha_2 = 0 \implies \alpha = \{20\}, p_\alpha = p_{20}$; for $\alpha_1 = 1$ and $\alpha_2 = 1 \implies \alpha = \{11\}, p_\alpha = p_{11}$; for $\alpha_1 = 0$ and $\alpha_2 = 2 \implies \alpha = \{02\}, p_\alpha = p_{02}$. Thus, $p = [p_{00}, p_{10}, p_{01}, p_{20}, p_{11}, p_{02}] = [1, -2, 0, 1, 0, 1]$. Finally the polynomial becomes:

$$p(\mathbf{x}) = p_{00}x^{00} + p_{10}x^{10} + p_{20}x^{20} + p_{02}x^{02} \tag{3.5}$$

The basic idea of the moment method is to substitute the monomials x^α with the scalar variable y_α (also called lifting variable). Thus, in the 'lifted space' polynomial (3.5) becomes linear:

$$p(\mathbf{y}) = p_{00}y_{00} + p_{20}y_{20} + p_{10}y_{10} + p_{02}y_{02} \tag{3.6}$$

Let $\mathbf{x} = [1, x_1, x_2, \ldots, x_n]^\top$ and $\mathbf{y}$ be the vector of lifting variables. The vector $\mathbf{y}$ is composed by variables that substituted the monomials in $\mathbf{x}$, and the number of components in $\mathbf{y}$ is $\binom{n+2d}{2d}$ for a polynomial of degree $2d$. For polynomial (3.5), its degree is $2d = 2$ with 2 variables (i.e. quadratic). Thus, $\binom{2+2}{2} = 6$. This shows an increase in the number of variables of the linearized equation.

Consider then the optimization problem:

$$\begin{array}{ll} \max\limits_{\mathbf{x}} & p(\mathbf{x}) \\ \text{subject to} & \mathbf{x} \geq 0. \end{array} \tag{3.7}$$

A relaxed solution to (3.7) can be obtained by solving the primal SDP problem [33]:

$$\begin{array}{ll} \max\limits_{\mathbf{X}} & \mathbf{C} \bullet \mathbf{X} \\ \text{subject to} & \mathbf{X} \succeq 0. \end{array} \tag{3.8}$$

where $\bullet$ is the inner product; $\succeq$ indicates positive semidefiniteness, that is $\mathbf{z}^\top \mathbf{X}\mathbf{z} \geq 0, \forall \mathbf{z} \in \mathbb{R}^n$; $\mathbf{C}$ is a constant symmetric matrix, and the symmetric matrix $\mathbf{X}$ is defined as:

$$\mathbf{X} = \mathbf{x}\mathbf{x}^\top = \begin{bmatrix} 1 & x_1 & \cdots & x_n \\ x_1 & x_1^2 & \cdots & x_1 x_n \\ \vdots & & \ddots & \\ x_n & x_1 x_n & \cdots & x_n^2 \end{bmatrix}. \tag{3.9}$$

The SDP relaxation (3.8) leads to a lower bound on the optimal cost of the original problem (3.7).

Notice that the only constraint in (3.7) limits the feasible solutions only to the nonnegative orthant. While, for the SDP equivalent (3.8), the constraint limits the feasible solutions to a convex closed cone K. The constraint in (3.8) can be enforced using the Sylvester's criterion for positive-semidefinite Hermitian matrices, i.e. the principal minor test.

If problem (3.7) has equality constraints, its relaxed SDP problem is written:

$$\begin{array}{ll} \max\limits_{\mathbf{X}} & \mathbf{C} \bullet \mathbf{X} \\ \text{subject to} & \\ & \mathbf{A}_j \bullet \mathbf{X} = b_j, j = 1, \ldots, J \\ & \mathbf{X} \succeq 0. \end{array} \tag{3.10}$$

where J is the number of constraints, b_j is the jth element of the fixed scalar column vector $\mathbf{b}$, and the sparse symmetric matrices $\mathbf{A}_j$ is the constant matrices for the constraints.

The optimal value of X can be more easily obtained by solving the dual SDP problem, which is expressed as follows [34]:

$$\begin{array}{ll} \min\limits_{\mathbf{X}} & \sum_{j=1}^{J} y_j b_j \\ \text{subject to} & \\ & \mathbf{C} - \sum_{j=1}^{J} y_j \mathbf{A}_j \succeq 0 \end{array} \tag{3.11}$$

Let the duality gap be $\mathbf{C} \bullet \mathbf{X} - \sum_{j=1}^{J} y_j b_j$. When solving for OPF SDP problem, if the duality gap is zero, then the SDP relaxation is exact. Moreover, if the duality gap is zero, then $\mathbf{X}$ is rank-one and the the optimal value of the objective function of the SDP problem is equal to the optimal values of $p(\mathbf{x})$ in (3.7) [35].

From (3.1) and (3.11), it is clear that the linear problem is a particular case of SDP. The linear problem can, therefore, be written as:

$$\begin{array}{lll} & \text{LP} & \\ \min & \sum_i^n c_i x_i & \\ \text{s.t.} & \sum_i^n a_{ji} x_i = b_j & \\ & \mathbf{x} \geq 0 & \\ & \text{for all } j & \end{array} \quad \Longrightarrow \quad \begin{array}{ll} & \text{SDP} \\ \min & \mathbf{C} \bullet \mathbf{X} \\ \text{s.t.} & \mathbf{A}_j \bullet \mathbf{X} = 0 \\ & \mathbf{X} \succeq 0 \\ & \text{for all } j \end{array} \tag{3.12}$$

where,

$$\mathbf{C} = \begin{bmatrix} c_0 & \frac{1}{2}c_1 & \cdots & \frac{1}{2}c_n \\ \frac{1}{2}c_1 & 0 & \cdots & 0 \\ \vdots & \vdots & \ddots & \vdots \\ \frac{1}{2}c_n & 0 & \cdots & 0 \end{bmatrix}, \quad \mathbf{A}_j = \begin{bmatrix} -b_j & \frac{1}{2}a_{j1} & \cdots & \frac{1}{2}a_{jn} \\ \frac{1}{2}a_{j1} & 0 & \cdots & 0 \\ \vdots & \vdots & \ddots & \vdots \\ \frac{1}{2}a_{jn} & 0 & & 0 \end{bmatrix}, \tag{3.13}$$

and

$$\mathbf{X} = \begin{bmatrix} 1 & x_1 & \cdots & x_n \\ x_1 & 0 & \cdots & 0 \\ \vdots & & \ddots & \vdots \\ x_n & 0 & \cdots & 0 \end{bmatrix}. \tag{3.14}$$

However, it is not desirable to convert a linear programming problem into an SDP, as it can be more efficiently solved in the original form.

3.3 POLYNOMIAL OPTIMIZATION PROBLEMS THROUGH SEMIDEFINITE PROGRAMMING

3.3.1 Sum of Squares

In this section, we demonstrate the relationship between nonnegative polynomials, sum of squares (SOS) and SDP. The main takeaway is that an SOS decomposition of a polynomial can be obtained by the use of SDP. Therefore, an SOS program is equivalent to SDP. An SOS program can be defined as a conic optimization problem and it can be written as:

$$\begin{array}{ll} \max\limits_{\mathbf{y}} & \sum_{j=1}^n y_j b_j \\ \text{subject to} & p_i(x;y) \text{ are SOS in } \mathbb{R}[x], \quad i = 1, \ldots, k, \end{array} \tag{3.15}$$

where $p_i(x;y) \coloneqq c_i(x) + a_{i1}(x)y_1 + \ldots + a_{in}(x)y_n$, and c_i and a_{ij} are given multivariate polynomials in $\mathbb{R}[x]$. One example of a SOS program is:

$$\begin{array}{ll} \max\limits_{\mathbf{y}} & y_1 + y_2 \\ \text{subject to} & x^4 + y_1 x + (2 + y_2) \text{ is SOS,} \\ & (y_1 - y_2 + 1)x^2 + y_2 x + 1 \text{ is SOS.} \end{array} \tag{3.16}$$

Consider an SOS constraint in (3.15). It implies that the polynomial $p_i(x;y)$ is nonnegative. This is true for all nonnegative polynomials. However, not all nonnegative polynomials are SOS [36].

A SOS polynomial $p(\mathbf{x})$ can be written as:

$$p(\mathbf{x}) = \sum_k q_k^2(\mathbf{x}) \geq 0,\ \mathbf{x} \in \mathbb{R}^2, \tag{3.17}$$

Another sufficient condition for nonnegativity is by using SDP. Let $p(x_1, \ldots, x_n)$ be a polynomial of degree $2d$, and the vector of monomials $[x]_d$ of size $\binom{n+d}{d}$. Therefore, $p(\mathbf{x})$ is SOS if and only if:

$$p(\mathbf{x}) = [x]_d^\top \mathbf{Q} [x]_d, \quad \mathbf{Q} \succeq 0. \tag{3.18}$$

where the rank of $\mathbf{Q}$ is equal to the number of squares (q_k).

The condition in (3.18) can be seen as an SDP, where in its primal form we have $[x]_d^\top \mathbf{Q} [x]_d = \mathbf{Q} \bullet \mathbf{X}$. As an example, consider the univariate polynomial [36]:

$$p(x) = x^4 + 4x^3 + 6x^2 + 4x + 5 \tag{3.19}$$

The polynomial (3.19) has degree $2d = 4$ and one variable ($n = 1$). As such, the vector of monomials has $\binom{1+2}{2} = 3$ components. Let $[x]_d = [1, x, x^2]^\top$. If we solve the condition (3.18) for the polynomial (3.19), we have:

$$\begin{aligned} p(x) = [x]_d^\top \mathbf{Q} [x]_d &= \begin{bmatrix} 1 \\ x \\ x^2 \end{bmatrix}^T \begin{bmatrix} q_{00} & q_{01} & q_{02} \\ q_{01} & q_{11} & q_{12} \\ q_{02} & q_{12} & q_{22} \end{bmatrix} \begin{bmatrix} 1 \\ x \\ x^2 \end{bmatrix} \\ &= q_{22}x^4 + 2q_{12}x^3 + (q_{11} + 2q_{02})\, x^2 + 2q_{01}x + q_{00} \end{aligned} \tag{3.20}$$

By matching coefficients between (3.19) and (3.20), we obtain the constraints:

$$\begin{aligned} q_{22} &= 1, \\ 2q_{12} &= 4, \\ q_{11} + 2q_{02} &= 6, \\ 2q_{01} &= 4, \\ q_{00} &= 5. \end{aligned}$$

Thus, in the SDP primal form, the matrices are:

$$\mathbf{A}_1 = \begin{bmatrix} 0 & 0 & 0 \\ 0 & 0 & 0 \\ 0 & 0 & 1 \end{bmatrix},$$
$$\mathbf{A}_2 = \begin{bmatrix} 0 & 0 & 0 \\ 0 & 0 & 1 \\ 0 & 1 & 0 \end{bmatrix},$$
$$\mathbf{A}_3 = \begin{bmatrix} 0 & 0 & 1 \\ 0 & 1 & 0 \\ 1 & 0 & 0 \end{bmatrix},$$
$$\mathbf{A}_4 = \begin{bmatrix} 0 & 1 & 0 \\ 1 & 0 & 0 \\ 0 & 0 & 0 \end{bmatrix},$$
$$\mathbf{A}_5 = \begin{bmatrix} 1 & 0 & 0 \\ 0 & 0 & 0 \\ 0 & 0 & 0 \end{bmatrix},$$
$$\mathbf{b} = [1, 4, 6, 4, 5]^\top.$$

Thus, by solving:

$$\begin{aligned} &\mathbf{A}_j \bullet \mathbf{Q} = b_j, \text{for } j = 1, \ldots, 5 \\ &\mathbf{Q} \succeq 0, \end{aligned} \tag{3.21}$$

we have,

$$\mathbf{Q} = \begin{bmatrix} 5 & 2 & 0 \\ 2 & 6 & 2 \\ 0 & 2 & 1 \end{bmatrix}. \tag{3.22}$$

The rank of $\mathbf{Q}$ is 3, so we can expect three squares. One way to extract q_j from the solution is to factorize $\mathbf{Q} = \mathbf{L}^\top \mathbf{L}$. Thus,

$$p(x) = \mathbf{y}^\top \mathbf{L}^\top \mathbf{L}\mathbf{y} = \|\mathbf{L}\mathbf{y}\|^2 = \sum_k (\mathbf{L}\mathbf{y})_k^2 = \sum_k q_k^2$$

By factorizing (3.22), we have:

$$\mathbf{L} = \begin{bmatrix} 0 & 2 & 1 \\ \sqrt{2} & \sqrt{2} & 0 \\ \sqrt{3} & 0 & 0 \end{bmatrix}. \tag{3.23}$$

which translates to $q_1 = y^2 + 2y$, $q_2 = \sqrt{2} + \sqrt{2}y$, and $q_3 = \sqrt{3}$. As such, the polynomial in the SOS decomposition is:

$$p(x) = (y^2 + 2y)^2 + 2(1 + y)^2 + 3.$$

3.3.2 Unconstrained Polynomial Optimization

One application of SOS is in a global optimization algorithm. Therefore, consider an unconstrained optimization problem:

$$\begin{array}{ll} \min\limits_{\mathbf{x}} & p(\mathbf{x}) \\ \text{subject to} & \mathbf{x} \in \mathbb{R}^n, \end{array} \tag{3.24}$$

where $p(\mathbf{x})$ is a generic polynomial, thus it can be nonconvex.

The idea is to approximate the lower bound (γ) to the optimal value for $p(\mathbf{x})$ [36]. As such, problem (3.24) can be described as:

$$\begin{array}{lll} \max & \gamma & \\ \text{s.t.} & p(\mathbf{x}) \geq \gamma & \iff \\ & \mathbf{x} \in \mathbb{R}^n & \end{array} \quad \begin{array}{lll} \max & \gamma & \\ \text{s.t.} & p(\mathbf{x}) - \gamma \geq 0 & \\ & \mathbf{x} \in \mathbb{R}^n & \end{array} \tag{3.25}$$

To obtain the best possible approximation, we can solve this convex optimization problem:

$$\begin{array}{ll} \max & \gamma \\ \text{subject to} & p(\mathbf{x}) - \gamma \geq 0. \end{array} \tag{3.26}$$

However, as seen previously, it is possible to approximate the nonnegative constraint in (3.26) for the condition that $p(\mathbf{x}) - \gamma$ must be SOS. The approximation comes from the fact that not all nonnegative polynomials are SOS. There are only three cases where (3.27) is equal to (3.26): univariate polynomials, and quadratic polynomials, bivariate quartics [36]. As such, (3.26) is can be approximated to:

$$\begin{array}{ll} \max & \gamma \\ \text{subject to} & p(\mathbf{x}) - \gamma \quad \text{is SOS}. \end{array} \tag{3.27}$$

This approach main advantage is that $p(\mathbf{x})$ may be nonconvex, but the convex problem (3.27) computes its global lower limit. When $p(\mathbf{x}) - \gamma$ is SOS, then the global minimum is obtained. Let $\mathbf{x}^\star$ be the global minimum for $p(\mathbf{x})$, and $\mathbf{x}_{sos}$ the optimal value of (3.27). Then, $p(\mathbf{x}_{sos}) \leq p(\mathbf{x}^\star)$.

Furthermore, the constraint "$p(\mathbf{x}) - \gamma \quad$ is SOS" in (3.27) is equivalent to the condition in (3.18). By using this relationship, and considering the univariate polynomial $p(x) = \sum_{k=0}^{2d} p_k x^k$, we can solve (3.27) through the following optimization problem:

$$\begin{array}{ll} \max\limits_{\gamma, \mathbf{Q}} & \gamma \\ \text{subject to} & \mathbf{H}_0 \bullet \mathbf{Q} = p_0 - \gamma, \\ & \mathbf{H}_1 \bullet \mathbf{Q} = p_1, \\ & \quad \vdots \\ & \mathbf{H}_{2d} \bullet \mathbf{Q} = p_{2d}, \\ & \mathbf{Q} \succeq 0, \end{array} \tag{3.28}$$

where,

$$\mathbf{H}_k(i,j) = \begin{cases} 1 \text{ if } i+j-2=k \\ 0 \text{ otherwise .} \end{cases} \tag{3.29}$$

The dual problem of (3.28) is:

$$\begin{array}{ll} \min_{\mu_k} & \sum_{k=1}^{2d} p_k \mu_k \\ \text{subject to} & \mu_0 = 1, \\ & \sum_{k=1}^{2d} \mu_k \mathbf{H}_k \succeq 0 \end{array} \tag{3.30}$$

The semidefinite constraint of (3.30) can be formulated as a moment matrix $\mathbf{M}$:

$$\mathbf{M} = \begin{bmatrix} \mu_0 & \mu_1 & \cdots & \mu_d \\ \mu_1 & \mu_2 & \cdots & \mu_{d+1} \\ \vdots & & \ddots & \\ \mu_d & \mu_{d+1} & \cdots & \mu_{2d} \end{bmatrix} \succeq 0. \tag{3.31}$$

where $\mu_0 = 1$ and $\mathbf{M} \succeq 0$.

Consider now a multivariate polynomial $p(\mathbf{x})$. Then the relaxed optimal solution to the problem (3.24) is given by solving the following SDP problem [37]:

$$\begin{array}{ll} \min\limits_{\mathbf{y}} & \sum_{\alpha} p_\alpha y_\alpha \\ \text{subject to} & \mathbf{M}(\mathbf{y}) \succeq 0. \end{array} \tag{3.32}$$

where $\mathbf{M}(\mathbf{y})$ has similarities to $\mathbf{X}$ defined in (3.9), but instead of monomials it is lifting variables $\mathbf{y}$. The monomials considered can also be the ones used in the vector $[x]_d$, defined in (3.18). Thus, an alternative way to define $\mathbf{X}$ is $[x]_d[x]_d^\top$. As $[x]_d$ has monomials up to degree d, $\mathbf{M}(\mathbf{y})$ will have the required lifting variables to represent a $2d$-degree polynomial. Hence, $\mathbf{M}(\mathbf{y})$ is defined as:

$$\mathbf{M}(\mathbf{y}) = \begin{bmatrix} 1 & y_{10\ldots0} & \cdots & y_{00\ldots1} \\ y_{10\ldots0} & y_{20\ldots0} & \cdots & y_{10\ldots1} \\ \vdots & & \ddots & \\ y_{00\ldots1} & y_{10\ldots1} & \cdots & y_{00\ldots2} \end{bmatrix}. \tag{3.33}$$

3.3.3 Constrained Polynomial Optimization

Consider a constrained optimization problem:

$$\begin{array}{ll} \min & p(\mathbf{x}) \\ \text{s.t.} & f_i(\mathbf{x}) = 0, \quad i = 1, \ldots, m, \\ \mathbf{x} \in \mathbb{R}^n & \end{array} \tag{3.34}$$

Using the Lagrangean relaxation, problem (3.34) can be rewritten as (3.27):

$$\begin{array}{ll} \max & p(\mathbf{x}) - \sum_i^m \lambda_i f_i \\ \text{s.t.} & \mathbf{x} \in \mathbb{R}^n \end{array} \tag{3.35}$$

As seen in (3.24) can be rewritten as:

$$\begin{array}{ll} \max & \gamma \\ \text{s.t.} & p(\mathbf{x}) - \sum_i^m \lambda_i f_i \geq \gamma \end{array} \tag{3.36}$$

By the same logic, we can approximate (3.36) with an SOS constraint [36]:

$$\begin{array}{ll} \max\limits_{\gamma} & \gamma \\ \text{subject to} & p(\mathbf{x}) - \gamma + \sum_{i=1}^m \lambda_i(\mathbf{x}) f_i(\mathbf{x}) \quad \text{is SOS.} \end{array} \tag{3.37}$$

Where problem (3.27) implies that the polynomial is nonnegative, problem (3.37) implies that $p(\mathbf{x})$ is nonnegative on the set of equality constraints. In other words, it only evaluates its nonnegativity inside the feasible set. Moreover, (3.37) is convex, just like its unconstrained counterpart.

In case the problem has inequality constraints, it is possible to convert them into equalities.

3.3.4 Non-SOS Example

As mentioned before, the SDP problem is an approximation of a polynomial problem. When the objective function or the constraints of the original problem are not SOS, then the SDP solution can be infeasible to the original problem. This is the case of the SCOPF problem. There are some algorithms that can reduce the degree of unfeasibility of SDP solutions, but they are not in the scope of this study [36–38].

Consider the example 4.6 from [39]:

$$\begin{array}{ll} \min\limits_{\mathbf{x}} & -x_1 - x_2, \\ \text{subject to} & \\ & x_2 \leq 2x_1^4 - 8x_1^3 + 8x_1^2 + 2, \\ & x_2 \leq 4x_1^4 - 32x_1^3 + 88x_1^2 - 96x_1 + 36, \\ & 0 \leq x_1 \leq 3, 0 \leq x_2 \leq 4. \end{array} \tag{3.38}$$

Problem (3.38) is depicted in Fig. 3.1, where the first constraints is represented by a straight line, the second constraint by a dashed line, and the shaded area is the feasible set. The problem has 6 stationary points: two local optima $(0.6116, 3.4421)$ and $(1.5996, 2.8204)$, are shown by triangles in Fig. 3.2; two local minima, $(1, 0)$ and $(3, 0)$, by squares; and the global minimum, $(2.3295, 3.1783)$, is shown by a star. The fourth stationary point $(7.4593, 3.3187 \times 10^3)$ is not shown in the figure. Also, the feasible space is almost disconnected at $(1, 0)$.

The solution to the SDP problem associated to (3.38) is $x^* = (3, 4)$, which is represented in Fig. 3.2 by a circle, while the shaded area shows the SDP feasible set. This solution violates the second constraint. The dotted line shows the distance between the global optimum and the SDP solution.

It should be noticed that the SDP solution is optimistic. In other words, it is unfeasible and its cost (-7) is lower than the cost of the global optimum, which is -5.5079. This follows the theory that $p(\mathbf{x}_{sos}) \leq p(\mathbf{x}^\star)$ [36].

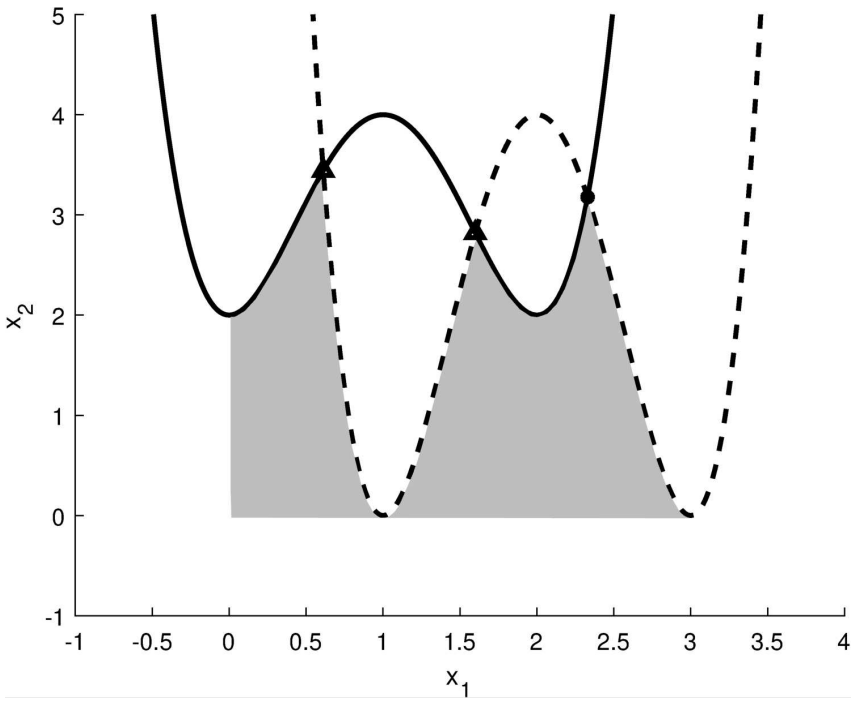

Figure 3.1: Feasible space of problem (3.38).

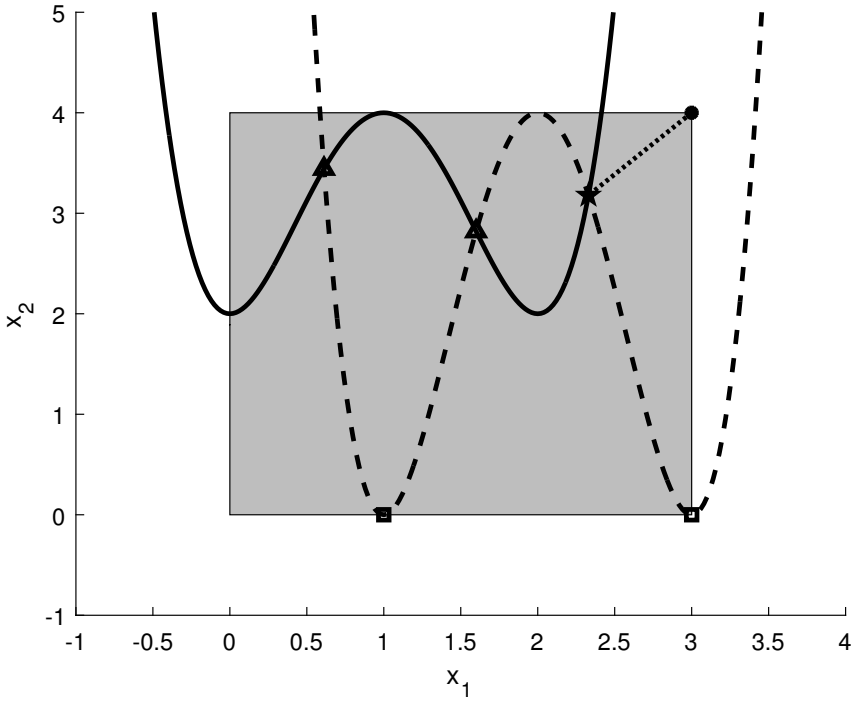

Figure 3.2: Feasible space of the SDP equivalent problem.

3.4 SDP RELAXATION OF THE SCOPF

As mentioned in the previous Chapter, the OPF problem is non-convex and NP-hard. Many studies approached the OPF problem through SDP relaxation, thus solving a convex problem [25, 38, 40]. The main disadvantage of this method is the increase in the number of variables. As the maximum polynomial degree of the OPF is $2d = 2$, this means that the number of monomials in the SDP problem is $\binom{2n_b+2}{2}$. By extension, the SDP equivalent of the SCOPF (SDP-SCOPF) problem has $\binom{2n_bn_c+2}{2}$ variables. Therefore, even a small SCOPF problem may lead to a very large SDP-SCOPF one. As an example, consider the SCOPF problem cast for the IEEE 14-bus system ($n_b = 14$ and $n_c = 10$). The SCOPF has $n = 2n_bn_c = 280$ variables. On the other hand, the SDP-SCOPF has $39,621$ lifting variables.

Consider the polynomial defined by (3.3). Let $L_y\{p\}$ be a linear functional that replaces the monomials x^α with scalar variables y^α [40]:

$$L_y\{p\} := \sum_{\alpha \in \mathbb{N}^n} p_\alpha y_\alpha \tag{3.39}$$

As an example, $L_y\{p\}$ of the quadratic polynomial (3.5) is the linear polynomial (3.6). If $p(x)$ is a matrix, then $L_y\{p\}$ is applied componentwise. An example of this operation in a matrix is $L_y\{\mathbf{x}\mathbf{x}^\top\}$, which yields the moment matrix (3.33).

Consider problem (2.48), its equivalent lifted problem is as follows:

$$\begin{aligned}
\min_{\mathbf{y}} \quad & L_y\{F_c\} && \text{(3.40a)}\\
\text{s.t.} \quad & P^{(k)}_{G_{i\min}} \le L_y\{f^{(k)}_{P_i}\} \le P^{(k)}_{G_{i\max}}, \forall k \in \mathcal{K}, \forall i \in \mathcal{N} && \text{(3.40b)}\\
& Q^{(k)}_{G_{i\min}} \le L_y\{f^{(k)}_{Q_i}\} \le Q^{(k)}_{G_{i\max}}, \forall k \in \mathcal{K}, \forall i \in \mathcal{N} && \text{(3.40c)}\\
& {V^{(k)}_{i_{\min}}}^2 \le L_y\{f^{(k)}_{V_i}\} \le {V^{(k)}_{i_{\max}}}^2, \forall k \in \mathcal{K}, \forall i \in \mathcal{N} && \text{(3.40d)}\\
& |L_y\{f^{(k)}_{F_l}\}| \le F^{(k)}_{l_{\max}}, \forall k \in \mathcal{K}, \forall l \in \mathcal{L} && \text{(3.40e)}\\
& L_y\{|f^{(k)}_{T_l}|\} \le F^{(k)}_{l_{\max}}, \forall k \in \mathcal{K}, \forall l \in \mathcal{L} && \text{(3.40f)}\\
& L_y\{|f^{(k)}_{S_{P_i}}|\} \le \Delta P^{(k)}_{i_{\max}}, \forall k \in \mathcal{K}, \forall i \in \mathcal{S} && \text{(3.40g)}\\
& L_y\{|f^{(k)}_{S_{Q_i}}|\} \le \Delta Q^{(k)}_{i_{\max}}, \forall k \in \mathcal{K}, \forall i \in \mathcal{S} && \text{(3.40h)}\\
& L_y\{f^{(k)}_{ref}\} = 0, \forall k \in \mathcal{K} \quad \text{(reference)} && \text{(3.40i)}
\end{aligned}$$

Consider the compact SCOPF problem (2.49). Therefore, the compact SDP-SCOPF optimization problem becomes:

$$\begin{aligned}
\min_{\mathbf{y}} \quad & L_y\{f_c\} \\
\text{subject to} \quad & L_y\{\mathbf{g}\} \le \mathbf{c}, \\
& \mathbf{M}(\mathbf{y}) \succeq 0,
\end{aligned} \tag{3.41}$$

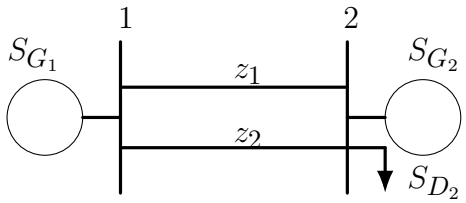

Figure 3.3: Two bus diagram.

After solving (3.41), if at the solution $\mathbf{M}(\mathbf{y})$ has rank-one, then the relaxation is labled as "exact" [38]. However, the SDP solution for general meshed networks is seldom exact [41]. This can be easily seen in the following two-bus example.

3.4.1 Two-bus Example

Consider the 2-bus system of Fig. 3.3, whose data can be found in Appendix A. For simplicity, the problem is cast only for $k = 0$ (non-contingency state, i.e. an OPF problem) and has no line constraint.

The bus admittance matrix of the system is

$$\mathbf{Y} = \mathbf{G} + \mathrm{j}\mathbf{B} = \begin{bmatrix} 0.8911 & -0.8911 \\ -0.8911 & 0.8911 \end{bmatrix} + \mathrm{j} \begin{bmatrix} -8.4359 & 8.9109 \\ 8.9109 & -8.4359 \end{bmatrix}$$

We use a generic optimization criterion (f_c) in the OPF problem. In matrix form,

the OPF is written

$$
\begin{aligned}
\min \quad & f_c \\
\text{s.t.} \quad & \\
& -diag(\mathbf{e})\left[\mathbf{G}\mathbf{e}-\mathbf{B}\mathbf{f}\right]-diag(\mathbf{f})\left[\mathbf{B}\mathbf{e}+\mathbf{G}\mathbf{f}\right] \leq \mathbf{P}_D-\mathbf{P}_{G_{\min}}, \\
& diag(\mathbf{e})\left[\mathbf{G}\mathbf{e}-\mathbf{B}\mathbf{f}\right]+diag(\mathbf{f})\left[\mathbf{B}\mathbf{e}+\mathbf{G}\mathbf{f}\right] \leq \mathbf{P}_{G_{\max}}-\mathbf{P}_D, \\
& diag(\mathbf{e})\left[\mathbf{B}\mathbf{e}+\mathbf{G}\mathbf{f}\right]+diag(\mathbf{f})\left[\mathbf{G}\mathbf{e}-\mathbf{B}\mathbf{f}\right] \leq \mathbf{Q}_D-\mathbf{Q}_{G_{\min}}, \\
& -diag(\mathbf{e})\left[\mathbf{B}\mathbf{e}+\mathbf{G}\mathbf{f}\right]-diag(\mathbf{f})\left[\mathbf{G}\mathbf{e}-\mathbf{B}\mathbf{f}\right] \leq \mathbf{Q}_{G_{\max}}-\mathbf{Q}_D, \\
& -diag(\mathbf{e})\mathbf{e}-diag(\mathbf{f})\mathbf{f} \leq -\mathbf{V}_{\min}^2, \\
& diag(\mathbf{e})\mathbf{e}+diag(\mathbf{f})\mathbf{f} \leq \mathbf{V}_{\max}^2, \\
& f_1 = 0 \quad (ref),
\end{aligned}
\tag{3.42}
$$

where $\mathbf{e}=[e_1,e_2]^\top$ and $\mathbf{f}=[f_1,f_2]^\top$.

Bus 1 is chosen as slack bus, therefore in (3.42) $f_1=0$. Also consider that the voltage magnitude at bus 1 is equal to 1 pu, which means that $e_1=1$. Substituting the elements of the admittance matrix and the loads of the system, the final representation of the OPF is:

$$
\begin{aligned}
\min \quad & f_c \\
\text{s.t.} \quad & \\
& 0.8911e_2+8.9109f_2-0.8911 \leq 0, \\
& -0.8911e_2-8.9109f_2-1.1089 \leq 0, \\
& 0.8911e_2-8.9109f_2-0.8911(e_2^2+f_2^2)-2 \leq 0, \\
& -0.8911e_2+8.9109f_2+0.8911(e_2^2+f_2^2)+0.5 \leq 0, \\
& 8.9109e_2-0.8911f_2-9.2359 \leq 0, \\
& -8.9109e_2+0.8911f_2+7.6359 \leq 0, \\
& 8.9109e_2+0.8911f_2-8.4359(e_2^2+f_2^2)-1.7 \leq 0, \\
& -8.9109e_2-0.8911f_2+8.4359(e_2^2+f_2^2)+0.3 \leq 0, \\
& -e_2^2-f_2^2+0.9025 \leq 0, \\
& e_2^2+f_2^2-1.1025 \leq 0.
\end{aligned}
\tag{3.43}
$$

The feasible set of (3.43) is the shaded area in Fig. 3.4. The solid lines are active power generation limits, the dashed lines are for reactive power generation limits, and the dotted lines represent the quadratic voltage limits. Notice that the feasible set is defined by four constraints: upper active power generation limit at bus 1 and 2, upper reactive power generation limit at bus 2, and lower quadratic voltage limit at bus 2.

The monomials of the SCOPF problem (3.43) and their associated lifted variables are:

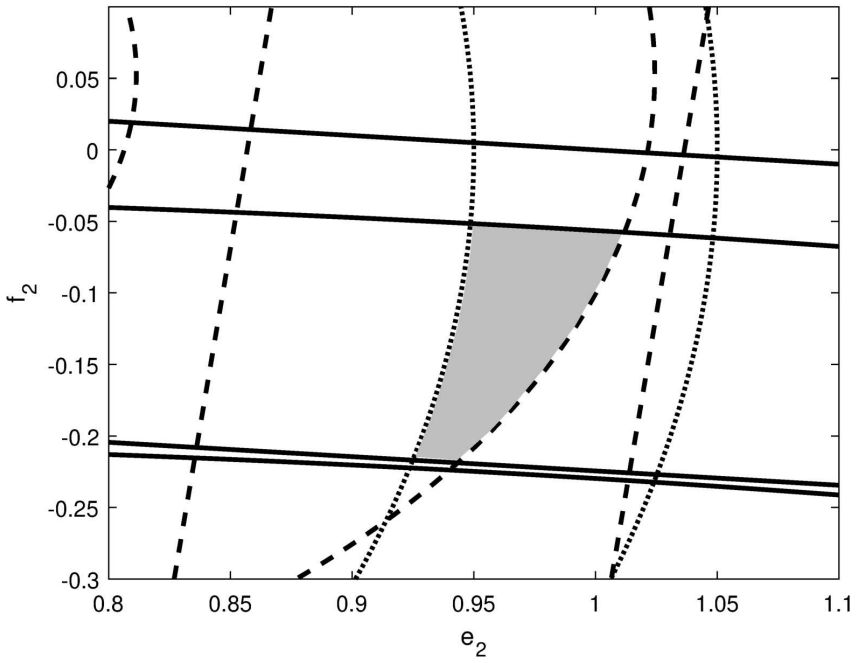

Figure 3.4: Feasible space of (3.43).

$$\begin{array}{ccccc} e_2 & f_2 & e_2^2 & e_2 f_2 & f_2^2 \\ \downarrow & \downarrow & \downarrow & \downarrow & \downarrow \\ y_1 & y_2 & y_3 & y_4 & y_5 \end{array}$$

Thus, the moment matrix is:

$$\mathbf{M}(\mathbf{y}) = \begin{bmatrix} 1 & y_1 & y_2 \\ y_1 & y_3 & y_4 \\ y_2 & y_4 & y_5 \end{bmatrix}$$

The SDP-SCOPF is written as:

$$
\begin{aligned}
\min \quad & L_y\{f_c\} \\
\text{subject to} \quad & \\
& 0,8911y_1 + 8,9109y_2 - 0,8911 \leq 0, \\
& -0,8911y_1 - 8,9109y_2 - 1,1089 \leq 0, \\
& 0,8911y_1 - 8,9109y_2 - 0,8911(y_3 + y_5) - 2 \leq 0, \\
& -0,8911y_1 + 8,9109y_2 + 0,8911(y_3 + y_5) + 0,5 \leq 0, \\
& 8,9109y_1 - 0,8911y_2 - 9,2359 \leq 0, \\
& -8,9109y_1 + 0,8911y_2 + 7,6359 \leq 0, \\
& 8,9109y_1 + 0,8911y_2 - 8,4359(y_3 + y_5) - 1,7 \leq 0, \\
& -8,9109y_1 - 0,8911y_2 + 8,4359(y_3 + y_5) + 0,3 \leq 0, \\
& -y_3 - y_5 + 0,9025 \leq 0, \\
& y_3 + y_5 - 1,1025 \leq 0, \\
& \mathbf{M}(\mathbf{y}) \succeq 0.
\end{aligned}
\tag{3.44}
$$

Notice that (3.44), has only linear and convex constraints. However, it is important to highlight the constraint $\mathbf{M}(\mathbf{y}) \succeq 0$. The constraint defines the feasible set through the closed cone K. An alternative to this constraint is to use the principal minor test:

$$
\begin{bmatrix} 1 & y_1 & y_2 \\ y_1 & y_3 & y_4 \\ y_2 & y_4 & y_5 \end{bmatrix} \succeq 0 \iff \begin{aligned} & 1 \geq 0, \\ & y_3 \geq 0, \\ & y_5 \geq 0, \\ & y_3 - y_1^2 \geq 0, \\ & y_5 - y_2^2 \geq 0, \\ & y_3 y_5 - y_4^2 \geq 0, \\ & y_3 y_5 + y_1^2 y_5 - y_4^2 - y_2^2 y_3 \geq 0. \end{aligned}
$$

In this small example it is possible to see how fast the number of variables increases when the problem is expressed in the lifted space. In (3.43) the number of variables is $n = 2$, but in its equivalent lifted problem (3.44), we have 5 lifting variables.

Fig. 3.5 shows the feasible set of the relaxed problem (shaded area). To have a better view of the SDP relaxation, all the constraints of the original problem are also shown in this figure. The SDP-OPF's feasible set is clearly larger than the original SCOPF one.

Fig. 3.5 is useful to highlight an important property of SDP solutions: they can be feasible or unfeasible to the original problem depending on the adopted optimization criterion. For example, if e_2 is maximized, the SDP solution will be feasible to the original problem, whereas if e_2 is minimized, the SDP solution will be unfeasible. Thus, the objective function can have a significant impact in the quality of the relaxed solution and may help achieve a rank-one or low-rank solution for (3.44) [38].

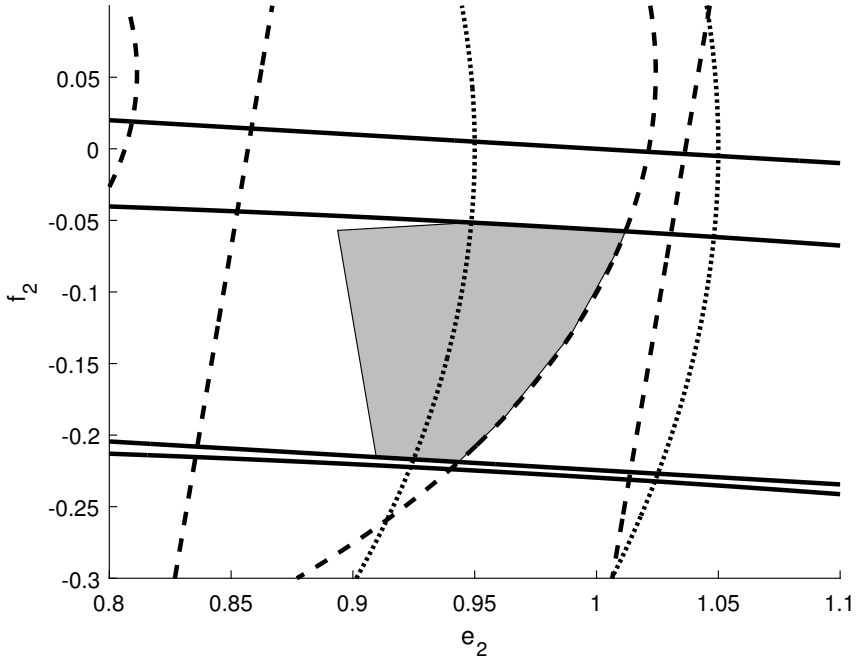

Figure 3.5: Feasible space of (3.44).

3.5 CONCLUSION

This chapter presented a brief introduction to semidefinite programming and analysed some properties of this methodology via illustrative examples. The first example is a problem which has rank-one solution, while the second demonstrates that the SOS approximation my yield unacceptable results. The last example shows how to apply SDP to the SCOPF problem. The next chapter introduces the umbrella discovery algorithm.

4 UMBRELLA CONSTRAINT DISCOVERY

4.1 INTRODUCTION

The SCOPF problem introduced by equation (2.49) is a nonlinear and NP-hard problem [25]. Furthermore, it can have a very high number of constraints. This can be shown by making the following consideration:when the $N-1$ criterion is defined by branch contingencies, $n_c = n_l + 1$. Hence, the number of constraints in (2.49) is $J_{AC} = (n_c + 1)(4n_g + 2n_b + 4n_l) - 4n_c$. As such, for the relatively small IEEE 118-bus network, the SCOPF problem has $222,908$ constraints. Therefore, there is a high computational cost for solving the problem. Furthermore, the complete problem can become computationally prohibitive for certain time-constrained operational conditions [29].

A possible solution is to remove the constraints that are not required to form the feasible set of the problem [2–4]. For that, an algorithm is adopted in [2–4] to identify those required inequalities, which are called *umbrella constraints*. However, the method is only valid for convex problems. As shown previously, the power balance from equation (2.32) can be manipulated to become linear, as in (2.45). When the DC representation of the network is adopted, the number of constraints in the SCOPF decreases, the problem becomes convex and the computational cost to find a solution is reduced, while the trade-off is the loss of reactive power representation in the model [4]. Nevertheless, the algorithm described in [2–4] can be use to obtain the umbrella constraints of the SC-LOPF.

This chapter analyzes the umbrella constraints concept and the Umbrella Constraint Discovery algorithm proposed in [4].

4.2 UMBRELLA CONSTRAINT AND DISCOVERY

Not all the inequality constraints of an optimization problem define its feasible set. Some of them are redundant and/or unnecessary [2]. These non-essential constraints are never binding at any solution. Therefore by identifying and removing them from the formulation of the SCOPF, we can reduce computational cost, while maintaining the same solution. To identify the minimum number of constraints necessary to form the feasible set, in other words, the umbrella constraints, the following properties are considered [4]:

- An umbrella constraint is not always biding at the optimal point. Nevertheless, it can potentially be biding;
- there is always at least one point lying on an umbrella constraint that is feasible with respect to all the other constraints of the problem. When a point lies on an inequality constraint, it means that the inequality is being satisfied with equality;
- in the case of a non-umbrella constraint, there is no single point lying on the constraint that can be feasible with respect to all the other constraints of the problem.

It is important to highlight that the term umbrella constraint is not interchangeable with active constraint. The former has the potential to become active at the solution, depending on the objective function. Another observation is the independence between the identified umbrella constraints and the objective function of the SCOPF. Consequently, the umbrella discovery algorithm searches in the constraint set of the optimization problem for potential biding constraints, disregarding the objective function.

Before introducing the Umbrella Constraint Discovery (UCD) optimization problem, consider the following trivial linear optimization example:

$$\begin{aligned} \min_{x} \quad & x \\ \text{subject to} \quad & -x \leq -2 \\ & x \leq 3, \\ & x \leq 4, \end{aligned} \tag{4.1}$$

whose optimal solution is $x = 2$.

Problem (4.1) is equivalent to:

$$\begin{aligned} \min_{x} \quad & x \\ \text{subject to} \quad & 2 \leq x \leq 3 \end{aligned} \tag{4.2}$$

Therefore, problem (4.1) has three constraints, but only two of them define its feasible set. In other words, there are two umbrella constraints, and they are shown in (4.2).

Another way is to verify if a constraint is umbrella is to check if problem (4.1) is feasible when the solution lies on that constraint. Consider constraint $x \leq 4$. To check if this constraint is umbrella, we build problem (4.3). As the constraint is not umbrella, (4.3) is clearly unfeasible.

$$\begin{aligned} \min_{x} \quad & x \\ \text{subject to} \quad & -x \leq -2 \\ & x \leq 3, \\ & x = 4 \end{aligned} \tag{4.3}$$

The same steps can be taken to check if the remaining constraints are umbrella. In this case, we would need to check the feasibility of two other problems. Another approach would be to split the equality constraint into two constraints ($\leq$ and $\geq$), add a slack variable, $s \geq 0$, in one of them, and obtain its minimum value. By doing so, we calculate the distance between the constraint and the feasible set. If the slack variable is 0, the equality holds and thus the problem is feasible with a point on the constraint.

Thus, to verify if $x \leq 4$ is an umbrella constraint of (4.1), we need to solve the following problem:

$$\begin{aligned} \min_{x,s} \quad & s \\ \text{subject to} \quad & -x \leq -2 \\ & x \leq 3, \\ & x \leq 4, \\ & x + s \geq 4, \\ & s \geq 0 \end{aligned} \tag{4.4}$$

Again, the solution for (4.4) is straightforward. At the solution the value of s is 1, the same as the distance between constraints $x \leq 4$ and $x \leq 3$. Finally, to check all the constraints, we can concatenate all the optimization problems, analogous to (4.4), which are built to check if the remaining constraints are umbrella. Therefore, the complete problem is:

$$\begin{aligned} \min_{x,y,z,s} \quad & \sum_{j=1}^{3} s_j \\ \text{subject to} \quad & -x \leq -2 \\ & -x + s_1 \geq -2, \\ & x \leq 3, \\ & x \leq 4, \\ & -y \leq -2, \\ & y \leq 3, \\ & y + s_2 \geq 3, \\ & y \leq 4, \\ & -z \leq -2, \\ & z \leq 3, \\ & z \leq 4, \\ & z + s_3 \geq 4, \\ & s_1, s_2, s_3 \geq 0 \end{aligned} \tag{4.5}$$

The first four constraints of the "umbrella detection problem" (4.5) are needed to check if $x \leq 2$ is umbrella; the next four constraints are introduced to check if constraint $x \leq 3$ is umbrella and the last constraints check constraint $x \leq 4$. Notice that every set of constraints is expressed by independent variables because it is not necessary that a single variable, x, respects all the constraints of (4.5), nor it is desirable.

As, in (4.5), there is no coupling between the sets of variables (x, s_1), (y, s_2) and (z, s_3), this optimization problem can be decomposed in three independent problems. To express (4.5) in a compact form, consider w_j to be the variable associated with constraint j (i.e. $w_1 = x$, $w_2 = y$, and $w_3 = z$) and define

$$\mathbf{A}_s = [-1, 1, 1]^\top, \tag{4.6}$$

$$\mathbf{b}_s = [-2, 3, 4]^\top \tag{4.7}$$

Let vector $\mathbf{a}_{s_j}$ the jth line of the constant matrix $\mathbf{A}_s$, b_{s_j} is jth line of the constant vector $\mathbf{b}_s$, and the set of constraints $\mathcal{J} = 1, 2, \ldots, J$. Thus, the compact representation of (4.5) is:

$$\begin{aligned} \min_{\mathbf{w},\mathbf{s}} \quad & \sum_{j=1}^{J} s_j \\ \text{subject to} \quad & \mathbf{A}_s \mathbf{w}_j \leq b_s, && \forall j \in \mathcal{J} \\ & \mathbf{a}_{s_j}^\top \mathbf{w}_j + s_j \geq b_{s_j}, && \forall j \in \mathcal{J} \\ & s_j \geq 0. && \forall j \in \mathcal{J} \end{aligned} \tag{4.8}$$

Problem (4.8) is feasible if the orignal is feasible. In addition (4.8) has a unique solution because the objective function is not colinear with any constraint of the problem. Therefore, problem (4.8) can be solved in polynomial time [16]. The number of constraints in (4.5) is equal to $J^2 + 2J$, where J is the number of constraints of (4.1).

In summary, problem (4.8) is very large. However, this problem can be decomposed into a set of J independent subproblems. It is possible and desirable to separate the constraints into smaller groups (up to J groups), each one expressed in terms of variables associated with a particular inequality constraint. The jth problem in this set is expressed only in terms of $\mathbf{w}_j$ and s_j. Let us now consider the SC-LOPF problem.

4.3 APPLICATION IN POWER SYSTEMS

To identify the umbrella constraints of SC-LOPF (2.53), the following optimization problem can be derived from (4.8):

$$\begin{aligned} \min_{\mathbf{w},\mathbf{s}} \quad & \sum_{j=1}^{J_{DC}} s_j \\ \text{subject to} \quad & \hat{\mathbf{a}}_{\delta_{j'}}^\top \mathbf{w}_j \leq \hat{c}_{\delta_{j'}}, && \forall j' \in \mathcal{J}, \forall j \in \mathcal{J} \\ & \hat{\mathbf{a}}_{\delta_j}^\top \mathbf{w}_j + s_j \geq \hat{c}_{\delta_j}, && \forall j \in \mathcal{J} \\ & s_j \geq 0, && \forall j \in \mathcal{J} \end{aligned} \tag{4.9}$$

where every vector $\mathbf{w}_j$ has $n_b - 1$ components, vector $\mathbf{s}$ has J_{DC} components, and $\mathcal{J} = \{1, \ldots, J_{DC}\}$. Thus, the number of variables of the umbrella detection problem is $J_{DC}\,(n_b - 1) + J_{DC}$.

If we consider n_c contingency states, the number of constraints in (4.9) is $J_{DC}^2 + J_{DC}$. Although this is usually a large number, the set of secure operating points (i.e., the feasible set of the problem) is defined by only a small portion of these constraints (i.e. umbrella constraints). As the system load changes over time, the set of umbrella

constraints may also change. However, if we know the umbrella constraints at each load level beforehand, the set of necessary constraints when calculating the secure power dispatch will be considerably smaller.

There are also two remarks regarding the applicability of (4.9):

- Any change in vector $\hat{\mathbf{c}}_\delta$, which contains the physical and operational limits of the system, may change the umbrella constraints set. Hence, requiring that (4.8) be solved again;
- the number of constraints ($J^2 + 2J$) and variables ($J(n_b - 1) + J$) from (4.9) increases significantly in relation to the original problem (J and $n_b - 1$, respectively). This may result in unsolvable problem due to computational limitations.

4.3.1 LOPF Two-Bus Example

In order to better demonstrate the umbrella discovery algorithm, the SC-LOPF umbrella constraints are identified for the two-bus system depicted in Fig. 3.3, whose data can be found in Appendix A. For simplicity, only the intact system will be considered (no contingency). The SC-LOPF is described using the following matrices:

$$\mathbf{B}_\delta = \begin{bmatrix} 9 & -9 \\ -9 & 9 \end{bmatrix}, \tag{4.10}$$

$$\mathbf{A}_{inc}^\top = \begin{bmatrix} 1 & -1 \\ 1 & -1 \end{bmatrix}, \tag{4.11}$$

$$\mathbf{\Gamma} = \begin{bmatrix} 5 & 0 \\ 0 & 4 \end{bmatrix}. \tag{4.12}$$

Choosing bus 1 as reference ($\delta_1 = 0$), the reduced matrices are:

$$\hat{\mathbf{B}}_\delta = [9], \tag{4.13}$$

$$\hat{\mathbf{A}}_{inc}^\top = \begin{bmatrix} -1 \\ -1 \end{bmatrix}, \tag{4.14}$$

$$\hat{\mathbf{P}}_G = [P_{G_2}], \tag{4.15}$$

$$\hat{\mathbf{P}}_D = [2] \tag{4.16}$$

From (2.41) we have

$$\mathbf{f} = \begin{bmatrix} -\frac{5}{9}P_{G_2} \\ -\frac{4}{9}P_{G_2} \end{bmatrix} + \begin{bmatrix} \frac{10}{9} \\ \frac{8}{9} \end{bmatrix} \tag{4.17}$$

Therefore, the optimization problem is:

$$\begin{aligned} \min \quad & c(P_{G_2}) \\ \text{subject to} \quad & 0 \leq 2 - P_{G_2} \leq 2 \\ & 0 \leq P_{G_2} \leq 1.5 \\ & -1 \leq -\frac{5}{9} P_{G_2} + \frac{10}{9} \leq 1 \\ & -1 \leq -\frac{4}{9} P_{G_2} + \frac{8}{9} \leq 1 \end{aligned} \tag{4.18}$$

The first constraint of (4.18) represents the upper and lower limits of P_{G_1}; the second constraint the limits on P_{G_2}; the third and fourth constraints represent the limits on the power flows over lines 1 and 2, respectively.

Problem (4.18) in compact form is:

$$\begin{aligned} \min \quad & P_{G_2} \\ \text{subject to} \quad & \mathbf{A}_\delta \hat{\mathbf{P}}_G \leq \mathbf{c}_\delta \end{aligned} \tag{4.19}$$

where,

$$\mathbf{A}_\delta = [-1, 1, 1, -1, -5, 5, -4, 4]^\top, \tag{4.20}$$

$$\mathbf{c}_\delta = [0, 2, 1.5, 0, -1, 19, 1, 17]^\top, \tag{4.21}$$

$$\hat{\mathbf{P}}_G = [P_{G_2}]. \tag{4.22}$$

As there is a single variable, the solution to this problem is trivial. Thus, the umbrella constraints can be identified analytically. Given $\mathbf{A}_\delta$ and $\mathbf{c}_\delta$, the equivalent problem is:

$$\begin{aligned} \min \quad & P_{G_2} \\ \text{subject to} \quad & P_{G_2} \geq 0, \\ & P_{G_2} \leq 2, \\ & P_{G_2} \leq 1.5, \\ & P_{G_2} \geq 0, \\ & P_{G_2} \geq 0.2, \\ & P_{G_2} \leq 3.8, \\ & P_{G_2} \geq -0.25, \\ & P_{G_2} \leq 4.25. \end{aligned} \tag{4.23}$$

Therefore, the umbrella constraints of (4.23) are:

$$0.2 \leq P_{G_2} \leq 1.5 \tag{4.24}$$

Thus, (4.23) is equivalent to:

$$\begin{aligned} \min \quad & P_{G_2} \\ \text{subject to} \quad & 0.2 \leq P_{G_2} \leq 1.5 \end{aligned} \tag{4.25}$$

As constraints 3 and 5 of (4.23) are umbrella, it is expected $s_3 = s_5 = 0$. For the sake of brevity, this chapter will only show on how to obtain s_2 and s_3, but the same steps shall be taken for the remaining constraints. The complete umbrella detection problem is:

$$
\begin{aligned}
\min \quad & \textstyle\sum_{j=1}^{8} s_j \\
\text{s.t.} \quad & \\
& \begin{bmatrix} -1 \\ 1 \\ 1 \\ -1 \\ -5 \\ 5 \\ -4 \\ 4 \end{bmatrix} w_j \leq \begin{bmatrix} 0 \\ 2 \\ 1.5 \\ 0 \\ -1 \\ 19 \\ 1 \\ 17 \end{bmatrix}, \\
& -w_1 + s_1 \geq 0, \\
& w_2 + s_2 \geq 2, \\
& w_3 + s_3 \geq 1.5, \\
& -w_4 + s_4 \geq 0, \\
& -5w_5 + s_5 \geq -1, \\
& 5w_6 + s_6 \geq 19, \\
& -4w_7 + s_7 \geq 1, \\
& 4w_8 + s_8 \geq 17, \\
& s_j \geq 0, \\
& \text{for } j = 1, \ldots, 8.
\end{aligned}
\tag{4.26}
$$

To check if the second constraint is umbrella we need to solve problem (4.27), which is obtained from (4.26) using decomposition.

$$
\begin{aligned}
\min \quad & s_2 \\
\text{s.t.} \quad & \\
& \begin{bmatrix} -1 \\ 1 \\ 1 \\ -1 \\ -5 \\ 5 \\ -4 \\ 4 \end{bmatrix} w_2 \leq \begin{bmatrix} 0 \\ 2 \\ 1.5 \\ 0 \\ -1 \\ 19 \\ 1 \\ 17 \end{bmatrix}, \\
& w_2 + s_2 \geq 2, \\
& s_2 \geq 0.
\end{aligned}
\tag{4.27}
$$

Expressing the constraints in terms of P_{G_2}, we have:

$$
\begin{aligned}
-P_{G_2} &\leq 0,\\
P_{G_2} &\leq 2,\\
P_{G_2} &\leq 1.5,\\
-P_{G_2} &\leq 0,\\
-P_{G_2} &\leq -0.2,\\
P_{G_2} &\leq 3.8,\\
-P_{G_2} &\leq 0.25,\\
P_{G_2} &\leq 4.25,\\
P_{G_2} + s_2 &\geq 2,
\end{aligned}
$$

which can be simplified to:

$$
\begin{aligned}
P_{G_2} &\leq 2,\\
0.2 \leq P_{G_2} &\leq 1.5,\\
P_{G_2} + s_2 &\geq 2
\end{aligned}
$$

It is trivial to see that the lowest value of s_2 that does not violate constraint $P_{G_2} + s_2 \geq 2$ is 0.5.

The same steps can be taken to check for another umbrella constraint, such as constraint 3:

$$
\begin{aligned}
&\min \quad s_3\\
&\text{subject to}\\
&\begin{bmatrix} -1 \\ 1 \\ 1 \\ -1 \\ -5 \\ 5 \\ -4 \\ 4 \end{bmatrix} \mathbf{w}_3 \leq \begin{bmatrix} 0 \\ 2 \\ 1.5 \\ 0 \\ -1 \\ 19 \\ 1 \\ 17 \end{bmatrix},\\
&\mathbf{w}_3 + s_3 \geq 1.5,\\
&s_3 \geq 0.
\end{aligned}
\tag{4.28}
$$

The constraints of (4.28) can be reduced to:

$$
\begin{aligned}
P_{G_2} &\leq 1.5,\\
P_{G_2} &\geq 0.2,\\
P_{G_2} + s_3 &\geq 1.5
\end{aligned}
$$

Again, the solution is straightforward. As the maximum P_{G_2} value is 1.5, then constraint $P_{G_2} + s_3 \geq 1.5$ implies that $s_3 = 0$.

Following the same constraint order of (4.18), Table 4.1 shows all the s values in this example. It is interesting to notice that only 2 out of 8 constraints define the feasible set (i.e. 75% reduction in the number of constraints).

Table 4.1: The s value for each associated LOPF constraint.

#	Constraint	s
1	$P_{G_{1_{\max}}}$	0.20
2	$P_{G_{1_{\min}}}$	0.50
3	$P_{G_{2_{\max}}}$	0.00
4	$P_{G_{2_{\min}}}$	0.20
5	$F_{1_{\max}}$	0.00
6	$F_{1_{\min}}$	0.20
7	$F_{2_{\max}}$	1.28
8	$F_{2_{\min}}$	1.22

4.3.2 SC-LOPF Two-Bus Example

As the problem presented here is not an SC-LOPF (but a linear optimal power flow, or LOPF), it is necessary to expand it to an SC-LOPF problem (2.53). The SC-LOPF problem follows the same structure as the problem (2.45), but with some extra security constraints and more variables. In this study, the SC-LOPF takes into consideration 2 contingencies ($k = 0, 1, 2$) and takes into account the active power security constraint $-\Delta P_{i_{\max}} \leq \hat{\mathbf{P}_{\mathbf{G}}}^{(0)} - \hat{\mathbf{P}_{\mathbf{G}}}^{(k)} \leq \Delta P_{i_{\max}}$ (2.54). The upper limit in the active power generated variation between contingencies, $\Delta P_{i_{\max}}$, is set at 10% of the maximum generation limits.

The procedure used to identify the umbrella constraints is the same. Table 4.2 shows the values obtained for the slack variables when the complete problem is solved in just one shot. Some important remarks are: reduction of 54% in the number of constraints, all the security constraints are umbrella, the upper limit of the generator at bus 2 is umbrella under all the contingencies, and the non-umbrella constraints of the LOPF problem (4.18) do not become umbrella with the tightening of the feasible set (i.e., with the inclusion of the security constraints). In summary, the set of umbrella constraints in this example is: $P_{G_{2_{\max}}}, S_{P_{1_{\max}}}, S_{P_{1_{\min}}}, S_{P_{2_{\max}}}$, and $S_{P_{2_{\min}}}$.

4.4 PROBLEM PARTITIONING

Many decomposition schemes were proposed in [16] for the umbrella discovery problem (4.9). In the present work, a combination of three types of decomposition is used, besides the one previously explained: contingency-based, line-based and security-based partitions.

It is in the best interest to obtain the most number of non-umbrella constraints in the least possible amount of iterations. This way, the umbrella discovery problem (4.8) is relatively small and not so costly.

Table 4.2: Optimal slack variables without decomposing the problem.

Constraint	s		
	$k=0$	$k=1$	$k=2$
$P_{G_{1_{\max}}}$	0.85	1.00	1.00
$P_{G_{1_{\min}}}$	0.50	0.50	0.50
$P_{G_{2_{\max}}}$	0.00	0.00	0.00
$P_{G_{2_{\min}}}$	0.85	1.00	1.00
$F_{1_{\max}}$	0.36	-	0.00
$F_{1_{\min}}$	1.28	-	1.50
$F_{2_{\max}}$	0.49	0.00	-
$F_{2_{\min}}$	1.22	1.50	-
$S_{P_{1_{\max}}}$	-	0.00	0.00
$S_{P_{1_{\min}}}$	-	0.00	0.00
$S_{P_{2_{\max}}}$	-	0.00	0.00
$S_{P_{2_{\min}}}$	-	0.00	0.00

Nevertheless, it is important to grasp some important concepts regarding feasible set and the umbrella constraints.

Firstly, the umbrella discovery problem (4.8) can be solved independently for each s_j and $\mathbf{w}_j$. As such, if desirable, problem (4.9) can be decomposed into J_{DC} subproblems. Each subproblem identify a single constraint and the umbrella set is the union of all the umbrella constraints identified separately. This is used to decompose problem (4.26) into (4.27).

Secondly, consider two constraint sets $\mathcal{J}$ and $\mathcal{J}_1$, where $\mathcal{J}_1 \subseteq \mathcal{J}$. If there is a constraint $j \in \mathcal{J}_1$ that does not define the feasible set (i.e. it is not a umbrella constraint) when solving the Umbrella Constraint Discovery algorithm (4.8), then the same constraint j is also considered not an umbrella constraint when solving the Umbrella Constraint Discovery (4.8) for the constraints in $\mathcal{J}$.

Finally, let $\mathcal{U}$ be the set of those constraints that are in $\mathcal{J}$ and are umbrella constraints when solving the Umbrella Constraint Discovery algorithm (4.8). Henceforth, $\subseteq_U$ is the operator that describes this type of subset composed of umbrella constraints, e.g. $\mathcal{U} \subseteq_U \mathcal{J}$. Furthermore, consider the constraint set $\mathcal{J}_2$, and two more umbrella sets $\mathcal{U}_1 \subseteq_U \mathcal{J}_1$, and $\mathcal{U}_2 \subseteq_U \mathcal{J}_2$. If $\mathcal{J} = \mathcal{J}_1 \bigcup \mathcal{J}_2$ and $\mathcal{J}_3 = \mathcal{J}_1 \bigcap \mathcal{J}_2 \neq \varnothing$, then $\mathcal{U}_3 = \mathcal{U}_1 \bigcap \mathcal{U}_2$, where $\mathcal{U}_3 \subseteq_U \mathcal{J}_3$.

4.4.1 Contingency-Based Partitioning

Consider the SC-LOPF problem (2.53). Its constraint set is composed by two subsets $\mathcal{J} = \mathcal{J}_\pi \bigcup \mathcal{J}_\lambda$. Let $\mathcal{J}_\pi(k)$ be the set of the power balance, generation and line limits constraints for each state k, and $\mathcal{J}_\lambda$ be the security constraint set. Therefore, $\mathcal{J}_\pi = \bigcup_{k \in \mathcal{K}} \mathcal{J}_\pi(k)$.

Consider that we solve the umbrella discovery problem (4.9) by taking into consideration only $\mathcal{J}_\pi$. Then, the problem can be decomposed into independent subproblems,

each one associated with a contingency state k, where $k = 0, 1, \ldots, n_c$. Each subproblem is called Umbrella Constraint Optimal Power Flow (UCOPF), due to the fact that its constraint set, $\mathcal{J}_\pi(k)$, is equivalent to the LOPF. Let each umbrella set of each UCOPF be denoted as $\mathcal{U}_k \subseteq_U \mathcal{J}_\pi(k)$.

Let the constraint set $\mathcal{J}_\pi^U = \bigcup_{k \in \mathcal{K}} \mathcal{U}_k$. Solve the umbrella discovery problem (4.9) for the constraints $\mathcal{J}_\pi^U \bigcup \mathcal{J}_\lambda$. By doing so, the identified umbrella set is $\mathcal{U}$, which it is the same as $\mathcal{U} \subseteq_U \mathcal{J}$. This brings an intuitive way to decompose the problem while reducing the number of total constraints. At the same time, the final solution is identical to the one obtained when (4.9) is solved considering the entire set of constraints $\mathcal{J}$.

To better illustrate this method, let $P_{G_{i_{\max}}}^{(k)}$ and $P_{G_{i_{\min}}}^{(k)}$ be the upper and lower active generation limits at bus i and state k, respectively; $F_{l_{\max}}^{(k)}$ and $F_{l_{\min}}^{(k)}$ the upper and lower power flow limits of line l at state k, respectively; $S_{P_{i_{\max}}}^{(k)}$ and $S_{P_{i_{\min}}}^{(k)}$ be, respectively, the upper and lower limits on the variation in the active power generation at bus i between states 0 and k. Then, for the two-bus example $\mathcal{J}_\pi$ is composed of $\{\mathcal{J}_\pi(0), \mathcal{J}_\pi(1), \mathcal{J}_\pi(2)\}$, where $\mathcal{J}_\pi(k) = \{P_{G_{1_{\max}}}^{(k)}, P_{G_{1_{\min}}}^{(k)}, P_{G_{2_{\max}}}^{(k)}, P_{G_{2_{\min}}}^{(k)}, F_{1_{\max}}^{(k)}, F_{1_{\min}}^{(k)}, F_{2_{\max}}^{(k)}, F_{2_{\min}}^{(k)}\}$, for $k = 0, 1, 2$; and $\mathcal{J}_\lambda = \{S_{P_{1_{\max}}}^{(1)}, S_{P_{1_{\min}}}^{(1)}, S_{P_{1_{\max}}}^{(2)}, S_{P_{1_{\min}}}^{(2)}, S_{P_{2_{\max}}}^{(1)}, S_{P_{2_{\min}}}^{(1)}, S_{P_{2_{\max}}}^{(2)}, S_{P_{2_{\min}}}^{(2)}\}$. As each $\mathcal{J}_\pi(k)$ has 8 constraints, then $\mathcal{J}_\pi$ has in total 24 constraints.

The next step is to solve the UCOPF for $k = 0, 1, 2$. The umbrella set for each state is:

$$\begin{aligned}
\mathcal{U}_0 &= \{P_{G_{2_{\max}}}^{(0)}, F_{1_{\max}}^{(0)}\}, \\
\mathcal{U}_1 &= \{P_{G_{2_{\max}}}^{(1)}, F_{2_{\max}}^{(1)}\}, \\
\mathcal{U}_2 &= \{P_{G_{2_{\max}}}^{(2)}, F_{1_{\max}}^{(2)}\},
\end{aligned}$$

thus, $\mathcal{J}_\pi^U = \{P_{G_{2_{\max}}}^{(0)}, P_{G_{2_{\max}}}^{(1)}, P_{G_{2_{\max}}}^{(2)}, F_{1_{\max}}^{(0)}, F_{1_{\max}}^{(2)}, F_{2_{\max}}^{(1)}\}$. The size of the set is 6, or in other words, there are 6 umbrella constraints from the original set $\mathcal{J}_\pi$.

To obtain the final umbrella set $\mathcal{U}$, we solve (4.9) taking into consideration all the 14 constraints in $\mathcal{J}_\pi^U \bigcup \mathcal{J}_\lambda$. Table 4.3 shows the optimal slack variables values for this problem. The umbrella constraints are those associated with $s = 0$. Although there is a substantial reduction in the number of constraints taken into consideration, the results are the same from Table 4.2. Notice that for the two-bus example, $\mathcal{J}$ has 32 constraints. In this small example, the number of constraints for the umbrella discovery algorithm changes from $32^2 + 32 = 1,056$ to $14^2 + 14 = 210$, or an 80% decrease. If we consider the number of constraints taken into account for each UCOPF problem, then this decomposition has in total 426 constraints. Among these, 210 are from the last optimization problem considering only $\mathcal{J}_\pi^U \bigcup \mathcal{J}_\lambda$.

Table 4.3: Optimal slack variables using decomposition.

Constraint	s		
	$k=0$	$k=1$	$k=2$
$P_{G_{2_{\max}}}$	0.00	0.00	0.00
$F_{1_{\max}}$	0.36	-	0.00
$F_{2_{\max}}$	-	0.00	-
$S_{P_{1_{\max}}}$	-	0.00	0.00
$S_{P_{1_{\min}}}$	-	0.00	0.00
$S_{P_{2_{\max}}}$	-	0.00	0.00
$S_{P_{2_{\min}}}$	-	0.00	0.00

4.4.2 Security-Based Partitioning

Let $\mathcal{J}_\lambda = \bigcup_{k\in\mathcal{K},\, k\neq 0} \mathcal{J}_\lambda(k)$, where $\mathcal{J}_\lambda(k)$ is the set of security constraints coupling the intact system state and the state k. Consider the SC-LOPF problem (2.53) with only the constraints $\mathcal{J}(k) = \{\mathcal{J}_\pi(0), \mathcal{J}_\pi(k), \mathcal{J}_\lambda(k)\}$, or in other words, with state $k=0$ plus only one contingency state.

Consider that we solve the umbrella discovery problem (4.9) for the constraints in $\mathcal{J}(k)$, thus obtaining the umbrella constraint set $\mathcal{U}(k) \subseteq_U \mathcal{J}(k)$. The umbrella set $\mathcal{U}(k)$ has two subsets $\{\mathcal{U}^0(k), \mathcal{U}^k(k)\}$, where $\mathcal{U}^0(k) \subseteq \mathcal{J}_\pi(0)$ and $\mathcal{U}^k(k) \subseteq \{\mathcal{J}_\pi(k), \mathcal{J}_\lambda(k)\}$.

After solving n_c subproblems (4.9) for each $\mathcal{J}(k)$, we have an approximation of the umbrella set $\mathcal{U}$. Let the approximated umbrella set be $\tilde{\mathcal{U}} = \{\bigcap \mathcal{U}^0(k), \bigcup \mathcal{U}^k(k) \,|\, k \in \mathcal{K}, k \neq 0\} \subseteq \mathcal{U}$. Finally, to obtain $\mathcal{U}$, we need to solve (4.9) considering all the constraints in $\tilde{\mathcal{U}}$.

The main advantage of this method is that it considers the coupling between the intact system and each contingency state through the security constraints, while maintaining the problem (4.9) manageable. However, its main setback is that the constraints of the intact system is tested n_c times, resulting in unnecessary computational cost.

As the two-bus system is too small to demonstrate the benefits of this approach, this decomposition is applied to the 34-bus equivalent of the Hydro-Québec system, whose data is in Appendix A.

4.4.2.1 Hydro-Québec Example

The Hydro-Québec system has 64 lines, however only 58 line outages are considered in SCOPF studies since 6 lines (# 1, 2 , 3 , 4 , 5, and 6) directly connect generator buses to the system. The removal of such lines would simulate a generator outage, which is not in the scope of this study. Consequently, for this system, we have $J_{DC} = 8,840$, and thus the umbrella detection problem (4.9) has $78,154,440$ constraints and $300,560$ variables. Knowing this, if the problem is decomposed trough the Security-Based Partitioning method, i.e. if we solve considering only the constraints in $\mathcal{J}(k)$, the umbrella discovery problem for the decomposed problem is reduced to $84,390$ constraints and

$9,860$ variables. However, to obtain $\tilde{\mathcal{U}}$, it is necessary to solve (4.9) n_c times, bringing the total number of constraints to $4,894,620$ and of variables to $571,880$.

After decomposition, there are 260 constraints in $\mathcal{J}(k)$ and 26 constraints in $\mathcal{U}(k)$, for $k = 1, \ldots, 59$. In other words, for all the contingency states, these sets have the same length. The results obtained from the decomposed problem are given in Table 4.4. In the first column of this table are given the type of the constraint, the second column is the number of constraints of each set $\{\bigcup\{\mathcal{J}_\pi(k), \mathcal{J}_\lambda(k)\} \,|\, k \in \mathcal{K}, k \neq 0\}$, the third column is the number of umbrella constraints in the set $\{\bigcup \mathcal{U}^k(k) \,|\, k \in \mathcal{K}, k \neq 0\}$, and the last column is the percentual reduction in the number of constraints between second and third columns.

Table 4.4: 34-bus system result for constraints of all contingency states.

Type of Constraint	# Constraints	# Umbrella	Reduction
$P_{G_{\max}}$	348	336	03.45%
$P_{G_{\min}}$	348	56	83.91%
$F_{\max}$	3,654	0	100.00%
$F_{\min}$	3,654	1	99.97%
$S_{G_{\max}}$	348	336	03.45%
$S_{G_{\min}}$	348	336	03.45%
Total	8,700	1,083	86.89%

As $\tilde{\mathcal{U}} = \{\bigcap \mathcal{U}^0(k), \bigcup \mathcal{U}^k(k) \,|\, k \in \mathcal{K}, k \neq 0\}$, it is also necessary to obtain $\bigcap \mathcal{U}^0(k)$, for $k \in \mathcal{K}, k \neq 0$. Therefore, Table 4.5 shows the results for the intact system. The first column shows the type of the constraint, the second column is the number of constraints in $\mathcal{J}_\pi(0)$, the third column is the number of umbrella constraints in $\{\bigcup \mathcal{U}^0(k) \,|\, k \in \mathcal{K}, k \neq 0\}$, and the last is the percentual reduction of constraints between column 2 and 3. As such, $\tilde{\mathcal{U}}$ has $1,090$ constraints, or a reduction of 87.67% in relation with J_{DC}.

Table 4.5: Total number of constraints and umbrella constraints for the intact system.

Type of Constraint	# Constraints	# Umbrella	Reduction
$P_{G_{\max}}$	6	6	00.00%
$P_{G_{\min}}$	6	1	83.33%
$F_{\max}$	64	0	100.00%
$F_{\min}$	64	0	100.00%
$S_{G_{\max}}$	0	0	-
$S_{G_{\min}}$	0	0	-
Total	140	7	95.00%

Next, when the umbrella constraint discovery problem is solved for the constraints in $\tilde{\mathcal{U}}$, the final umbrella set $\mathcal{U} = \tilde{\mathcal{U}}$. As such, this example has an exact approximation of umbrella set.

Both Tables 4.4 and 4.5 shows an impressive decrease in the number of line constraints. This observation inspires a line-based decomposition scheme [16], as discussed in the next section.

4.4.3 Line-Based Partitioning

Let $\mathcal{J} = \{\mathcal{J}_\pi^g, \mathcal{J}_\pi^l, \mathcal{J}_\lambda\}$, where $\mathcal{J}_\pi^g$ is the set of power generation constraints and $\mathcal{J}_\pi^l$ is the set of line constraints. These sets can be rewritten as $\mathcal{J}_\pi^g = \{P_{G_{i\max}}, P_{G_{i\min}} \,|\, i \in \mathcal{G}\}$, and $\mathcal{J}_\pi^l = \{F_{l_{\max}}, F_{l_{\min}} \,|\, l \in \mathcal{L}\}$.

Instead of solving problem (4.9) with all the constraints in $\mathcal{J}$, it is possible to solve it by first identifying the constraints in $\mathcal{J}_\pi^l$:

$$\begin{aligned} \min_{\mathbf{w},\mathbf{s}} \quad & \sum_{j \in \mathcal{J}_\pi^l} s_j \\ \text{subject to} \quad & \hat{\mathbf{A}}_\delta \mathbf{w}_j \leq \hat{\mathbf{c}}_\delta, && \forall j \in \mathcal{J}_\pi^l \\ & \hat{\mathbf{a}}_{\delta_j}^\top \mathbf{w}_j + s_j \geq \hat{c}_{\delta_j}, && \forall j \in \mathcal{J}_\pi^l \\ & s_j \geq 0. && \forall j \in \mathcal{J}_\pi^l \end{aligned} \tag{4.29}$$

Let $\mathcal{U}^l$ be the set of umbrella constraints obtained by solving (4.29). As seen before, there is a potentially significant number of non-umbrella constraints in $\mathcal{J}_\pi^l$. Let $\tilde{\mathcal{J}} = \{\mathcal{J}_\pi^g, \mathcal{U}^l, \mathcal{J}_\lambda\}$, then $\tilde{\mathcal{J}}$ is expected to be significantly smaller than $\mathcal{J}$. Finally, we can solve the reduced problem:

$$\begin{aligned} \min_{\mathbf{w},\mathbf{s}} \quad & \sum_{j \in \tilde{\mathcal{J}}} s_j \\ \text{subject to} \quad & \mathbf{A}_\epsilon \mathbf{w}_j \leq \mathbf{c}_\epsilon, && \forall j \in \tilde{\mathcal{J}} \\ & \mathbf{a}_{\epsilon_j}^\top \mathbf{w}_j + s_j \geq c_{\epsilon_j}, && \forall j \in \tilde{\mathcal{J}} \\ & s_j \geq 0, && \forall j \in \tilde{\mathcal{J}} \end{aligned} \tag{4.30}$$

where $\mathbf{A}_\epsilon$ and $\mathbf{c}_\epsilon$ are $\hat{\mathbf{A}}_\delta$ and $\hat{\mathbf{c}}_\delta$ considering only the constraints in $\tilde{\mathcal{J}}$, respectively.

To demonstrate the effectiveness of this approach, consider the same 34-bus example. The cardinality of $\mathcal{J}_\pi^l$ is $7,436$, but $\mathcal{U}^l$ has only one constraint. The only umbrella line constraint in $\mathcal{U}^l$ is the lower power flow limit of line 20 at the contingency state 20, when line 26 is disconnected. Hence, for this problem, there are $1,405$ constraints in $\tilde{\mathcal{J}}$. This is already a significant reduction from the original $J_{DC} = 8,840$ constraints, and a good approximation for $\mathcal{U}$, which contains $1,090$ umbrella constraints.

4.5 CONCLUSION

The umbrella discovery algorithm was introduced with two SC-LOPF examples to showcase the algorithm potential in reducing the number of constraints. Furthermore, some partitioning schemes were described to decrease computational cost of the umbrella discovery problem, among them two were first introduced in this thesis (Contingency-based and Security-based partitionings).

Next chapter derives a new umbrella discovery algorithm for non-linear problems based on the use of semidefinite programming.

5 SEMIDEFINITE UMBRELLA DISCOVERY ALGORITHM

5.1 INTRODUCTION

The main advantage of solving the UCD problem is to identify the constraints that form the feasible set, i.e. the minimal number of constraints needed to solve a problem. This is specially beneficial for very large problems, such as the SC-LOPF. There is a substantial reduction of constraints in the SC-LOPF when the UCD is solved, as shown in [4]. Nonetheless, there are some shortcomings in using SC-LOPF, e.g. it does not take into consideration reactive power and voltage constraints [23].

In this study, we propose an extended UCD problem to identify the umbrella constraints of the SCOPF problem, although the UCD is only capable of solving convex problems. As previously shown, the SDP is a powerful tool to convexify a problem and to obtain an approximate global solution. The convexification is essential to extend the UCD algorithm to the SCOPF.

This chapter extends the UCD algorithm to detect the umbrella constraints of the SCOPF problem and proposes some strategies to reduce computational cost of the UCD algorithm.

5.2 NON-CONVEX UMBRELLA CONSTRAINT IDENTIFICATION

Consider a set of non-convex inequalities constraints $C = \{x \in \mathbb{R}^n \,|\, h_i(\mathbf{x}) \leq c_i \,,\, i = 1, \ldots, m\}$, and the following optimization problem:

$$\begin{array}{ll} \min\limits_{\mathbf{x}} & p(\mathbf{x}) \\ \text{subject to} & h_i(\mathbf{x}) \leq c_i,\ i = 1, \ldots, m \end{array} \tag{5.1}$$

The identification of the umbrella constraints of (5.1) imposes a challenge, as the use of slack variables to identify umbrella constraints is only valid for convex problems, such as the SC-LOPF. This becomes clear when we analyze Fig. 5.1, which depicts a non-convex set defined by two umbrella constraints (h_1 and h_2). Consider that the umbrella detection algorithm is initialized at two different points, a and b, and due to the nonlinearities, follows two different directions represented by the arrows in the figure. When starting at point a, the algorithm will indicate only h_1 as umbrella constraint. On the other hand, if the initial point is b, only h_2 will be identified as umbrella constraint. The two identifications would be wrong since both h_1 and h_2 are umbrella constraints.

Therefore, problem (4.8) can only be used to detect the umbrella constraints of convex problems, else there may not be an unique solution. However, some of the observations made in Chapter 4 are still valid:

- There is at least a point $\mathbf{w}$ lying on an umbrella constraint that is feasible to all the other constraints;
- There is not a point on a non-umbrella constraint that is feasible to all constraints of the problem.

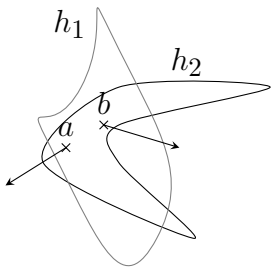

Figure 5.1: Non-convex feasible space defined by two constraints.

These observations indicate that the approach taken in Chapter 4 is still viable, but it can provide an incorrect umbrella constraint set. Consider the following problem, which is built from (5.1) in order to identify the umbrella constraints of this problem:

$$\min_{\mathbf{w}} \quad F = \sum_{j=1}^{m} s_j \tag{5.2a}$$

$$\text{subject to} \quad h_{j'}(\mathbf{w}_j) \leq c_{j'},\ j' = 1, \ldots, m \tag{5.2b}$$

$$h_j(\mathbf{w}_j) + s_j \geq c_j, \tag{5.2c}$$

$$s_j \geq 0 \tag{5.2d}$$

$$\text{for all } j = 1, \ldots, m \tag{5.2e}$$

Unfortunately, the solution to (5.2) may not be unique, whereas there is only one set of umbrella constraints. This is true, as (5.2) convexity is not guaranteed. Thus, it is necessary to ensure that the solution to this problem is unique and correctly indicates the set of umbrella constraints. One way to achieve this is by using SDP, as it will approximate the feasible set of problem (5.2) by a convex feasible set. In case (5.1) is a quadratically constrained quadratic problem, as the SCOPF, so is problem (5.2). Therefore, a second-order SDP relaxation can be applied to (5.2) [32]. If second-order approximation is used, constraints $h_j(\mathbf{x}), j = 1, \ldots, m$ are linear in the lifted space. Due to these properties, the optimal solution to the lifted umbrella detection problem is unique. Hence, the SDP Umbrella Constraint Discovery (SDP-UCD) problem is as follows:

$$\min_{\mathbf{y}} \quad L_y\{F = \sum_{j=1}^{m} s_j^2\} \tag{5.3a}$$

$$\text{subject to} \quad L_y\{h_{j'}(\mathbf{w}_j)\} \leq c_{j'},\ j' = 1, \ldots, m \tag{5.3b}$$

$$L_y\{h_j(\mathbf{w}_j) + s_j\} \geq c_j, \tag{5.3c}$$

$$L_y\{s_j\} \geq 0, \tag{5.3d}$$

$$L_y\{\mathbf{Z}\} \succeq 0, \tag{5.3e}$$

$$\text{for all } j = 1, \ldots, m, \tag{5.3f}$$

$L_y\{\mathbf{Z}\}$ is the order-1 moment matrix, which is defined as follows: Define vector $\mathbf{z} = [1, \mathbf{w}^\top, \mathbf{s}^\top]$ and matrix $\mathbf{Z} = \mathbf{z}\mathbf{z}^\top$, where $\mathbf{w}^\top = [\mathbf{w}_1^\top, \mathbf{w}_2^\top, \ldots, \mathbf{w}_m^\top]$. The components of $\mathbf{Z}$ are all the monomials in $\mathbf{w}_j$ and s_j, $\forall j$, with degree 0, 1 and 2. After building $\mathbf{Z}$, replace each monomial in this matrix by the associated lifted variable. The resulting matrix is $L_y\{\mathbf{Z}\}$, which is symmetric.

The solution of (5.3) is relaxed, i.e. there may be non-umbrella constraints in the solution. In addition, by comparing problem (5.3) with problem (4.9), we notice that the objective functions are different. This occurs because simulations have shown that numerical conditioning of the lifted problem improves if the original objective function is $F = \sum_{j=1}^{m} s_j^2$.

As mentioned in Chapter 3 , the optimal cost of the solution to the SDP relaxed problem is a lower bound to the optimal cost of the solution to the original problem. In the case of problem (5.3), the cost function is the sum of squared slack variables. As a consequence of this optimistic approach, we obtain a conservative answer, i.e. an increase in false-positive for the umbrella constraint identification (as s tends to 0). This may be problematic to determine a limit value for a slack variable, below which the associated constraint is considered umbrella. One way to tackle this issue is by creating a recovery method to obtain a solution to the original problem.

However, the recovery method must differentiate an umbrella constraint ($s_j = 0$) from a non-umbrella one ($s_j > 0$). The difficulty arises when the lifted variable associated to s, due to algorithm tolerance and SDP approximation, is very close to zero (e.g, 10^{-5}), but the related constraint is not umbrella. The opposite can also be true, that is, the lifted variable is slightly higher that a given tolerance (e.g., 10^{-4}), but is associated to an umbrella constraint.

5.2.1 Example

In order to better illustrate the SDP-UCD algorithm, consider the following non-convex optimization problem:

$$\begin{array}{ll} \min\limits_{\mathbf{x}} & f_c = x_1 + x_2 \\ \text{subject to} & h_1(\mathbf{x}) = x_2 - 10 \leq 0, \\ & h_2(\mathbf{x}) = -x_2 + x_1^2 \leq 0, \\ & h_3(\mathbf{x}) = -x_1 + x_2 - 6 \leq 0 \\ & h_4(\mathbf{x}) = -\frac{1}{2}x_2 + \frac{1}{2}x_1^2 + 2.5 \geq 0. \end{array} \tag{5.4}$$

The optimal solution to (5.4) is $x_1 = -0.50$ and $x_2 = 0.25$, while its graphical representation is shown by Fig. 5.2, where the solid line is the constraint h_1, the dashed line is for h_2, the dash-dotted line is for h_3, and the dotted line is for h_4. The feasible set is the area between both parabolas (shaded in light gray) and limited by the dash-dotted line.

By analyzing Fig. 5.2, it can be easily concluded that constraints h_2, h_3 and h_4 are umbrella, while h_1 is not. To reach the same conclusion, it is possible to use the SDP-UCD problem (5.3). Thus, (5.4) equivalent lifted problem is:

$$\begin{array}{ll} \min\limits_{\mathbf{y}} & L_y\{s_1^2 + s_2^2 + s_3^2 + s_4^2\} \\ \text{subject to} & L_y\{h_1(\mathbf{w}_1)\} \leq 0, \\ & L_y\{h_2(\mathbf{w}_1)\} \leq 0, \\ & L_y\{h_3(\mathbf{w}_1)\} \leq 0, \\ & L_y\{-h_4(\mathbf{w}_1)\} \leq 0, \\ & L_y\{h_1(\mathbf{w}_1) + s_1\} \geq 0, \\ & L_y\{h_1(\mathbf{w}_2)\} \leq 0, \\ & L_y\{h_2(\mathbf{w}_2)\} \leq 0, \\ & L_y\{h_3(\mathbf{w}_2)\} \leq 0, \\ & L_y\{-h_4(\mathbf{w}_2)\} \leq 0, \\ & L_y\{h_2(\mathbf{w}_2) + s_2\} \geq 0, \\ & L_y\{h_1(\mathbf{w}_3)\} \leq 0, \\ & L_y\{h_2(\mathbf{w}_3)\} \leq 0, \\ & L_y\{h_3(\mathbf{w}_3)\} \leq 0, \\ & L_y\{-h_4(\mathbf{w}_3)\} \leq 0, \\ & L_y\{h_3(\mathbf{w}_3) + s_3\} \geq 0, \\ & L_y\{h_1(\mathbf{w}_4)\} \leq 0, \\ & L_y\{h_2(\mathbf{w}_4)\} \leq 0, \\ & L_y\{h_3(\mathbf{w}_4)\} \leq 0, \\ & L_y\{-h_4(\mathbf{w}_4)\} \leq 0, \\ & L_y\{-h_4(\mathbf{w}_4) + s_4\} \geq 0, \\ & L_y\{\mathbf{s}\} \geq 0, \\ & L_y\{\mathbf{Z}\} \succeq 0, \end{array} \tag{5.5}$$

where vectors $\mathbf{w}_1$, $\mathbf{w}_2$, $\mathbf{w}_3$ e $\mathbf{w}_4$ have two components, which correspond to x_1 and x_2 in the original problem.

Table 5.1 presents the solution to problem (5.5). The feasible set of the equivalent lifted problem of (5.4) is the shaded area (light and dark gray) in Fig. 5.2. Notice that the feasible set is larger than the original one.

Table 5.1: Optimal values of the lifted variables.

Constraint tested	$L_y\{x_1\}$	$L_y\{x_2\}$	$L_y\{x_1^2\}$	$L_y\{s\}$
$L_y\{h_1\}$	-3.00	9.00	9.00	1.00
$L_y\{h_2\}$	-0.05	1.49	1.49	1.94×10^{-4}
$L_y\{h_3\}$	1.17	4.83	3.28	1.97×10^{-4}
$L_y\{h_4\}$	-0.18	5.36	0.36	2.11×10^{-4}

The optimal point for $L_y\{h_1\}$ is $(L_y\{x_1\}, L_y\{x_2\})$ and is shown as a bullet, for $L_y\{h_2\}$ is $(\sqrt{L_y\{x_1^2\}}, L_y\{x_2\})$ and is shown as a triangle, for $L_y\{h_3\}$ is $(L_y\{x_1\}, L_y\{x_2\})$ and is shown as a star, for $L_y\{h_4\}$ is $(\sqrt{L_y\{x_1^2\}}, L_y\{x_2\})$ and is shown as a hexagram. The coordinates chosen are in accordance with each monomials used in each constraint. Therefore, there are some important remarks to be made for this result:

1. If we follow the same procedure used by the linear UCD, from the optimal values of $L_y\{s\}$ it seems very straightforward to classify a constraint as umbrella or not. However, $L_y\{s\}$ is the lifted variable for the monomial s. Therefore, $L_y\{s\}$ and s may have significant divergence in value if the SDP approximation is not good;

2. When checking a linear constraint, the optimal points $(L_y\{x_1^*\}, L_y\{x_2^*\})$ are on the constraint in the original problem. Nevertheless, the same cannot be said when the constraint is non-convex. This happens because the solution of the lifted problem is not the same for the original one. In other words, the optimal value of the SDP problem is a point in the lifted space, not in the original problem;

3. As the solution given by Table 5.1 is to the lifted problem, one can say that if the approximation made is not good enough, then optimal point $(L_y\{x_1^*\}, L_y\{x_2^*\})$ on the lifted constraint may not lie on the original constraint. This may cause two problems: a very conservative solution (i.e. more umbrella constraints detected than there are in fact) and a harder solution recovery. This can be observed in Table 5.1, where $(L_y\{x_1\})^2$ is not always equal to $L_y\{x_1^2\}$, such as in constraints h_2, h_3, and h_4 (all non-linear);

4. One possible consequence of the SDP-UCD is that a solution for a given constraint may have a very small $L_y\{s\}$, but such small $L_y\{s\}$ is only valid for the lifted space. If this approximation is not good enough, the equivalent original constraint may not be umbrella, even with a small $L_y\{s\}$. This is expected, as the SDP is a conservative algorithm (provides a lower bound for the optimal value of the objective function), but the approximation may cause some constraints to be wrongly classified if only $L_y\{s\}$ is checked;

By taking into consideration all these remarks, one can conclude that a method to recover the set of umbrella constraints should be implemented. One possible approach is to consider a $L_y\{s\}$ threshold to eliminate evident non-umbrella constraints (e.g.

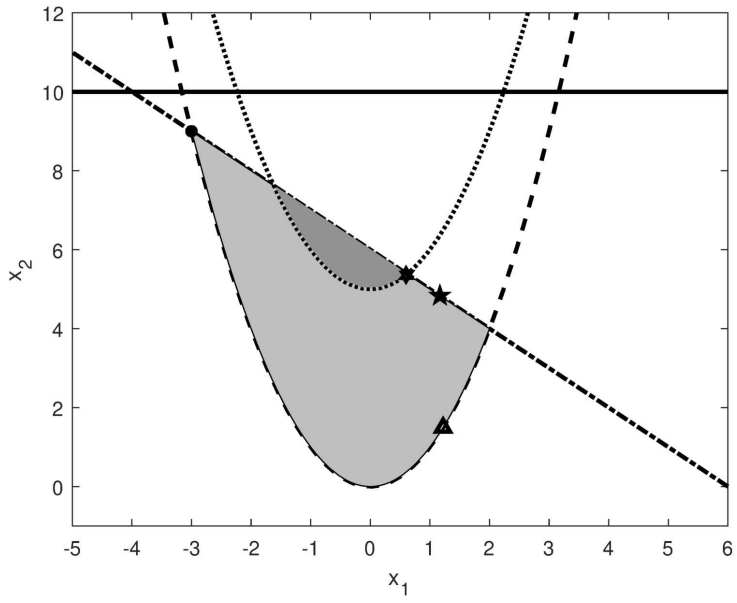

Figure 5.2: Graphical representation of (5.4).

$L_y\{s\} \geq 1$). If it is over the threshold, it is classified as non-umbrella. Otherwise, recover the solution.

Therefore, the SDP-UCD identified correctly all the constraints of problem (5.4). However, the algorithm has some shortcomings regarding the umbrella constraint detection. The main one is that the the value of $L_y\{s\}$ at the optimal solution to (5.5) do not indicate with certainty that a given constraint is umbrella or not, as the optimal solution is in the lifted space. In this study, we propose a method to classify each constraint after solving problem (5.3), which will be discussed in section 5.3.2.

5.3 SCOPF-UCD

Previous applications of SDP to obtain global solutions to the SCOPF have shown that SDP provides good approximations for the feasible set of this problem [38, 40, 42]. The SCOPF is a quadratically constrained quadratic problem, and so is the non-convex UCD problem to identify SCOPF umbrella constraints.

Our goal is to determine the set of umbrella constraints that defines the feasible set of (2.48). As such, to check for the umbrella constraints of the SCOPF problem, vector $\mathbf{w_j}$ has $2n_b - 1$ components and J_{AC} slack variables will be needed. Furthermore, the ratio of the number of constraints in the SCOPF and SC-LOPF is given in (5.6). As the SCOPF is considerably larger that the SC-LOPF, to identify the umbrella constraints of the SCOPF, we need to solve a very large umbrella detection problem. In addition to being very large, the non-linear SCOPF problem is also non-convex. Some methods proposed to address this issue are presented in section 5.3.1.

$$\frac{J_{AC}}{J_{DC}} \approx \frac{4n_g + n_b + 2n_l - 2}{2n_g + n_l - 1} > 2 \tag{5.6}$$

Taking into consideration the properties discussed in section 5.2, we can solve the SDP-UCD problem (5.3) by taking consideration the J_{AC} SCOPF constraints of problem (2.49).

5.3.1 Computational Complexity Reduction

Problem (5.3) is useful for obtaining the umbrella constraints of a non-convex problem. However, the SCOPF can be a considerably large problem, and SDP relaxation has some shortcomings, especially the increase in the number of variables of the optimization problem. This combination of negative points can make problem (5.3) extremely large and computationally demanding.

In order to address this issue, the present study reduces the number of variables in (5.3) by first introducing a series of procedures are used to decompose (5.3) into smaller problems that can be independently solved. Subsequently, by replacing matrix $\mathbf{M}(\mathbf{y})$ by a block diagonal matrix $\hat{\mathbf{M}}(\mathbf{y})$. Afterwards, the constraint $\mathbf{M}(\mathbf{y}) \succeq 0$ is substituted by a set of constraints which imposes that each submatrix of $\hat{\mathbf{M}}(\mathbf{y})$ be semidefinite positive.

5.3.1.1 Partitioning

The partitioning of problem (5.3) is accomplished by using the methodologies described in section 4.4. All considerations established in that section are still valid. Thus, consider the inequality constraint set $\mathcal{J} = \{\mathcal{J}_\pi^{g,v}, \mathcal{J}_\pi^l, \mathcal{J}_\lambda\}$, where $\mathcal{J}_\pi^{g,v}$ is the set of power generation and bus voltage constraints. Hence, problem (5.3) can be partitioned in the following way:

1. Determine the constraint set $\mathcal{J} = \{\mathcal{J}_\pi^{g,v}, \mathcal{J}_\pi^l, \mathcal{J}_\lambda\}$;
2. By using contingency-based partitioning, it is possible to define the constrain set $\mathcal{J}_\pi(k) = \{\mathcal{J}_\pi^{g,v}(k), \mathcal{J}_\pi^l(k)\}$, where k is the contingency index;
   a) By using line-based partitioning, solve (5.3) for $\mathcal{J}_\pi^l(k)$, where $k = 0, \ldots, n_c$. Define each umbrella set identified after solving it as $\mathcal{U}_k^l$;
   b) Consider the constraint set $\tilde{\mathcal{J}}_\pi(k) = \{\mathcal{J}_\pi^{g,v}(k), \mathcal{U}_k^l\}$. Solve problem (5.3) for each $\tilde{\mathcal{J}}_\pi(k)$, where $k = 0, \ldots, n_c$. The output of each iteration is the umbrella set $\tilde{\mathcal{U}}_k$;
   c) Set an initial umbrela set: $\tilde{\mathcal{U}}^\alpha = \bigcup \tilde{\mathcal{U}}_k$;
3. Define $\tilde{\mathcal{J}}_\alpha = \{\tilde{\mathcal{U}}^\alpha, \mathcal{J}_\lambda\}$;
4. By using security-based partitioning, we can obtain the constraint set $\tilde{\mathcal{J}}_\alpha(k) = \{\tilde{\mathcal{U}}^\alpha(0), \tilde{\mathcal{U}}^\alpha(k), \mathcal{J}_\lambda(k)\}$;
5. Solve problem (5.3) for each $\tilde{\mathcal{J}}_\alpha(k)$, where $k = 1, \ldots, n_c$. The umbrella set determined by the solution of the problem is $\tilde{\mathcal{U}}^\beta(k)$;
6. The approximate umbrella constraint set is $\tilde{\mathcal{U}} = \bigcup \tilde{\mathcal{U}}^\beta(k)$;

7. If an exact approximation is required, solve problem (5.3) by considering only the constraints in $\tilde{\mathcal{U}}$. The solution is the original problem exact umbrella set $\mathcal{U}$.

Notice that two approximate umbrella sets are obtained: $\tilde{\mathcal{U}}^{\alpha}$ and $\tilde{\mathcal{U}}$. It is expected that the cardinality of $\tilde{\mathcal{U}}^{\alpha}$ be considerably lower than that of $\mathcal{J}$. This is due to the fact that the partitioning in step 2 splits the SCOPF problem into $n_c + 1$ OPF problems, each one with a different network characteristic due to the contingency or pre-contingency. Thus, $\tilde{\mathcal{U}}^{\alpha}$ is the set of all umbrella constraints for all $n_c + 1$ OPF problems. Therefore, it is expected that step 2 to be the most impactful step in the partitioning method. Simulations have shown that the benefits of steps 3 to 7 are marginal, in comparison to steps those of 1 to 2.

5.3.1.2 Sparsity Exploitation

One difficulty faced in solving large scale SDP problems is that the moment matrix $\mathbf{M}(\mathbf{y})$ is fully dense, even when all coefficients matrices $\mathbf{A}_j$ in the SDP problem (3.11) are sparse [43]. One approach reduce the number of variables of the SDP problem is to solve a matrix completion problem for $\mathbf{M}(\mathbf{y})$.

The objective of the matrix completion problem is to determine whether partially specified matrices can be completed to fully specified matrices satisfying certain desired properties.

Consider the induced subgraph of an undirected graph $G = (V, E)$, where V is a set of nodes and E a set of edges, being of the form $H = (U, F)$ where $U \subseteq V$ and $F \coloneqq \{ij \in E : i, j \in U\}$. As the moment matrix is a partial semidefinite matrix, there is a matrix completion if and only if it has a sparsity pattern expressed by a chordal graph, H [44]. In the case of the SDP problem, the goal is to determine a block diagonal matrix $\hat{\mathbf{M}}(\mathbf{y})$ that is semidefinite positive if and only if the moment matrix also is. If we can find $\hat{\mathbf{M}}(\mathbf{y})$, then the constraint $\mathbf{M}(\mathbf{y}) \succeq 0$ can be replaced by a set of constraints imposing that the submatrices in the diagonal of $\hat{\mathbf{M}}(\mathbf{y})$ be semidefinite positive, which can substantially reduce the number of variables in the problem.

To obtain $\hat{\mathbf{M}}(\mathbf{y})$ it is necessary to know the sparsity structure of the original problem, that is, to derive a symmetric zero-one matrix, $\mathbf{R}$, with number of rows/columns equal to the number of variables of the original problem, and with $\mathbf{R}_{ij} = 1$ if and only if variables x_i and x_j appear together in a given constraint or in the objective function of this problem. For the UCD-SCOPF problem, $\mathbf{R}$ is obtained from the bus admittance matrices of the system, $\mathbf{Y}^{(k)}$, defined for every contingency state, k. The reason for such choice is that a nonzero element in the ith line and jth column of $\mathbf{Y}^{(k)}$, determines which variables $e_i^{(k)}$, $e_j^{(k)}$, $f_i^{(k)}$ and $f_j^{(k)}$ appear together in a constraint of the SCOPF problem.

For the UCD-SCOPF problem, it is also necessary to indicate whether a given slack variable appear together with variables $e_i^{(k)}$, $e_j^{(k)}$, $f_i^{(k)}$ or $f_j^{(k)}$ in the same constraint. However, as a particular slack variable is assigned to each constraint of (5.2), to obtain matrix $\mathbf{R}$ for the UCD problem, first of all, $\mathbf{R}$ is derived using the bus admittance matrices. Subsequently, new rows/columns are added to $\mathbf{R}$, each one corresponding to a slack variable of (5.2), and new nonzero elements are introduced in $\mathbf{R}$ at the positions

corresponding the variables $e_i^{(k)}$, $e_j^{(k)}$, $f_i^{(k)}$ or $f_j^{(k)}$ that appear in the same constraint as the slack variable. $\mathbf{R}$ is the adjacency matrix of $G = (V, E)$.

For demonstration purposes, consider the example (3.43). We want to check if the upper and lower voltage limit inequality are umbrella or not. The UCD-SCOPF problem has twice the number of constraints of (3.43) plus 2 additional constraints:

$$\mathbf{w}_{1_{e_2^2}} + \mathbf{w}_{1_{f_2^2}} + 1.1025 + s_1 \geq 0, \tag{5.7a}$$

$$-\mathbf{w}_{2_{e_2^2}} - \mathbf{w}_{2_{f_2^2}} + 0.9025 + s_2 \geq 0, \tag{5.7b}$$

where the variable vector is $[\mathbf{w}_1, \mathbf{w}_2, s_1, s_2]$ and has size 6. This is due to the fact that $\mathbf{w}_1$ and $\mathbf{w}_2$ each has size 2.

To show the sparsity of the problem, consider the $\bar{\mathbf{Y}}$ matrix. As the constraints of (2.49) appear twice in the UCD-SCOPF, we can consider that we have two OPF problems. Thus, we create a block diagonal matrix, where each submatrix is derived from the admittance matrix of the system, $\bar{\mathbf{Y}}$, by substituting nonzero elements of $\bar{\mathbf{Y}}$ by 1:

$$\begin{bmatrix} 1 & 1 & 0 & 0 \\ 1 & 1 & 0 & 0 \\ 0 & 0 & 1 & 1 \\ 0 & 0 & 1 & 1 \end{bmatrix} \tag{5.8}$$

Then, we add to the block diagonal matrix in (5.8) two rows and columns corresponding to s_1 and s_2. To each line i of the new columns (columns 5 and 6) corresponds a variable in $\mathbf{w}_1$ or $\mathbf{w}_2$. The component at position $(i, 6)$ is set to 1 if the corresponding variable appears together with s_1 in a constraint of the problem. Similar procedure is adopted to complete column 6. Finally, as the matrix is symmetric, two new rows are set equal to the two new columns. The final matrix is:

$$\mathbf{R} = \begin{bmatrix} 1 & 1 & 0 & 0 & 1 & 0 \\ 1 & 1 & 0 & 0 & 1 & 0 \\ 0 & 0 & 1 & 1 & 0 & 1 \\ 0 & 0 & 1 & 1 & 0 & 1 \\ 1 & 1 & 0 & 0 & 1 & 0 \\ 0 & 0 & 1 & 1 & 0 & 1 \end{bmatrix} \tag{5.9}$$

Once $\mathbf{R}$ is obtained, the matrix completion problem can be solved. As $\mathbf{M}(\mathbf{y})$ is a partial semidefinite matrix, there is a matrix completion if and only if it has sparsity pattern expressed by a chordal[1] graph [44]. However, if $\mathbf{M}(\mathbf{y})$ does not satisfy the requirements of being expressed via chordal graph, there are many algorithms to determine and add the number of necessary edges to obtain a chordal graph [44]. In this

[1]A chordal graph is one in which all cycles of four or more vertices have a chord, which is an edge that is not part of the cycle but connects two vertices of the cycle. Equivalently, every induced cycle in the graph should have exactly three vertices.

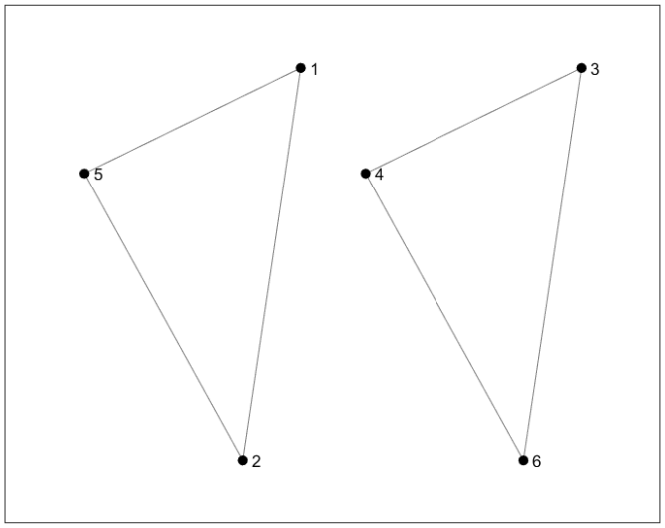

Figure 5.3: The graph G plot.

study, we use the decomposing algorithm introduced in [45]. To show case how it works, let's use it on example (3.43). Remember that example (3.43) has a sparse structure $\mathbf{R}$ derived earlier, and it is the adjacency matrix of the graph G, shown by Fig. 5.3. The variables $e_i^{(k)}$, $e_j^{(k)}$, $f_i^{(k)}$, $f_j^{(k)}$, s_1, and s_2 are represented by nodes 1, 2, 3, 4, 5, and 6, respectively.

The algorithm first solves the minimum fill-in problem of graph G using the sparse structure. That is, it finds a triangulation of a graph that minimizes the number of added edges [46]. After identifying the node with the minimum fill-in, the triangulation is stored (called bag, $\mathcal{B}$) and the node is removed from the graph. Repeat this process until the all nodes were accounted for. This means that at least the last bag ($\mathcal{B}_p$) have only one node. The identified bags are shown by Fig. 5.4.

For illustrative purposes, if we add an edge linking nodes 2 and 4, almost all the bags will be the same, except that instead of a bag with only node 5, there will be one with nodes 2 and 4.

Now let each bag ($\mathcal{B}_i$) act as an index of $\mathbf{M}(\mathbf{y})$'s elements to create a submatrix. This means that the $\hat{\mathbf{M}}(\mathbf{y})$ matrix is:

$$\hat{\mathbf{M}}(\mathbf{y}) = \begin{bmatrix} \mathbf{M}(\mathbf{y})\{\mathcal{B}_1, \mathcal{B}_1\} & \mathbf{0} & \cdots & \mathbf{0} \\ \mathbf{0} & \mathbf{M}(\mathbf{y})\{\mathcal{B}_2, \mathcal{B}_2\} & \cdots & \mathbf{0} \\ \vdots & & \ddots & \\ \mathbf{0} & \cdots & & \mathbf{M}(\mathbf{y})\{\mathcal{B}_p, \mathcal{B}_p\} \end{bmatrix}. \tag{5.10}$$

Concluding the example shown, the original SDP problem had a 6 by 6 moment matrix. This means we would have to consider 21 lifted variables. By decomposing the problem into 6 small matrices, we now only have 12 variables. For completeness sake, the submatrices are as follows: $\mathbf{M}(\mathbf{y})\{\mathcal{B}_1, \mathcal{B}_1\}$ is a 3 by 3 matrix composed by rows/columns

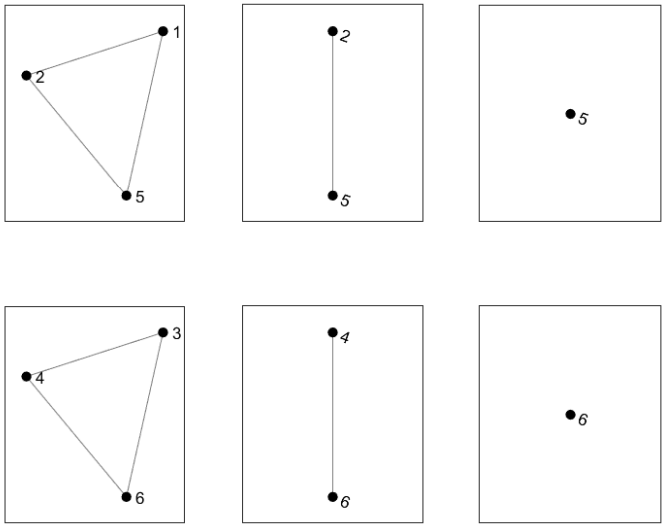

Figure 5.4: The bags of graph G.

1,2, and 5 of $\mathbf{M}(\mathbf{y})$; $\mathbf{M}(\mathbf{y})\{\mathcal{B}_2, \mathcal{B}_2\}$ is a 2 by 2 matrix composed by rows/columns 2, and 5; $\mathbf{M}(\mathbf{y})\{\mathcal{B}_3, \mathcal{B}_3\}$ is a 1 by 1 matrix composed by the fifth row and column; $\mathbf{M}(\mathbf{y})\{\mathcal{B}_4, \mathcal{B}_4\}$ is a 3 by 3 matrix composed by rows/columns 3,4, and 6 of $\mathbf{M}(\mathbf{y})$; $\mathbf{M}(\mathbf{y})\{\mathcal{B}_5, \mathcal{B}_5\}$ is a 4 by 6 matrix composed by rows/columns 2, and 5; and $\mathbf{M}(\mathbf{y})\{\mathcal{B}_6, \mathcal{B}_6\}$ is a 1 by 1 matrix composed by the sixth row and column. Therefore, $\hat{\mathbf{M}}(\mathbf{y})$ is a 6×6 block diagonal matrix.

Finally, if $\mathbf{M}(\mathbf{y})\{\mathcal{B}_m, \mathcal{B}_m\} \succeq 0$ for every $m \in \{1, \ldots, p\}$, then $\mathbf{M}(\mathbf{y})$ is also semidefinite positive. Therefore, the optimal objective value of the SCOPF-UCD does not change if the constraint $\mathbf{M}(\mathbf{y}) \succeq 0$ is replaced by the equivalent constraints $\mathbf{M}(\mathbf{y})\{\mathcal{B}_m, \mathcal{B}_m\} \succeq 0$ for every $m \in \{1, \ldots, p\}$.

After solving the SCOPF-UCD problem using this decomposition algorithm, the moment matrix's elements that wasn't considered in the sparse structure matrix $\mathbf{R}$ may have been disregarded by the numerical algorithm. Therefore, the solution matrix is a partial semidefinite matrix. This means that we can use any well-known polynomial-time algorithm to fill a partially-known real-valued matrix. The resulting matrix will have the same rank as the highest rank among all bags [44].

5.3.2 Recovery Method

Consider that problem (5.3) was solved, and at the solution, $\mathbf{y}_j = L_y\{\mathbf{w}_j\}$ and $y_{s_j} = L_y\{s_j\}$. By solving (5.3), the objective is to determine an umbrella constraint set, and the same can be said about the recovery method. In other words, it is not in the scope of the algorithm to recover $\mathbf{w}_j$ and s_j, but to indicate whether or not a constraint is umbrella.

One way to recover the original's problem solution is by searching for the local optimal close to the optimal solution to (5.3). This can be achieved by minimizing the

difference between the original's and SDP-UCD's optimal solutions, while solving for the same constraints in SDP-UCD. The recovery problem is then:

$$\begin{array}{ll} \min\limits_{\mathbf{w}_j} & F = \frac{1}{2}\left\|\mathbf{w}_j - \mathbf{y}_j\right\| \\ \text{subject to} & h_{j'}(\mathbf{w}_j) \leq c_{j'},\ j' = 1,\ldots,m, \\ & h_j(\mathbf{w}_j) + s_j \geq c_j, \\ & s_j \geq 0, \end{array} \tag{5.11}$$

where j is the number of the constraint that needs to be tested for, and the starting point is $\mathbf{y}_j$ and y_{s_j}.

Problem (5.11) is solved by using IPOPT [47] and checks for a feasible solution for the original problem close to the solution to the lifted one. Another way to look into the recovery method is that (5.3) provides a starting point to (5.2). As we want a solution close to SDP's optimal point, then we solve an adapted (5.2), which is problem (5.11). Nevertheless, we still have the same problem of identifying whether $h(\mathbf{x})_j$ is umbrella or not by checking s_j, as s_j can yet be close to zero although the constraint is not umbrella. Another drawback with of this procedure is the need to calculate s_j and $\mathbf{w}_j$.

As mentioned before, the main purpose is to obtain the umbrella constraint set. This can be achieved by modifying (5.11) in the following way:

$$\begin{array}{ll} \min\limits_{\mathbf{w}_j} & F = \frac{1}{2}\left\|\mathbf{w}_j - \mathbf{y}_j\right\| \\ \text{subject to} & h_{j'}(\mathbf{w}_j) \leq c_{j'},\ j' = 1,\ldots,m,\ j' \neq j \\ & h_j(\mathbf{w}_j) = c_j \end{array} \tag{5.12}$$

However, instead of solving (5.12), we can check its feasibility around the starting point. If deemed unfeasible, then $h(\mathbf{x})_j$ is not an umbrella constraint. However, if judged possibly feasible, then (5.12) needs to be solved. It is expected that the solution given by (5.3) is near-feasible, therefore problem (5.12) should have a solution next to the starting point. If (5.12) converges in a few steps, then the constraint is umbrella. In case of non-convergence in a predetermined number of steps, then the constraint is not umbrella.

Moreover, there is no need to solve (5.12) for every j, as we already have information regarding s_j in the lifted variable y_{s_j}. We can check (5.12) feasibility only if y_{s_j} is lower than a user defined tolerance.

Simulations have shown that the recovery method can be improved if a good starting point is adopted for the algorithm that solves (5.12). As shown in Table 5.1, the SDP solution may not be of low-rank, i.e. $\mathbf{M}(\mathbf{y})$ is not necessarily low-rank at the solution. As we only need a near-feasible starting point, and the SCOPF is a quadratically constrained quadratic program, thus a good starting point is the square root of the main diagonal of $\mathbf{M}(\mathbf{y})$ [38].

To better illustrate it, consider the following moment matrix for an SCOPF-UCD that checks a single constraint:

$$\mathbf{M}(\mathbf{y}) = \begin{bmatrix} L_y\{1\} & L_y\{e_1\} & \cdots & L_y\{e_{n_b}\} & L_y\{f_1\} & \cdots & L_y\{f_{n_b}\} & L_y\{s_1\} \\ L_y\{e_1\} & L_y\{e_1^2\} & & & & & & \\ \vdots & & \ddots & & & & & \\ L_y\{e_{n_b}\} & & & L_y\{e_{n_b}^2\} & & & & \vdots \\ L_y\{f_1\} & & & & L_y\{f_1^2\} & & & \\ \vdots & & & & & \ddots & & \\ L_y\{f_{n_b}\} & & & & & & L_y\{f_{n_b}^2\} & \\ L_y\{s_1\} & & & \cdots & & & & L_y\{s_1^2\} \end{bmatrix}. \quad (5.13)$$

As the first element in (5.13) is a constant, the lifted variables of interest are $\mathbf{y}_{e^2} = \{L_y\{e_1^2\}, \ldots, L_y\{e_{n_b}^2\}\}$ and $\mathbf{y}_{f^2} = \{L_y\{f_1^2\}, \ldots, L_y\{f_{n_b}^2\}\}$. Consider the following lifted variables $\mathbf{y}_e = \{L_y\{e_1\}, \ldots, L_y\{e_{n_b}\}\}$ and $\mathbf{y}_f = \{L_y\{f_1\}, \ldots, L_y\{f_{n_b}\}\}$.

Now, we can obtain a better starting point by setting:

$$\mathbf{e}_{rec_i} = (sign(\mathbf{y}_{e_i})\sqrt{\mathbf{y}_{e^2{}_i}})_{i\in\mathcal{N}} \quad (5.14)$$

$$\mathbf{f}_{rec_i} = (sign(\mathbf{y}_{f_i})\sqrt{\mathbf{y}_{f^2{}_i}})_{i\in\mathcal{N}} \quad (5.15)$$

where $sign(\cdot)$ is the sign of the variable.

Let $\mathbf{x}_{rec} = [\mathbf{e}_{rec}, \mathbf{f}_{rec}]$ and $\mathbf{x}_{rec_j}$ is the vector of variables obtained by solving for $\mathbf{w}_j$, then solve the problem:

$$\begin{array}{ll} \min\limits_{\mathbf{x}_j} & dev = \sum\limits_i \left(\mathbf{x}_{j_i} - \mathbf{x}_{rec_{j_i}}\right)^2 \\ \text{subject to} & h_{j'}(\mathbf{x}_j) \leq c_{j'},\ j' = 1, \ldots, m,\ j' \neq j \\ & h_j(\mathbf{x}_j) = c_j \end{array} \quad (5.16)$$

After solving (5.16), if the problem is infeasible, then constraint j is not umbrella. Otherwise, constraint j is umbrella.

5.4 CONCLUSION

This chapter described a new approach to obtain the umbrella constraint set of the SCOPF problem by using semidefinite programming. It also described how to reduce the computational cost of solving the SDP problem by the use of some partitioning strategies and sparsity exploitation. Finally, a procedure was proposed to obtain the umbrella set from the solution of the SCOPF-UCD problem.

Next chapter will present the results obtained with the SCOPF-UCD algorithm.

6 RESULTS AND DISCUSSIONS

6.1 INTRODUCTION

This chapter showcase the applicability of the SDP-UCD on one illustrative example, a 34-bus equivalent of the Hydro-Québec system, and the New England test system. All the power networks are described in Appendix A.

The SDP-UCD problem identifies the umbrella constraints of the nonlinear SCOPF problem introduced by equation (2.49). The $N-1$ security criterion considering line contingencies was used to formulate the SCOPF problem. To ensure that line contingencies would not result in disconnecting generators, thus defining a double contingency, the outages of all the lines, with the exception of those connecting generators to the system, were considered.

The sets of umbrella constraints for the test systems were obtained, after solving the SDP problem (5.3), by applying the recovery method described in Section $5.3.2$. Therefore, no threshold was used for the value of $L_y\{s\}$ to determine if a constraint is umbrella or not, as all constraints were tested in during the recovery method.

The simulations were run in a Ryzen 1600 with 16 Gb of RAM computer via MATLAB [48]. The SDP problems were modeled with the use of YALMIP [49] and solved by the MOSEK solvers [50]. In the recovery step, the solution to the nonlinear problem (5.16) was obtained by the IPOPT solver [47].

6.2 ILLUSTRATIVE EXAMPLE

6.2.1 The Network

The test system used here is the same as in the example in Section $3.4.1$. The SDP-OPF problem is described in details by equation (3.44). Only the intact system was considered ($k=0$). Therefore, the system has $n_b=2$ buses, $n_l=2$ transmission lines, $n_g=2$ generators, and $n_c=0$ contingencies. Its diagram is represented by Fig. 3.3. It should be remembered that, in this example, $e_1=1$ and $f_1=0$.

By considering the constraints in (3.44), it is possible to formulate the umbrella identification problem, as shown by (5.3). If we count down the number of constraints in (3.44), we conclude that there are only 10 constraints to be checked. As the umbrella identification problem has only 110 constraints in total (10^2+10), it can be solved without using partition mechanisms.

6.2.2 Results

The nonlinear feasible space of (3.43) is depicted in Fig. 3.4. Fig. 6.1 shows all the constraints of the OPF problem (3.43) and, in the shaded area, the relaxed feasible set obtained via SDP (3.44). Furthermore, the arrows indicate the direction of the feasible space. Each constraint is labelled by a number shown in the figure and the optimal solution to the nonlinear problem when minimizing e_2 is represented by a circle. By inspecting Fig. 6.1, it is possible to analytically determine that the umbrella set of the nonlinear problem is composed by: constraints 1, 3, 7, and 10.

Notice that the feasible set of the SDP-OPF contains the feasible set of the nonlinear OPF problem, as constraint 10 goes through the SDP-OPF feasible space. The values of the slack variables at the solution to the umbrella identification problem are given in Table 6.1. In the last columns of this table are presented the umbrella constraints obtained in the recovery step.

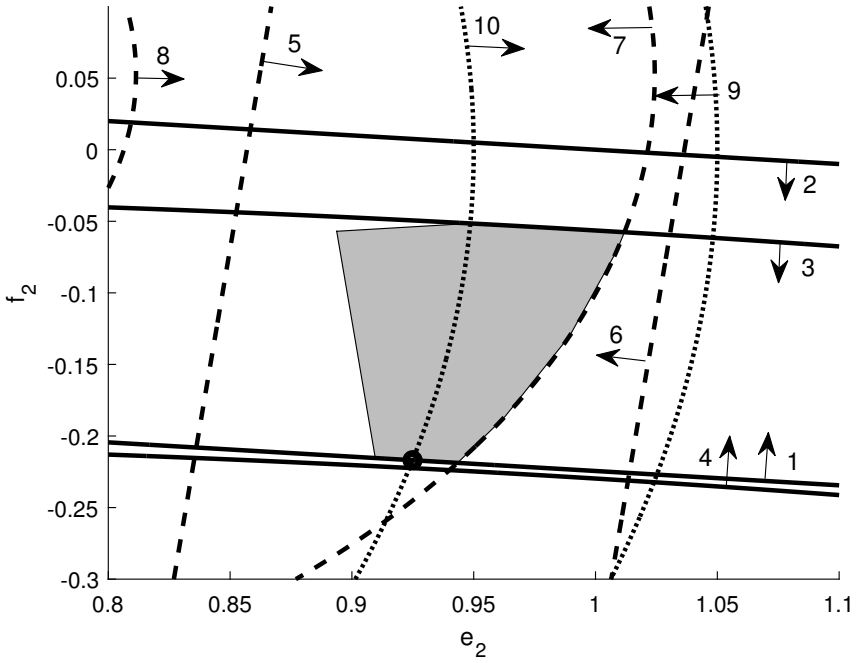

Figure 6.1: Feasible space for (3.44).

Table 6.1: Results for the illustrative example.

Label	Constraints	$L_y\{s\}$	Recovery
1	$P_{G_{1_{\max}}}$	0.0000	Umbrella
2	$P_{G_{1_{\min}}}$	0.5028	-
3	$P_{G_{2_{\max}}}$	0.0000	Umbrella
4	$P_{G_{2_{\min}}}$	0.0455	-
5	$Q_{G_{1_{\max}}}$	0.3791	-
6	$Q_{G_{1_{\min}}}$	0.1680	-
7	$Q_{G_{2_{\max}}}$	0.0000	Umbrella
8	$Q_{G_{2_{\min}}}$	0.9064	-
9	$V^2_{2_{\max}}$	0.0753	-
10	$V^2_{2_{\min}}$	0.0000	Umbrella

There are some important remarks regarding the solution given in Table 6.1. First, the umbrella identification problem has correctly detected all the umbrella constraints. Moreover, all $L_y\{s\}$ were very close to zero, e.g. for the first constraint, $L_y\{s\} = 4.34 \times 10^{-5}$. As shown in Fig. 6.1, constraint 4 is very close to the feasible space, thus its $L_y\{s\}$ should be small, but not zero. However, constraint 9 is further away from

the feasible set than constraint 6, but its $L_y\{s\}$ is smaller. The reason for that is that constraint 6 is linear, while 9 is not, thus, distorting the mathematical meaning of $L_y\{s\}$, as $L_y\{s\}$ now is the distance of of the constraint to the feasible space in the lifted space.

Nevertheless, by solving (5.3), 60% of the problem constraints were identified as not umbrella, thus they are redundant and can be removed from the optimization problem. By only leaving the umbrella constraints in the nonlinear problem (3.43), we have the following optimization problem:

$$
\begin{aligned}
\min \quad & e_2 \\
\text{s.t.} \quad & \\
& -0.8911e_2 - 8.9109f_2 - 1.1089 \leq 0, \\
& -0.8911e_2 + 8.9109f_2 + 0.8911(e_2^2 + f_2^2) + 0.5 \leq 0, \\
& -8.9109e_2 - 0.8911f_2 + 8.4359(e_2^2 + f_2^2) + 0.3 \leq 0, \\
& -e_2^2 - f_2^2 + 0.9025 \leq 0,
\end{aligned}
\tag{6.1}
$$

The solutions to (6.1) and (3.43) are equal.

6.3 39-BUS EQUIVALENT OF THE NEW ENGLAND NETWORK

6.3.1 The Network

This system has $n_b = 39$ buses, $n_l = 46$ transmission lines, and $n_g = 10$ generators. Its diagram is shown in Fig. 6.2, where the square and triangle nodes indicate load and generation buses, respectively.

When solving an SCOPF problem, there are $n_c = 36$ contingency scenarios. The loss of any of lines 5, 14, 20, 32, 33, 34, 37, 39, 41, and 46 disconnects power generators, thus their contingencies are neglected. Therefore, we have $4n_g(n_c + 1) = 1480$ generation limits, $2n_b(n_c + 1) = 2886$ voltage limits, $4(n_l - 1)n_c + 4n_l = 6664$ power flow, and $4n_g n_c = 1440$ security constraints, as demonstrated by (2.52). Consequently, we need to identify which of the $\mathcal{J}_{AC} = 12470$ constraints define the feasible set.

6.3.2 Results

For this system, there are over 150 million ($\mathcal{J}_{AC}^2 + \mathcal{J}_{AC}$) constraints to be identified as umbrella or not. Therefore, the contingency-based and line-based partitioning are required to solve this problem. Table 6.2 summarizes the results after finishing step 2. All the upper active power generation limits are considered umbrella, as, when they are enforced, the detection problem is infeasible or run into numerical problems.

According to the Appendix A, line 3 connects buses 2 and 3; line 4 connects buses 2 and 25; line 30 connects buses 17 and 18; line 40 connects buses 25 and 26; and line 42 connects buses 26 and 27. Among the constraints identified as umbrella in Table

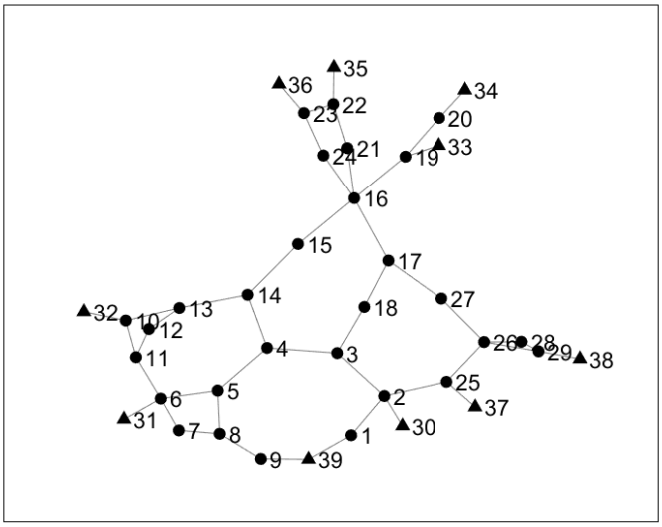

Figure 6.2: Network diagram for the New England system.

Table 6.2: Results after step 2 for the New England system.

Constraint tested	# of Constraints	# of Umbrella	Reduction
Upper voltage	1443	566	60.78%
Lower voltage	1443	625	56.69%
Lower active power	370	177	52.16%
Upper reactive power	370	328	11.35%
Lower reactive power	370	317	14.32%
Upper direct power flow	1666	53	96.82%
Lower direct power flow	1666	0	100.00%
Upper reverse power flow	1666	88	94.72%
Lower reverse power flow	1666	0	100.00%

6.2, the upper direct power flow umbrella constraints are the following: the limit on line 3; and the limit on lines 4, 40, and 42, which become umbrella when line 3 is removed. The other power flow limits that are considered umbrella are associated with the reduction of the capacity of transferring power between a generator an a load after given contingencies.

From Table 6.2 we see that the cardinality of $\mathcal{J}_\pi$ is reduced by 59.14%, as $\bigcup \mathcal{U}_k^l$ has 141 constraints (53 + 88). Therefore, $\tilde{\mathcal{J}}_\pi$ has cardinality of $4,507$ ($1,480 + 2,886 + 141$). Finally, the $\tilde{\mathcal{U}}^\alpha$ has 2524 "umbrella" constraints (as an approximation), a reduction of 77.12% from the total number of constraints in $\mathcal{J}_\pi$. This second step in the partitioning strategy required 77 hours to be completed. This can be broken down into almost 76 hours to model plus 37 minutes to solve the problem.

Table 6.3 contains the percentage of the constraints with the $L_y\{s\}$ value higher

than the highest $L_y\{s\}$ associated with an umbrella constraint. Comparing the results obtained for the upper voltage limits in Tables 6.3 and 6.2, the adoption of a threshold is effective in reducing the number of non-umbrella constraints. The threshold is set at 0.0053, as it is the highest value of $L_y\{y\}$ associated with an umbrella constraint in the upper voltage limits constraint set. Nonetheless, as we can observe in Fig. 6.3, there is a large concentration of non umbrella constraints near this value. This indicates that the threshold is sensitive for small values, i.e. a small change to its value implies a large change in the number of constraints filtered out by it. In this case, 47.75% of all the lifted slack variables falls in the interval between 0.0053 and 0.05. For comparison, for 40.40% of the lifted slack variables are in the $L_y\{s\} \leq 0.0053$ range. Finally, we notice, in Table 6.3 that most power flow non-umbrella constraints can be properly identified as such with the use of a threshold.

Table 6.3: Number of non umbrella constraints with $L_y\{s\}$ higher than the threshold value for the New England system.

Constraint	Threshold	% of Constraints over threshold
Upper voltage	5.50×10^{-3}	59.32%
Lower voltage	2.08×10^{-4}	0.01%
Lower active power	3.97	0.06%
Upper reactive power	5.32×10^{-4}	0.00%
Lower reactive power	1.95×10^{-5}	0.14%
Upper direct power flow	4.70×10^{-3}	93.04%
Lower direct power flow	0.00	100.00%
Upper reverse power flow	3.69×10^{-3}	93.28%
Lower reverse power flow	0.00	100.00%

In the case of the lower limits on voltages, active power and reactive power generation, and also, the upper limits on reactive power generation, as show in Tables 6.6 and 6.3, it is not effective to use thresholds to eliminate non-umbrella constraints. The histograms of the lifted slack variables associated with the limits on the direct power flow is shown in Fig. 6.4. A vertical dashed line is inserted in each figure to indicate the highest value of $L_y\{s\}$ that is associated with an umbrella constraint identified by the recovery method. Notice the large number of constraints with large $L_y\{s\}$. For example, the lifted slack variables, $L_y\{s\}$, of almost 90% of these limits are above 1. This is better shown in Table 6.3, where 93.04% of all non-umbrella constraints has a lifted slack variable value above the highest one for an umbrella constraint. By comparing these results with Table 6.2, it is possible to conclude that constraints further away from the border of the feasible set are effectively identified as non-umbrella based on the values of the lifted slack values, $L_y\{s\}$. However, the same is not true for constraints associated to small $L_y\{s\}$.

After the second step of the partitioning algorithm (section $5.3.1.1$), we obtain $\tilde{\mathcal{U}}^{\alpha}$. Therefore, $\tilde{\mathcal{J}}_{\alpha}$ and $\tilde{\mathcal{J}}_{\alpha}(k)$ are defined (steps 3 and 4, respectively). Following the

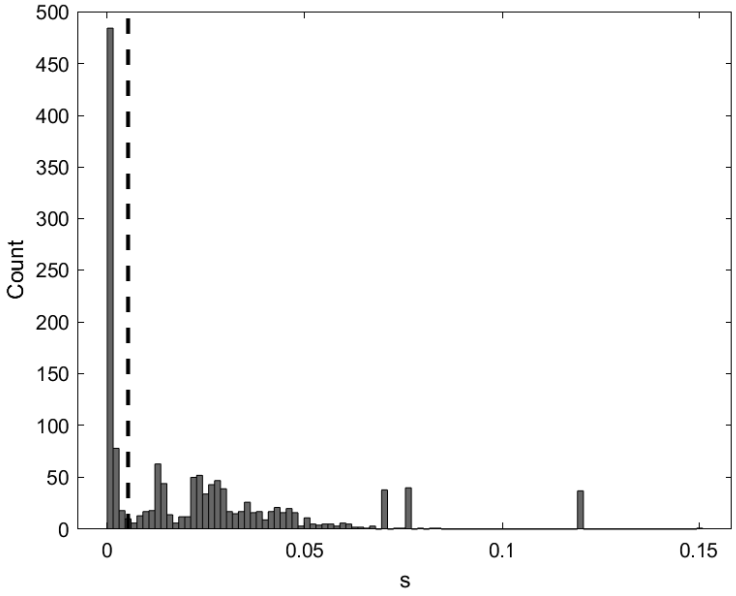

Figure 6.3: Histogram of $L_y\{s\}$ values for upper voltage limit constraint for the New England system.

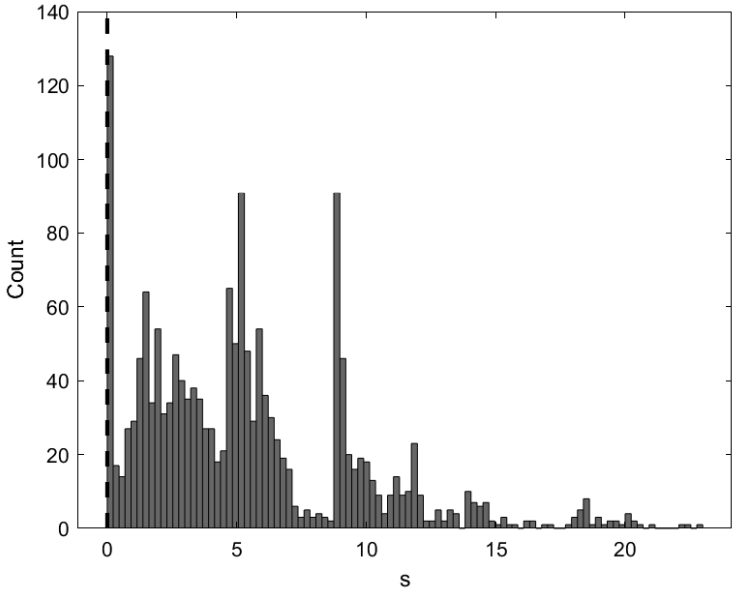

Figure 6.4: Histogram of $L_y\{s\}$ values for upper direct power flow constraint.

algorithm, it is now required to identify the umbrella constraints in each $\tilde{\mathcal{J}}_\alpha(k)$ set, for $k = 1, \ldots, n_c$; thus, obtaining $\tilde{\mathcal{U}}$. Table 6.4 summarizes the results from the umbrella identification problem for $\tilde{\mathcal{U}}$. As expected, the effectiveness in identifying umbrella constraints has been reduced. This can be explained by the reduction of the feasible set after introducing the security constraints. The cardinality of $\tilde{\mathcal{U}}$ is 3438, a reduction of 72.43% in relation to $\mathcal{J}$. Nevertheless, if comparing only the constraints considered in $\tilde{\mathcal{U}}^\alpha$, there is a reduction of only 13.67%. The time required to finish these steps $(3-6)$

is 28 hours to model plus 40 minutes to solve the umbrella identification problem.

Table 6.4: Results after steps 3 – 6 for the New England system.

Constraint tested	# of Constraints	# of Umbrella	Reduction
Upper voltage	566	527	6.89%
Lower voltage	625	506	19.04%
Lower active power	177	82	53.67%
Upper reactive power	328	313	4.57%
Lower reactive power	317	303	4.42%
Upper security active power	360	312	13.33%
Lower security active power	360	317	11.94%
Upper security reactive power	360	317	11.94%
Lower security reactive power	360	313	13.06%
Upper direct power flow	53	25	52.83%
Lower direct power flow	0	0	0.00%
Upper reverse power flow	88	53	39.77%
Lower reverse power flow	0	0	0.00%

To test if the umbrella identification problem eliminated an umbrella constraint by mistake, problem (2.32) is solved considering only the umbrella constraints in Table 6.4. After solving the nonlinear SCOPF problem, no constraint in $\mathcal{J}$ is violated.

6.4 34-BUS EQUIVALENT OF THE HYDRO-QUÉBEC NETWORK

6.4.1 The Network

This system has $n_b = 34$ buses, $n_l = 64$ transmission lines, and $n_g = 20$ generators. Its single-line diagram is shown in Fig. 6.5, where the square and triangle nodes indicate a load and generation buses, respectively.

When solving an SCOPF problem, there are $n_c = 58$ contingency scenarios. This is due to the fact that the loss of one of the lines 1, 2, 3, 4, 5, and 6 disconnects power generators, thus creating double contingencies. In addition, if line 28 is eliminated, we have an infeasible problem, as bus 29 would be disconnected from the network. Therefore, we have $4n_g(n_c + 1) = 4720$ generation limits, $2n_b(n_c + 1) = 4012$ voltage limits, $4(n_l - 1)n_c + 4n_l = 14872$ power flow, and $4n_g n_c = 9280$ security constraints, as demonstrated by (2.52). Consequently, we need to identify which of the $\mathcal{J}_{AC} = 32884$ constraints define the feasible set.

6.4.2 Results

To obtain the umbrella constraints of this problem, it is necessary to consider $(32884^2 + 32884)$ constraints, as shown in section 4.2. This results in over 1 billion constraints. Due to its size, the umbrella detection problem is decomposed and partitioned.

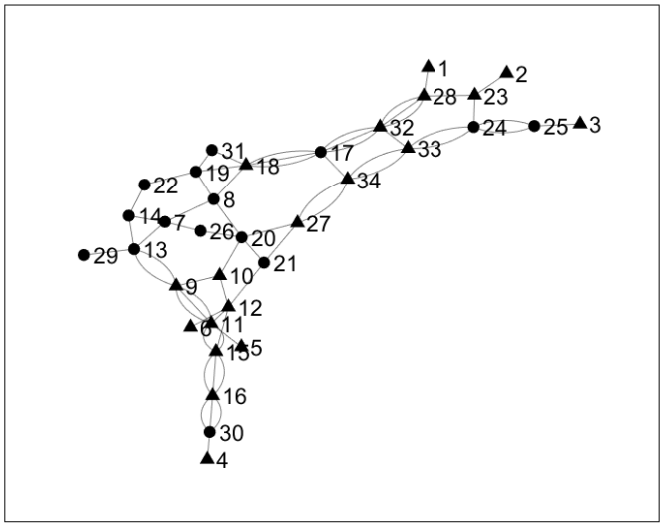

Figure 6.5: Network diagram for the Hydro-Québec system.

As shown in section $5.3.1.1$, the first umbrella set to be obtained is $\mathcal{U}_k^l$ (step $2.a$). For that, contingency-based and line-based partitioning are used. At the beginning of step $2.a$, the cardinality of $\mathcal{J}_\pi^l(k)$ is 256 for $k = 0$, and 252 for $k > 0$. Therefore, for each k, over 100 thousand ($400 \times 252 + 252$) constraints are tested, where 400 is the cardinality of $\mathcal{J}_\pi(k)$ (i.e., the voltage, power generation, and power flow constraints for the contingency state k). This results in the elimination of all but one power flow constraint (99.99% reduction). The only umbrella constraint in $\mathcal{J}_\pi^l$ is the maximal limit on the reverse power flow over the line 20 for $k = 26$. Its slack variable value is 0.027 and it is identified as umbrella by the recovery method.

The next step ($2.b$) is to obtain the umbrella set for $\tilde{\mathcal{J}}_\pi(k)$. The algorithm indicates that $\tilde{\mathcal{J}}_\pi(k)$ has cardinality equal to 148 for $\forall k \neq 26$ ($400 - 252$, where 400 and 252 are the cardinalities of $\mathcal{J}_\pi(k)$ and $\mathcal{J}_\pi^l(k)$, respectively), and 149 for $k = 26$ (as it is the only contingency state with a power flow constraint), totalling 8733 constraints ($148n_c + 149$). In step $2.c$, solving the SDP-UCD problem for all $\tilde{\mathcal{J}}_\pi(k)$ constraint sets, the number of identified umbrella constraints ($\tilde{\mathcal{U}}^\alpha$) is 7259 (15.45% reduction from $\bigcup \tilde{\mathcal{J}}_\pi(k)$). The summary of the results is given in Table 6.5. The lower active power limit are not included in this table as, when they are tested, the umbrella detection problem is unfeasible.

At the end of step 2, the number of constraints is reduced from 32884 to 16539 (where 7259 is from $\tilde{\mathcal{U}}^\alpha$ and 9280 are the security constraints), or a 49.71% decrease in the number of constraints.

To show the importance of a recovery method, Fig. 6.6, 6.7, 6.8, 6.9, and 6.10 represent the histograms of the values of $L_y\{s\}$ for each constraint type: upper and lower voltage limits, upper active power generation limits, and upper and lower reactive power limits, respectively. A vertical dashed line is inserted in each figure to indicate the highest value of $L_y\{s\}$ that is associated with an umbrella constraint identified by

Table 6.5: Results after step $2.c$ for the Hydro-Québec system.

Constraint tested	# of Constraints	# of Umbrella	Reduction
Upper voltage	1972	1372	30.43%
Lower voltage	1972	1479	25.00%
Upper active power	1160	1160	0.00%
Upper reactive power	1160	1043	10.09%
Lower reactive power	1160	1044	10.00%
Upper direct power flow	3718	0	100.00%
Lower direct power flow	3718	0	100.00%
Upper reverse power flow	3718	1	99.99%
Lower reverse power flow	3718	0	100.00%

the recovery method.

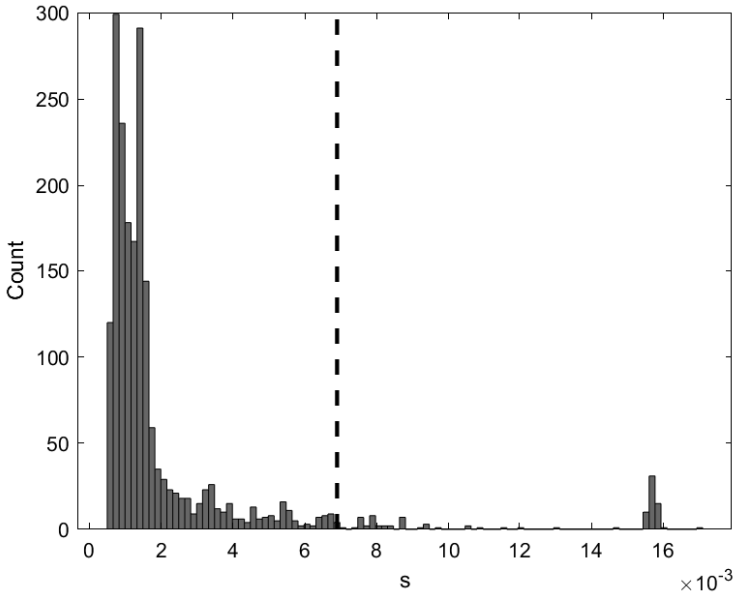

Figure 6.6: Histogram of $L_y\{s\}$ values for upper voltage limit constraint.

Consider that we set the threshold for $L_y\{s\}$ equal to the highest value associated to an umbrella constraint (i.e., the optimal threshold value). If $L_y\{s\}$ value of a given constraint is higher than the threshold, then the constraint is not umbrella. Table 6.6 contains the percentage of the constraints identified as non umbrella based on the $L_y\{s\}$ value. By comparing the results with Table 6.5, it is possible to conclude that to adopt such threshold value is not an efficient way to determine the umbrella constraint set. For example, there is a 30.43% reduction in the number of upper voltage constraints by using the recovery method; but only 5.22% when using the threshold value for $L_y\{s\}$.

As the Hydro-Québec network has a very tight feasible region [51], it is expected that almost all the constraints would be close to the feasible set, i.e., the slack vari-

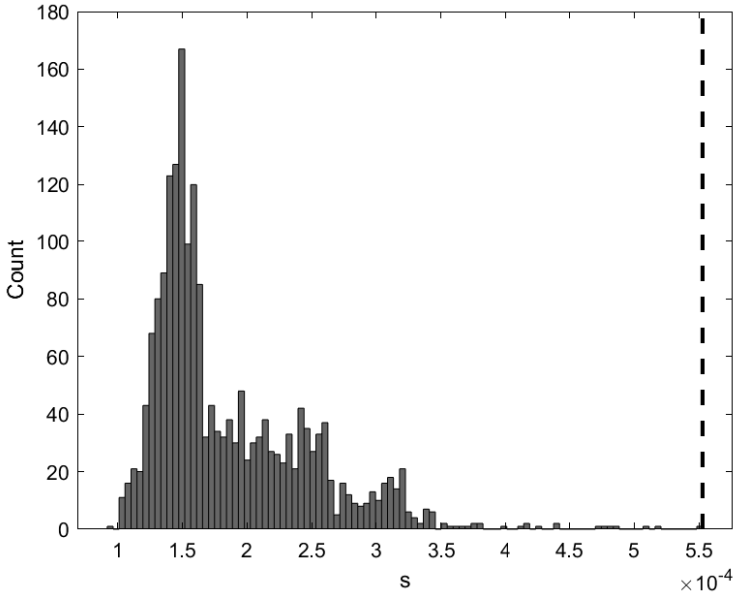

Figure 6.7: Histogram of $L_y\{s\}$ values for lower voltage limit constraint.

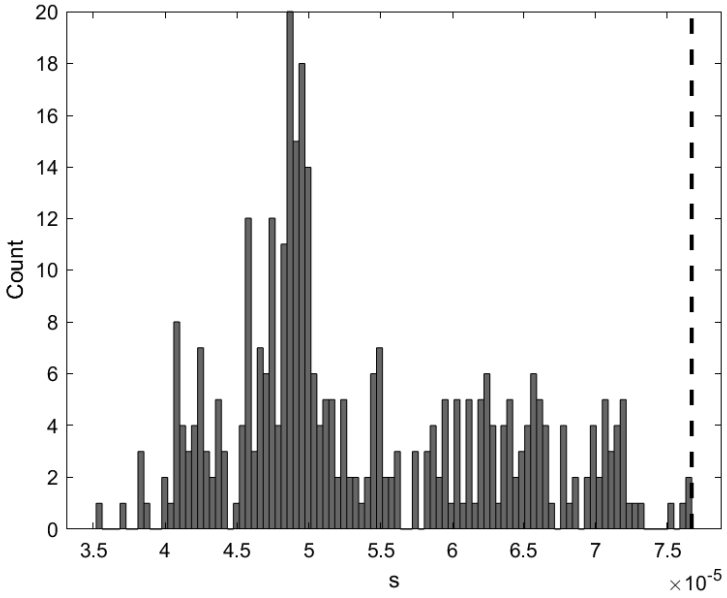

Figure 6.8: Histogram of $L_y\{s\}$ values for upper active power limit constraint.

ables (or, the associated lifting variables $L_y\{s\}$) are small even for the non umbrella constraints. Nevertheless, the opposite can be true. That is, the value of $L_y\{s\}$ can filter-out non umbrella constraints, instead of identifying the umbrella ones. This is due to the fact that all the $L_y\{s\}$ values are very small for constraints close to or which form the border of the feasible set. Thus, by setting a high enough threshold for $L_y\{s\}$, we can filter-out some non-umbrella constraints. As all umbrella constraints have a small value of $L_y\{s\}$ associated to it. As an example, Fig. 6.11 is the histogram of the values of $L_y\{s\}$ associated to the upper reverse power flow limits. If the threshold is set as 1,

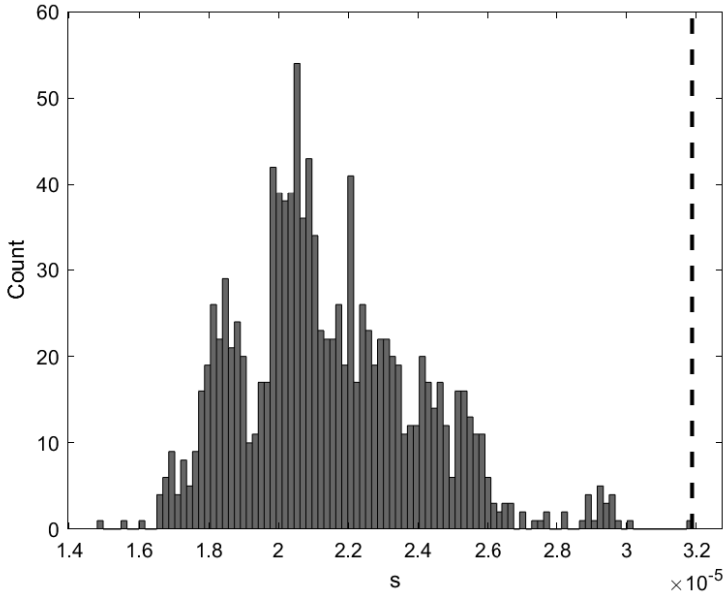

Figure 6.9: Histogram of $L_y\{s\}$ values for upper reactive power limit constraint.

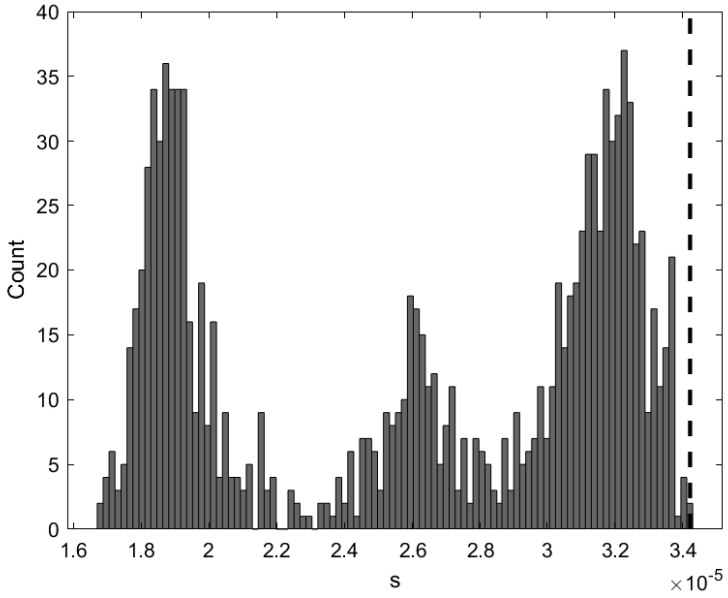

Figure 6.10: Histogram of $L_y\{s\}$ values for lower reactive power limit constraint.

then there is a reduction of 99.67% in the number of non umbrella constraints. This means that it is possible to discard those before solving the recovery method, therefore reducing the computational cost.

As mentioned earlier, it is possible to say that the Hydro-Québec equivalent system has a very tight feasible region by comparing tables 6.2 and 6.5. Therefore, further umbrella identification problems (steps 3 to 7) will not result in a considerable reduction in the number of constraints to justify its computational cost. To better understand how demanding the umbrella identification problem is, for this system, to complete step $2.a$

Table 6.6: Number of non umbrella constraints with $L_y\{s\}$ higher than the threshold value for the Hydro-Québec system.

Constraint	Threshold	% of Constraints over threshold
Upper voltage	6.90×10^{-3}	5.22%
Lower voltage	5.53×10^{-4}	0.00%
Upper active power	7.67×10^{-5}	0.00%
Upper reactive power	3.42×10^{-5}	0.00%
Lower reactive power	3.19×10^{-5}	0.00%

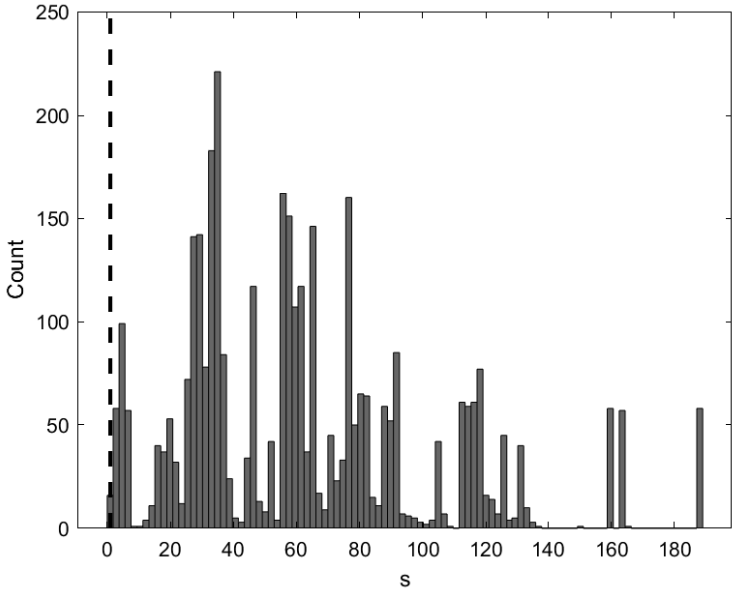

Figure 6.11: Histogram of $L_y\{s\}$ values for upper reverse power flow constraint.

of the umbrella detection algorithm, almost 58 hours is required to model the problem plus 34 minutes to solve it. On the other hand, to model and solve the problem in step $2.b$, 23 hours plus 11 minutes are required. Thus, step 2 requires around 82 hours of processing time.

6.5 CONCLUSION

The UCD-SDP results for three test systems were discussed in this chapter: an illustrative example, the New England 39-bus equivalent system, and the Hydro-Québec 34-bus equivalent system. In the illustrative example, the lifted slack variable values were consistent with the figure of the feasible space, except for the one associated with the nonlinear constraint. This behavior is also present in the other two test systems, as a consequence of the SDP relaxation. The recovery method demonstrated capable of solving this issue.

Next chapter discuss the thesis conclusions and proposes future work based on this

work.

7 CONCLUSION

7.1 INTRODUCTION

The problem analyzed in this thesis is introduced in Chapter 2 by the formulations of the OPF, SC-LOPF, and SCOPF problems. These are very large problems. Many of the constraints of these problems are redundant; that is, they can be eliminated from the formulations without affecting the optimal solutions. The constraints that define the feasible set of these problems are denoted umbrella constraints. Although procedures can be found in the literature that calculate the umbrella constraints of the SC-LOPF, the detection of the umbrella constraints of the nonlinear SCOPF is still an open problem. This thesis aims at contributing to the resolution of this problem. For that, it relaxes the umbrella detection problem via SDP. The relaxed problem (SDP-UCD) is formulated using YALMIP and solved by MOSEK.

The the solution to the SDP-UCD problem need to be recovered to obtain a proper umbrella constraint set. The proposed recovery method is based on the resolution of problem (5.12). Due to the increase in computational complexity, Section 5.3.1 introduces partitioning and decomposition strategies to decrease the number of constraints in the SDP-UCD problem.

7.2 DISCUSSION ON THE PROPOSED METHOD

The proposed SDP-UDC problem is capable of correctly identifying the umbrella constraints of the OPF and SCOPF problems. To showcase how the optimization problem identifies the umbrella constraints, an illustrative example is analyzed in Chapter 6.

The umbrella constraints of the SCOPF problem were also identified for the New England and the Hydro-Québec systems. It can be noticed that the SDP-UCD results by themselves are quite conservative, i.e. many non-umbrella constraints have a small lifted slack variables. As mentioned by [4], in the linear umbrella discovery constraint problem, the slack variable is the distance between the linear constraint and the border of the feasible space. However, after lifting a nonlinear constraint to linearize it, this is not necessarily true. The reason is that the lifted slack variable is now the distance between the lifted space border and the lifted constraint. However, this may not have a direct correlation with the nonlinear feasible space. Such property is better shown by the illustrative example, where linear constraint 6, although closer to the feasible space border, has an associated lifted slack variable larger than that of constraint 9.

As the lifted slack variable does not necessarily correlates to the nonlinear feasible space. If we only check its value to determine whether the constraint is umbrella or not, we would have a very conservative umbrella set. That is, there would be many non-umbrella constraints incorrectly identified as umbrella. This is expected, as the semidefinite problem computes the global lower limit; in other words, the objective function at the SDP solution is either equal or lower than at the global optimum. As the objective function is the sum of the lifted squared slack variables, their values tend to be lower than expected. Another way to see how conservative the SDP-UCD is the following: tables 6.3 and 6.6 indicates the number of nonlinear constraints that have

$L_y\{s\}$ higher than the highest lifted slack variable associated to an umbrella constraint. If we remove all those constraints by considering them non-umbrella, the overall reduction of constraints is significantly smaller than the one obtained after the recovering step, shown in tables 6.2 and 6.5.

Due to the SDP conservative solution, it is necessary to recover the solution in order to obtain a reduced umbrella set. This study proposes to solve a nonlinear recovery problem using as starting point the solution of the SDP-UCD problem. By recovering the solution, it is clear that there is a large number of non-umbrella constraints with small lifted slack variables. For the test systems, the recovery method seems to be able to identify all the umbrella constraints, as when solving the SCOPF problem with only the identified umbrella set the solution is the same as that of the full SCOPF problem. However, it is possible that non-umbrella constraints can still be found in the identified umbrella set.

This study also shows that, for the test systems, most power flow limits are not umbrella constraints. This is consistent with the results obtained when solving the linear umbrella identification problem [4]. There is also a considerable reduction in the number of constraints after step 2 in the partitioning strategy. Nonetheless, a considerable computational effort is required to solve the umbrella identification problem. As there is a significant number of constraints and variables, identifying the umbrella set requires a considerable amount of system memory. By partitioning the problem, the demand for memory is reduced, making it possible to solve larger test systems.

7.3 RECOMMENDATIONS FOR FUTURE RESEARCH

This study proposes a new method to obtain the constraints that form the feasible space border, i.e. the umbrella constraints. Although the method was successfully applied to small systems, some of its limitations need to be addressed. Therefore, the proposed future research has the following objectives:

- Reduce the computational cost: as previously mentioned, the SDP-UCD can have a massive number of constraints even for small problems. Although partitioning methods were adopted in this thesis, it is still costly to obtain check for all umbrella constraints;

- Introduce a pre-processing step: it may be possible to identify and remove some non-umbrella constraints before solving the SDP-UCD problem. For example, one can analyze the problem analytically to eliminate a constraint before solving the SDP-UCD problem. Another possible approach is to use facial reduction in the SDP-UCD problem as a pre-processing step;

- Improve the recovery method: in spite of being effective, the proposed recovery method is computationally costly. This is due to the fact that it must be run for each umbrella constraint tested. The number of constraints that needs to be tested can be reduced through the use of a threshold for the lifted slack variables. However, as mentioned in the previous chapter, many constraints are expected to have small

$L_y\{s\}$ values. Sometimes the same constraint is tested more than once when partitioning is used, thus bringing the number of nonlinear optimization problem to the thousands;

- Propose a method to obtain a low-ranking solution to the SDP-UCD problem: the lower the rank of the relaxed solution, the closer this solution is to the feasible set of the nonlinear UCD problem. This means that non-umbrella constraints will be known with more certainty and, thus be eliminated before the recovery step;
- Use other relaxation methods to solve the umbrella detection problem: this study proposes the use of SDP relaxation in order to identify its umbrella constraints. Although effective, this procedure proved to be computationally costly. There are many other convexification methods that may be used for this same purpose, e.g. convex conic programming.

REFERENCES

1 Fink, L. H.; Carlsen, K. Operating under stress and strain [electrical power systems control under emergency conditions]. *IEEE Spectrum*, v. 15, n. 3, p. 48–53, 1978.

2 Bouffard, F.; Galiana, F. D.; Arroyo, J. M. Umbrella contingencies in security-constrained optimal power flow. In: *15th Power Systems Computation Conf., 2005. Proceedings of the*. [S.l.: s.n.], 2005. p. 22–26.

3 Bouffard, F.; Galiana, F. D.; Conejo, A. J. Market-clearing with stochastic security-part ii: case studies. *IEEE Transactions on Power Systems*, v. 20, n. 4, p. 1827–1835, Nov 2005.

4 Ardakani, A. J.; Bouffard, F. Identification of umbrella constraints in dc-based security-constrained optimal power flow. *IEEE Transactions on Power Systems*, v. 28, n. 4, p. 3924–3934, Nov 2013. ISSN 1558-0679.

5 YORINO, N. et al. Robust power system security assessment under uncertainties using bi-level optimization. *IEEE Transactions on Power Systems*, v. 33, n. 1, p. 352–362, 2018.

6 WEINHOLD, R.; MIETH, R. Fast security-constrained optimal power flow through low-impact and redundancy screening. *IEEE Transactions on Power Systems*, v. 35, n. 6, p. 4574–4584, 2020.

7 SHOR, N. Z. Quadratic optimization problems. *Soviet Journal of Computer and Systems Sciences*, v. 25, p. 1–11, 1987.

8 SEDANO, R. P.; BROWN, M. H. Electricity transmission: a primer. *National Council on Electricity Policy, June, Washington, DC*, 2004.

9 Joo, S.; Kim, J.; Liu, C. Empirical analysis of the impact of 2003 blackout on security values of u.s. utilities and electrical equipment manufacturing firms. *IEEE Transactions on Power Systems*, v. 22, n. 3, p. 1012–1018, 2007.

10 FELIZARDO, N.; DIAS, T. *Apagão no Amapá: a série de negligências da empresa que tentava se livrar do serviço*. 2020. Disponível em: <https://theintercept.com/2020/11/14/apagao-amapa-negligencia-lmte-isolux-aneel/>.

11 AMAPá: os impactos do apagão na população periférica: "me sinto um nada". 2020. Disponível em: <https://apublica.org/2020/11/amapa-os-impactos-do-apagao-na-populacao-periferica-me-sinto-um-nada/>.

12 ALSAC, O.; STOTT, B. Optimal load flow with steady-state security. *IEEE transactions on power apparatus and systems*, IEEE, n. 3, p. 745–751, 1974.

13 LIACCO, T. E. D. Power/energy: System security: The computer's role: Several security-related functions can be aided by the digital computer, and linked together by a software scheme. *IEEE Spectrum*, v. 15, n. 6, p. 43–50, 1978.

14 ZIMA, M.; ANDERSSON, G. On security criteria in power systems operation. In: *IEEE Power Engineering Society General Meeting, 2005*. [S.l.: s.n.], 2005. p. 3089–3093 Vol. 3.

15 FENG, W.; SHRESTHA, G. Allocation of tcsc devices to optimize total transmission capacity in a competitive power market. In: *2001 IEEE Power Engineering Society Winter Meeting. Conference Proceedings (Cat. No.01CH37194)*. [S.l.: s.n.], 2001. v. 2, p. 587–593 vol.2.

16 ARDAKANI, A. *Identification of Umbrella Constraints in Power Generation Scheduling Problems*. Tese (Doutorado) — McGill University, Montréal, Canada, aug 2014.

17 Ejebe, G. C.; Wollenberg, B. F. Automatic contingency selection. *IEEE Transactions on Power Apparatus and Systems*, PAS-98, n. 1, p. 97–109, 1979.

18 STOTT, B.; ALSAC, O.; MONTICELLI, A. J. Security analysis and optimization. *Proceedings of the IEEE*, IEEE, v. 75, n. 12, p. 1623–1644, 1987.

19 CARPENTIER, J. Contribution to the economic dispatch problem. *Bulletin de la Societe Francoise des Electriciens*, v. 3, n. 8, p. 431–447, 1962.

20 MONTICELLI, A.; PEREIRA, M. V. F.; GRANVILLE, S. Security-constrained optimal power flow with post-contingency corrective rescheduling. *IEEE Transactions on Power Systems*, v. 2, n. 1, p. 175–180, 1987.

21 STOTT, B.; HOBSON, E. Power system security control calculations using linear programming, part i. *IEEE Transactions on Power Apparatus and Systems*, PAS-97, n. 5, p. 1713–1720, 1978.

22 STOTT, B.; HOBSON, E. Power system security control calculations using linear programming, part ii. *IEEE Transactions on Power Apparatus and Systems*, PAS-97, n. 5, p. 1721–1731, 1978.

23 Overbye, T. J.; Xu Cheng; Yan Sun. A comparison of the ac and dc power flow models for lmp calculations. In: *37th Annual Hawaii International Conference on System Sciences, 2004. Proceedings of the*. [S.l.: s.n.], 2004. p. 9 pp.–.

24 SQUIRES, R. B. Economic dispatch of generation directly rrom power system voltages and admittances. *Transactions of the American Institute of Electrical Engineers. Part III: Power Apparatus and Systems*, IEEE, v. 79, n. 3, p. 1235–1244, 1960.

25 Low, S. H. Convex relaxation of optimal power flow—part i: Formulations and equivalence. *IEEE Transactions on Control of Network Systems*, v. 1, n. 1, p. 15–27, March 2014. ISSN 2372-2533.

26 WOOD, A.; WOLLENBERG, B.; SHEBLÉ, G. *Power Generation, Operation, and Control*. [S.l.]: Wiley, 2013. ISBN 9781118733912.

27 MONTICELLI, A. *State Estimation in Electric Power Systems*. [S.l.]: 3Island Press, 1999. ISBN 9781461550006.

28 ZHU, J. *Optimization of power system operation*. [S.l.]: John Wiley & Sons, 2015.

29 Capitanescu, F. et al. Contingency filtering techniques for preventive security-constrained optimal power flow. *IEEE Transactions on Power Systems*, v. 22, n. 4, p. 1690–1697, 2007.

30 BERTSIMAS, D.; TSITSIKLIS, J. N. *Introduction to linear optimization*. [S.l.]: Athena Scientific Belmont, MA, 1997. v. 6.

31 ANJOS, M. F.; LASSERRE, J. B. *Handbook on semidefinite, conic and polynomial optimization*. [S.l.]: Springer Science & Business Media, 2011. v. 166.

32 LASSERRE, J. B. Global optimization with polynomials and the problem of moments. *SIAM*, v. 11, p. 796–817, 2001.

33 ANTONIOU, A.; LU, W.-S. *Practical optimization: algorithms and engineering applications*. [S.l.]: Springer, 2007. v. 19.

34 FREUND, R. M. Introduction to semidefinite programming (sdp). *Massachusetts Institute of Technology*, p. 8–11, 2004.

35 LAVAEI, J.; LOW, S. H. Zero duality gap in optimal power flow problem. *IEEE Transactions on Power Systems*, IEEE, v. 27, n. 1, p. 92–107, 2011.

36 BLEKHERMAN, G.; PARRILO, P. A.; THOMAS, R. R. *Semidefinite optimization and convex algebraic geometry*. [S.l.]: SIAM, 2012.

37 LASSERRE, J. B.; LAURENT, M.; ROSTALSKI, P. Semidefinite characterization and computation of zero-dimensional real radical ideals. *Foundations of Computational Mathematics*, Springer, v. 8, n. 5, p. 607–647, 2008.

38 MADANI, R. *Computational Methods for Nonlinear Optimization Problems: Theory and Applications*. Tese (Doutorado) — Columbia University, 2015.

39 FLOUDAS, C. A.; PARDALOS, P. M. *A collection of test problems for constrained global optimization algorithms*. [S.l.]: Springer Science & Business Media, 1990. v. 455.

40 MOLZAHN, D. K.; JOSZ, C.; HISKENS, I. A. Moment relaxations of optimal power flow problems: beyond the convex hull. In: IEEE. *2016 IEEE Global Conference on Signal and Information Processing (GlobalSIP)*. [S.l.], 2016. p. 856–860.

41 LESIEUTRE, B. C. et al. Examining the limits of the application of semidefinite programming to power flow problems. In: IEEE. *2011 49th annual Allerton conference on communication, control, and computing (Allerton)*. [S.l.], 2011. p. 1492–1499.

42 Lesieutre, B. C. et al. Examining the limits of the application of semidefinite programming to power flow problems. In: *2011 49th Annual Allerton Conference on Communication, Control, and Computing (Allerton)*. [S.l.: s.n.], 2011. p. 1492–1499. ISSN null.

43 FUKUDA, M. et al. Exploiting sparsity in semidefinite programming via matrix completion i: General framework. *SIAM Journal on optimization*, SIAM, v. 11, n. 3, p. 647–674, 2001.

44 LAURENT, M. Matrix completion problemsmatrix completion problems. In: _____. *Encyclopedia of Optimization*. Boston, MA: Springer US, 2009. p. 1967–1975. ISBN 978-0-387-74759-0. Disponível em: <https://doi.org/10.1007/978-0-387-74759-0_355>.

45 MADANI, R.; ASHRAPHIJUO, M.; LAVAEI, J. Promises of conic relaxation for contingency-constrained optimal power flow problem. *IEEE Transactions on Power Systems*, v. 31, n. 2, p. 1297–1307, 2016.

46 BOUCHITTÉ, V.; TODINCA, I. Treewidth and minimum fill-in: Grouping the minimal separators. *SIAM Journal on Computing*, SIAM, v. 31, n. 1, p. 212–232, 2001.

47 WACHTER, A.; BIEGLER, L. On the implementation of a primal—dual interior point filter line search algorithm for large-scale nonlinear programming, mathematical programming. *Math. Program*, v. 106, n. 1.

48 MATLAB. *9.8.0.1538580 (R2020a)*. Natick, Massachusetts: The MathWorks Inc., 2020.

49 LÖFBERG, J. Yalmip : A toolbox for modeling and optimization in matlab. In: *In Proceedings of the CACSD Conference*. Taipei, Taiwan: [s.n.], 2004.

50 APS, M. *MOSEK Optimization Toolbox for MATLAB 9.3.8*. [S.l.], 2021. Disponível em: <https://docs.mosek.com/9.3/toolbox/index.html>.

51 ALMEIDA, K. C.; GALIANA, F. D. Critical cases in the optimal power flow. *IEEE Transactions on Power Systems*, IEEE, v. 11, n. 3, p. 1509–1518, 1996.

TESTS SYSTEMS DATA

REMARKS

All systems used in this study and present here had the following characteristics:

- All data is in per-unit ($p.u.$) with the base power of 100 MVA,
- All SVCs were converted to SCs,
- The active power flow limits were chosen in a way to help converge and show the effects of the algorithm proposed in this study.

2-BUS SYSTEM

Table A.1: Line data for the 2-bus system.

Line	From	To	r_{lm}	x_{lm}	b_{sh}	$F_{lm_{\max}}$
1	1	2	0.020	0.200	0.500	1
2	1	2	0.025	0.250	0.450	1

Table A.2: Generator data for the 2-bus system.

Bus	$P_{G_{\max}}$	$P_{G_{\min}}$	$Q_{G_{\max}}$	$Q_{G_{\min}}$
1	2.00	0.00	0.80	−0.80
2	1.50	0.00	0.70	−0.70

Table A.3: Bus data for the 2-bus system.

Bus	$V_{\max}$	$V_{\min}$	P_D	Q_D
1	1.05	0.95	0.00	0.00
2	1.05	0.95	2.00	1.00

34-BUS EQUIVALENT OF THE HYDRO-QUÉBEC NETWORK

Table A.4: Line data for the Hydro-Québec system.

Line	From	To	r_{lm}	x_{lm}	b_{sh}	$F_{lm_{\max}}$
1	1	28	0.00005	0.00269	0.0000	1.20
2	2	23	0.00004	0.00643	0.1360	1.00
3	3	25	0.00010	0.00444	0.0000	1.00
4	4	30	0.00003	0.00226	−0.0340	1.50
5	5	11	0.00014	0.00898	−0.0610	0.77
6	6	12	0.00014	0.00581	0.0000	1.20
7	7	8	0.00008	0.00185	0.7380	0.55
8	7	13	0.00023	0.00681	2.5760	0.45
9	7	14	0.00006	0.00150	0.6260	1.02
10	7	26	0.00011	0.00314	1.3740	0.50
11	8	19	0.00009	0.00255	1.1230	0.37
12	8	20	0.00055	0.01307	5.5530	0.53
13	8	18	0.00053	0.01493	6.6410	0.46
14	9	10	0.00007	0.00172	0.6890	1.00
15	9	13	0.00023	0.00692	2.8010	1.01
16	9	13	0.00023	0.00692	2.8010	1.01
17	9	11	0.00078	0.02295	9.8210	0.30
18	9	11	0.00078	0.02295	9.2810	0.30
19	9	11	0.00094	0.02253	9.9290	0.31
20	10	12	0.00101	0.02434	10.878	0.28
21	10	20	0.00010	0.00228	0.9530	1.00
22	11	12	0.00013	0.00379	1.5460	1.00
23	11	15	0.00045	0.01042	4.4020	0.67
24	11	15	0.00045	0.01042	4.4020	0.67
25	12	15	0.00048	0.01126	4.7660	0.62
26	12	21	0.00068	0.01517	6.4880	0.46
27	13	14	0.00027	0.00851	3.6790	0.82
28	13	29	0.00015	0.00426	1.8390	1.00
29	14	22	0.00009	0.00279	1.2250	1.00
30	15	16	0.00058	0.01351	5.7550	0.51
31	15	16	0.00058	0.01351	5.7540	0.51
32	15	16	0.00058	0.01351	5.7540	0.51
33	16	30	0.00060	0.01411	6.0180	0.49
34	16	30	0.00060	0.01411	6.0180	0.49
35	16	30	0.00060	0.01411	6.0180	0.49
36	17	18	0.00054	0.01608	7.2820	0.43
37	17	18	0.00054	0.01610	7.2670	0.43

Table A.5: Line data for the Hydro-Québec system (continuation).

Line	From	To	r_{lm}	x_{lm}	b_{sh}	$F_{lm_{\max}}$
38	17	18	0.00054	0.01647	7.5980	0.42
39	17	32	0.00044	0.01311	5.8550	0.53
40	17	32	0.00044	0.01311	5.8550	0.53
41	17	32	0.00049	0.01422	6.5520	0.49
42	17	34	0.00012	0.00345	1.5130	1.00
43	18	19	0.00050	0.01513	6.8060	0.46
44	18	31	0.00037	0.01059	4.8650	0.66
45	19	22	0.00019	0.00551	2.4260	1.27
46	19	31	0.00016	0.00471	2.0640	1.48
47	20	21	0.00052	0.01149	4.8620	0.60
48	20	26	0.00045	0.01083	4.6110	0.64
49	20	27	0.00053	0.01561	6.7450	0.44
50	21	27	0.00024	0.00709	3.1110	0.80
51	23	24	0.00022	0.00622	2.8050	0.90
52	23	28	0.00032	0.00942	4.1280	0.74
53	24	25	0.00025	0.00706	3.1820	0.90
54	24	25	0.00025	0.00706	3.1820	0.90
55	24	33	0.00045	0.01318	5.8770	0.53
56	24	33	0.00045	0.01318	5.8770	0.53
57	27	34	0.00039	0.01155	5.1380	0.60
58	27	34	0.00039	0.01155	5.1380	0.60
59	28	32	0.00055	0.01649	7.4560	0.42
60	28	32	0.00055	0.01649	7.4580	0.42
61	28	32	0.00055	0.01649	7.5310	0.42
62	32	33	0.00007	0.01900	0.8560	0.36
63	33	34	0.00048	0.01387	6.3980	0.50
64	33	34	0.00048	0.01387	6.3980	0.50

Table A.6: Generator data for the Hydro-Québec system.

Bus	$P_{G_{\max}}$	$P_{G_{\min}}$	$Q_{G_{\max}}$	$Q_{G_{\min}}$
1	53.7000	0	10.0000	−3.0000
2	23.2000	0	10.0000	−3.0000
3	26.1000	0	10.0000	−3.0000
4	47.4000	0	10.0000	−3.0000
5	15.4000	0	10.0000	−3.0000
6	50.0000	0	10.0000	−3.0000
18	0	0	10.0000	−3.0000
27	0	0	13.4650	−6.5700
9	0	0	6.9300	−7.0350
10	0	0	3.4650	−3.5700
11	0	0	3.4650	−3.5700
12	0	0	3.4650	−3.5700
15	0	0	6.9300	−7.0350
16	0	0	8.6625	−8.7150
18	0	0	3.4650	−3.5700
23	0	0	3.4650	−3.5700
28	0	0	3.4650	−3.5700
32	0	0	3.4650	−3.5700
33	0	0	3.4650	−3.5700
34	0	0	3.4650	−3.5700

Table A.7: Bus data for the Hydro-Québec system.

Bus	$V_{\max}$	$V_{\min}$	P_D	Q_D
1	1.05	0.95	0.0000	0.0000
2	1.05	0.95	0.0000	0.0000
3	1.05	0.95	0.0000	0.0000
4	1.05	0.95	0.0000	0.0000
5	1.05	0.95	0.0000	0.0000
6	1.05	0.95	0.0000	0.0000
7	1.05	0.95	32.0326	4.0382
8	1.05	0.95	27.8528	0.7733
9	1.05	0.95	24.7537	−6.5129
10	1.05	0.95	9.1963	−0.0082
11	1.05	0.95	0.0000	0.0000
12	1.05	0.95	0.0000	0.0000
13	1.05	0.95	11.6150	0.4902
14	1.05	0.95	21.3966	0.1042
15	1.05	0.95	2.4618	0.4492
16	1.05	0.95	1.1464	0.2127
17	1.05	0.95	3.7194	−0.7294
18	1.05	0.95	0.0000	0.0000
19	1.05	0.95	17.4624	−1.0848
20	1.05	0.95	7.8867	−0.2046
21	1.05	0.95	4.7270	1.9766
22	1.05	0.95	8.0475	0.5300
23	1.05	0.95	0.0000	0.0000
24	1.05	0.95	0.0000	0.0000
25	1.05	0.95	0.0000	0.0000
26	1.05	0.95	11.1031	−0.4204
27	1.05	0.95	0.0000	0.0000
28	1.05	0.95	0.0000	0.0000
29	1.05	0.95	12.0500	1.1311
30	1.05	0.95	0.6000	0.1100
31	1.05	0.95	2.6449	0.3130
32	1.05	0.95	0.0000	0.0000
33	1.05	0.95	0.0000	0.0000
34	1.05	0.95	0.0000	0.0000

39-BUS EQUIVALENT OF THE NEW ENGLAND NETWORK

Table A.8: Line data for the 39-bus system.

Line	From	To	r_{lm}	x_{lm}	b_{sh}	$F_{lm_{\max}}$
1	1	2	0.0035	0.0411	0.6987	6
2	1	39	0.0010	0.0250	0.7500	10
3	2	3	0.0013	0.0151	0.2572	5
4	2	25	0.0070	0.0086	0.1460	5
5	2	30	0	0.0181	0	9
6	3	4	0.0013	0.0213	0.2214	5
7	3	18	0.0011	0.0133	0.2138	5
8	4	5	0.0008	0.0128	0.1342	6
9	4	14	0.0008	0.0129	0.1382	5
10	5	6	0.0002	0.0026	0.0434	12
11	5	8	0.0008	0.0112	0.1476	9
12	6	7	0.0006	0.0092	0.1130	9
13	6	11	0.0007	0.0082	0.1389	4
14	6	31	0	0.0250	0	18
15	7	8	0.0004	0.0046	0.0780	9
16	8	9	0.0023	0.0363	0.3804	9
17	9	39	0.0010	0.0250	1.2000	9
18	10	11	0.0004	0.0043	0.0729	6
19	10	13	0.0004	0.0043	0.0729	6
20	10	32	0	0.0200	0	9
21	12	11	0.0016	0.0435	0	5
22	12	13	0.0016	0.0435	0	5
23	13	14	0.0009	0.0101	0.1723	6
24	14	15	0.0018	0.0217	0.3660	6
25	15	16	0.0009	0.0094	0.1710	6
26	16	17	0.0007	0.0089	0.1342	6
27	16	19	0.0016	0.0195	0.3040	6
28	16	21	0.0008	0.0135	0.2548	6
29	16	24	0.0003	0.0059	0.0680	6
30	17	18	0.0007	0.0082	0.1319	6
31	17	27	0.0013	0.0173	0.3216	6
32	19	20	0.0007	0.0138	0	9
33	19	33	0.0007	0.0142	0	9
34	20	34	0.0009	0.0180	0	9
35	21	22	0.0008	0.0140	0.2565	9
36	22	23	0.0006	0.0096	0.1846	6
37	22	35	0	0.0143	0	9

Table A.9: Line data for the 39-bus system (continuation).

Line	From	To	r_{lm}	x_{lm}	b_{sh}	$F_{lm_{\max}}$
38	23	24	0.0022	0.0350	0.3610	6
39	23	36	0.0005	0.0272	0	9
40	25	26	0.0032	0.0323	0.5310	6
41	25	37	0.0006	0.0232	0	9
42	26	27	0.0014	0.0147	0.2396	6
43	26	28	0.0043	0.0474	0.7802	6
44	26	29	0.0057	0.0625	1.0290	6
45	28	29	0.0014	0.0151	0.2490	6
46	29	38	0.0008	0.0156	0	12

Table A.10: Generator data for the 39-bus system.

Bus	$P_{G_{\max}}$	$P_{G_{\min}}$	$Q_{G_{\max}}$	$Q_{G_{\min}}$
30	10.40	0.00	4.00	1.40
31	6.46	0.00	3.00	−1.00
32	7.25	0.00	3.00	1.50
33	6.52	0.00	2.00	0
34	5.08	0.00	1.00	0
35	6.87	0.00	3.00	−1.00
36	5.80	0.00	2.00	0
37	5.64	0.00	2.00	0
38	8.65	0.00	3.00	−1.50
39	11.00	0.00	3.00	−1.00

Table A.11: Bus data for the 39-bus system.

Bus	$V_{\max}$	$V_{\min}$	P_D	Q_D
1.0000	1.0600	0.9400	0.9760	0.4420
2.0000	1.0600	0.9400	0	0
3.0000	1.0600	0.9400	3.2200	0.0240
4.0000	1.0600	0.9400	5.0000	1.8400
5.0000	1.0600	0.9400	0	0
6.0000	1.0600	0.9400	0	0
7.0000	1.0600	0.9400	2.3380	0.8400
8.0000	1.0600	0.9400	5.2200	1.7660
9.0000	1.0600	0.9400	0.0650	−0.6660
10.0000	1.0600	0.9400	0	0
11.0000	1.0600	0.9400	0	0
12.0000	1.0600	0.9400	0.0853	0.8800
13.0000	1.0600	0.9400	0	0
14.0000	1.0600	0.9400	0	0
15.0000	1.0600	0.9400	3.2000	1.5300
16.0000	1.0600	0.9400	3.2900	0.3230
17.0000	1.0600	0.9400	0	0
18.0000	1.0600	0.9400	1.5800	0.3000
19.0000	1.0600	0.9400	0	0
20.0000	1.0600	0.9400	6.8000	1.0300
21.0000	1.0600	0.9400	2.7400	1.1500
22.0000	1.0600	0.9400	0	0
23.0000	1.0600	0.9400	2.4750	0.8460
24.0000	1.0600	0.9400	3.0860	−0.9220
25.0000	1.0600	0.9400	2.2400	0.4720
26.0000	1.0600	0.9400	1.3900	0.1700
27.0000	1.0600	0.9400	2.8100	0.7550
28.0000	1.0600	0.9400	2.0600	0.2760
29.0000	1.0600	0.9400	2.8350	0.2690
30.0000	1.0600	0.9400	0	0
31.0000	1.0600	0.9400	0.0920	0.0460
32.0000	1.0600	0.9400	0	0
33.0000	1.0600	0.9400	0	0
34.0000	1.0600	0.9400	0	0
35.0000	1.0600	0.9400	0	0
36.0000	1.0600	0.9400	0	0
37.0000	1.0600	0.9400	0	0
38.0000	1.0600	0.9400	0	0
39.0000	1.0600	0.9400	11.0400	2.5000